Newsletter of the Climate Variability and Predictability Programme (CLIVAR)

Exchanges

No. 25 (Vol. 7, No. 3/4) September 2002

Special issue on: CLIVAR Atlantic

Latest CLIVAR News

- New in this issue: CLIVAR Data Section, see pages 68-73.
- New Version of the CLIVAR Calendar: www.clivar.org/calendar/. Bookmark the new address and edit/add entries yourself.
- Coming soon: Bookmark **www.clivar2004.org**, the official CLIVAR conference website.
- ICPO worldwide: Mike Sparrow works out of his new base in China. See www.clivar.org/organization/icpo/sparrow.htm for more information.

Visit our news page:
http://www.clivar.org/recent/

CLIVAR is an international research programme dealing with climate variability and predictability on time-scales from months to decades.

CLIVAR is a component of the World Climate Research Programme (WCRP).

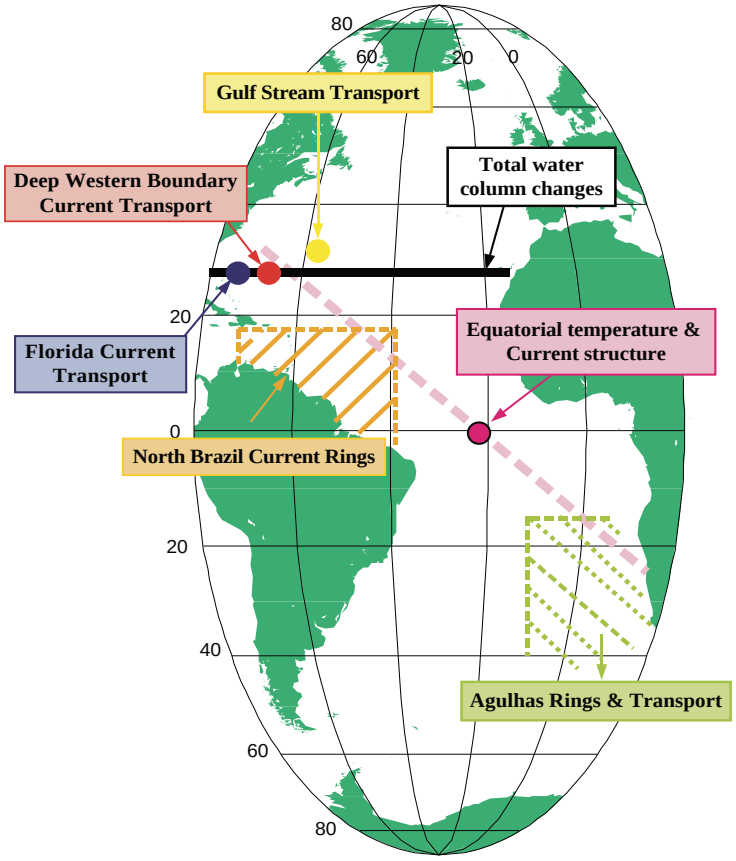

Figure 1 from paper *'Benchmarks for Atlantic Ocean Circulation'* by R. Molinari et al.: *Benchmarks being monitored and available on http://www.aoml.noaa.gov/benchmarks/index.html.* The paper appears on page 6.

Call for Contributions

We would like to invite the CLIVAR community to submit papers to CLIVAR Exchanges for the next issue.The overarching topic will be on **science related to the WOCE / CLIVAR transition. The deadline for this issue is January, 31, 2003.**

Guidelines for the submission of papers for CLIVAR Exchanges can be found under: http://www.clivar.org/publications/exchanges/guidel.htm

Editorial

Dear CLIVAR community,

As we reported in out previous issue, the ICPO has a new director. Dr. Howard Cattle has taken over the responsibilities from Dr. John Gould who retired from his CLIVAR job beginning of August. Again, a warm welcome to Howard and deepest thanks and highest regards to John for leading the ICPO over the past 4 years. Howard is the fourth director of the ICPO, following Dr. Michael Coughlan (1995-97), Dr. Lydia Dümenil (1997-1998) and Dr. John Gould (1998-2002). Together with the CLIVAR Scientific Steering Group, its panels and working groups (currently 12) and the ICPO staff, his challenge will be, to steer and develop CLIVAR further into its fully mature phase.

About 5 years after the publication of the Initial Implementation Plan, CLIVAR has entered its mature phase. National projects are being funded, international coordination is taking place within many parts of the programme and most important, scientific results are being published. For us in the ICPO it is important to monitor the scientific progress of the programme, since this is one of the key parameters to measure the success of the programme, and somehow also a legacy for the community. However it turns out to be much more tricky in many cases to decide what is a CLIVAR publication than for other, more focused programmes like WOCE which, because of their nature, have specific national grants which are referred to. Such acknowledgement will clearly be made if there is indeed a nationally funded programme for CLIVAR (and such programmes do exist in some countries). But acknowledgement may also to some extent be a cultural issue in terms of making the community itself feel it is a part of a programme which it is naturally appropriate to refer to, irrespective of funding lines. This is clearly an issue which CLIVAR as a programme needs to work on, but it would be helpful if authors of CLIVAR-relevant papers could consider if a reference to CLIVAR is appropriate.

To get a broader overview of what is published within the CLIVAR related science, we have started to collect the titles of CLIVAR related publications of about a dozen peer-reviewed journals and provide this information on our website, along with links to abstracts, and some kind of indication about the relevance to specific parts of CLIVAR. This is by no means an objective and comprehensive approach but it provides a tool to monitor the progress of the programme. Please feel free to visit: http://www.clivar.org/publications/journals/literature.htm. We will try to maintain and extend this service in the future.

Another tool to demonstrate the progress and the achievements of the programme has been our newsletter. During the first years, it was mainly a communication forum reporting about the progress in building up the organizational and programmatic structure of CLIVAR. Shortly after the publication of the Initial Implementation Plan and CLIVAR Conference we changed the scope of the newsletter and invited the community to report about scientific progress on topics related to CLIVAR. Certainly, not everybody is in favour of this approach. Because the articles published in Exchanges are not reviewed they form part of grey literature and not every contribution might be well balanced and as of high quality as papers are in the peer-reviewed literature. We are taking this risk into account and the response to our calls for contributions has proved the wide interest of the community to have and use this forum. If controversial discussions about papers in Exchanges arise, we are happy to expose the community to this and we are willing to publish letters to the editor as we have done in the past. We feel that different views are part of living and developing science and these discussions often contribute to scientific progress.

Until today, we have published more than 120 scientific articles in Exchanges and this 25th issue is a very special one. Not only, because it is a double number 3/4 2002, but we have never received as many contributions as we have for this issue. Of course, the overarching theme CLIVAR Atlantic is broad and encompasses many research topics within CLIVAR, but the response has also shown that we are on the right track with Exchanges. We think that a wide overview about CLIVAR related research within the Atlantic has been provided.

In addition, we are starting a new regular section on CLIVAR data and data management in Exchanges. We like would to report new efforts within this area as well to provide information about existing data sets, data centres and data management efforts within WCRP and other relevant programmes. We encourage submissions of contributions relevant to this topic.

As many of you know, WOCE is coming to a conclusion at the end of this year. The final WOCE conference in San Antonio, Texas, USA will highlight this very successful WCRP programme in a very comprehensive way. In order to honour the accomplishments of WOCE and the legacy to CLIVAR we will dedicate the next issue of Exchanges (1/2003) on the WOCE-CLIVAR transition. Although we will specifically approach a number of scientists for contributions, papers submitted by the community are very welcome. The deadline for submissions is January 31, 2003.

We hope that you will enjoy this very special issue of Exchanges.

Andreas Villwock

From the Director of the ICPO

Dear CLIVAR community,

I am grateful to Andreas Villwock for his words of welcome above and like him must firstly pay tribute to John Gould for all he has done for CLIVAR during his time as Director of the ICPO. I have taken over a well-run office and an enthusiastic team and I only hope I can maintain the momentum. As one person emphasised, at the SSG in Xian, China this year, I have some big shoes to fill. The regard in which John is held is, I am sure, reflected in the very warm welcome everyone has given me on my entry into the CLIVAR world, a welcome I have been much encouraged by. John is still close by in the office across the corridor helping to bring WOCE to its conclusion. Having his advice and wisdom at hand is very welcome at this (very steep) stage of my learning curve.

As Andreas has said, CLIVAR is now in its mature phase and, as I am learning, there are many and varied initiatives underway under the CLIVAR banner. Ultimately, CLIVAR exists as a project of WCRP to set the agenda for and to facilitate international collaboration in research on climate variability and predictability. This is, of course carried out through the Scientific Steering Group and its panels and working groups and it is a primary role of the ICPO to assist with the practical implementation of their work. I am looking forward to working with others in the ICPO as well as all in the CLIVAR panels and working groups and the wider community on the variety of CLIVAR activities and initiatives.

It is clear that there will be many challenges ahead. A key outcome of the meeting of the Joint Scientific Committee (JSC) for WCRP when it met in Hobart in March 2002 was a proposal for an overall WCRP banner on predictability. This is an issue of which lies at the heart of CLIVAR (indeed sitting within its very title). CLIVAR has the natural lead within WCRP for this therefore, but there is a need to clarify the issues and CLIVAR has a key contribution to make to formulate the way ahead, together with the other WCRP projects.

WOCE is, as I have mentioned, coming to an end. It has done a wonderful job in providing us amongst other things with an unparalleled database of ocean climate. For the future, however, the issue of monitoring the variability of the ocean on climate time-scales and the role CLIVAR has to play as the lead within WCRP for this is a key one, as John Gould has emphasised on more than one occasion. With the exception of its modelling groups, the CLIVAR panel structure itself largely addresses the variability of the climate system on regional and basin-scale. One of the concerns of the JSC at its last meeting was the need for us to better articulate how these contribute to and build into an overall global picture. We need to think how we best do this. Another issue for CLIVAR, described at the last SSG meeting as "getting your arms around the data elephant" is that of CLIVAR data management and how we go about it, This is an area of concern not only to CLIVAR but to WCRP as a whole. From a CLIVAR perspective, it is one that needs to be addressed with the help of all the panels and working groups as well as the ICPO.

These are but a few examples of the many challenges facing us. An event still a little way off, but one which will soon become larger in our minds is that of the First International CLIVAR Science Conference, to be held in Baltimore, USA from 21-25 July 2004. Planning for this exciting event is already well underway. The Conference will be a real opportunity for us to assess progress in CLIVAR science against our implementation plan and to consider the directions CLIVAR should take in the second half of the decade.

So, there is much work to be done and I am looking forward to our future involvement together. Whilst I am no stranger to WCRP projects, I trust you will bear with me as I settle into my new role. At the same time please provide me with appropriate advice and correction whenever you feel I am taking the wrong turn. I will always be pleased to receive and hopefully to respond positively to comments on CLIVAR, its structure and activities and in particular the role of those of us at the ICPO. We are here to be as helpful as we can.

Howard Cattle

CLIVAR in the Atlantic Sector

M. Visbeck (chair)[1], David Marshall[2] and the CLIVAR-Atlantic Implementation Panel
[1] Lamont Doherty Earth Laboratory, Palisades, NY, USA
[2] University of Reading, Reading, UK
corresponding e-mail: visbeck@ldeo.columbia.edu

Introduction

Our panel looks after the implementation of CLIVAR in the Atlantic sector with an emphasis on three phenomena: Tropical Atlantic Variability, the North Atlantic Oscillation, and changes in the ocean's meridional overturning. The primary goal is to improve our description and understanding of those modes of variability and then explore to what degree they might be predictable on seasonal to decadal time scales. An important objective is to study the interaction between those phenomena and large scale forcings of the global climate system such as due to El Niño and/or anthropogenic climate change.

The CLIVAR Atlantic panel has met approximately annually during the last 3 years. In December 2000 the focus was on implementation issues associated with the North Atlantic Oscillation in conjunction with the Chapman Conference (Visbeck et al., 2001). In September 2001 we reviewed ongoing and planned activities in the tropical Atlantic following a CLIVAR sponsored workshop on the subject (Garzoli, 2001). This year's meeting (July 2002 in Bermuda) focused on CLIVAR activities and plans regarding the oceans meridional overturning circulation. A number of invited experts and representatives from WGCM and WGOMD were present to enrich the discussions. A brief review on the MOC and related CLIVAR activities is given below.

Atlantic Meridional Overturning Circulation: Issues for Models and Observations

The Meridional Overturning Circulation (MOC) in the Atlantic transports approximately 20 Sv of warm water northward in surface layers, with compensating southward flow at depth. Associated with this overturning is a northward heat transport, peaking at about 1PW in the subtropical North Atlantic. It is widely (though not universally) accepted that this heat is an important factor in determining surface air temperatures over much of the North Atlantic Sector. On long time scales the strength of the MOC is dominated by this thermohaline driving (a balance between surface buoyancy loss in high latitudes and buoyancy gain by diapycnal mixing in the tropical oceans and/or the Southern Ocean). In contrast, on interannual and shorter time scales wind-driven Ekman cells dominate its variability. This mix of forcing poses significant challenges for sustained observations.

A significant number of projections of greenhouse-gas induced climate change over the next century indicate a weakened MOC in the North Atlantic due to freshening of the subpolar ocean, although there is little consensus on the rate and magnitude of the projected change (IPCC, 2001). A key issue is therefore to understand the spread in these predictions, and to determine whether this is indicative of shortcomings in the models or an inherent lack of predictability in the response of the MOC, and to attempt to reduce the uncertainties. Observations reveal consistent evidence of long-term changes in the properties of the overflows and in convectively renewed water masses in the Labrador Sea; the present observational network seems inadequate, however, to directly determine whether the strength of the MOC is in the process of decreasing by 10-20% as anticipated. In addition, even with perfect observations it would be difficult to detect an MOC climate change signal without an adequate understanding of the natural variability of the MOC. This argues both for improved understanding of the fundamental processes controlling the MOC and its variability, such as can be achieved through theoretical and modelling studies, and for efforts to quantify the natural variability of the MOC.

The thermohaline circulation responds to surface forcing on a range of time-scales. The initial dynamical adjustment occurs via the propagation of Kelvin waves and Rossby waves on the time-scale of months-decades; in contrast thermodynamic equilibrium is approached over several centuries. Thus, while eddy-permitting models can be used to study the initial dynamical adjustment of the thermohaline circulation, it is still necessary to employ relatively coarse-resolution models in order to study the time-mean circulation and anthropogenic climate-change scenarios. These latter models not only fail to resolve the geostrophic eddy field, but also fail to adequately resolve the narrow boundary currents and their recirculations within which most of the heat transport occurs; thus the results of such coarser models need to be treated with caution. Even in eddy-permitting models, there remain several important processes that require careful parameterisation such as shelf and open-ocean convection, overflows and sea-ice. Models can be particularly sensitive to these parameterisations, for example Dengg and Böning (2002) have found that subtle changes in the density of the water flowing over the Denmark Straits can lead to dramatic changes in MOC downstream due to entrainment in the overflows.

A critical issue is to improve our understanding of how the coupled system responds to changes in MOC. Johnson and Marshall (2002) have shown that the equator acts as a low pass filter to MOC anomalies. In contrast to the time-mean, where there is some debate over whether the MOC is "pushed" by convection in the high-

Participants of the 3rd Meeting of the CLIVAR Atlantic Panel in Bermuda, July 2002.

latitude North Atlantic, or "pulled" by Ekman transports in the Southern Ocean and/or diapycnal mixing in the ocean interior, temporal anomalies in MOC are likely to be confined to the hemisphere in which they are generated on decadal and shorter time-scales. However the Atlantic MOC may still have a rapid global impact. Dong and Sutton (2002) have performed a provocative calculation in which the thermohaline circulation is abruptly halted by an impulsive reduction in high-latitude salinity. Circulation anomalies are found in the tropical Atlantic within 6 months via the propagation of a Kelvin wave. These anomalous currents modify the cross equatorial Atlantic SST gradient (with cooling in the North Atlantic) and shift the mean position of the ITCZ southward; the latter in turn leads to a global atmospheric response within seven years. While a somewhat extreme scenario, this experiment serves as a useful reminder that the response of the climate system to a change in high latitude ocean conditions is likely to involve a combination of oceanic and atmospheric teleconnections, with coupling most likely occurring in the tropical belt. In the absence of an abrupt shutdown, natural variations in MOC are likely to be significantly smaller, but still possibly important. For example, recent observational analyses (Landsea et al., 1999) have noted a link between Atlantic multidecadal SST variations and hurricane activity. To the extent that these multidecadal fluctuations in SST are related to variations in the MOC, this points to a potentially important role for the MOC in modulating Atlantic hurricanes.

A further motivation for improving our ability to understand and model the dynamical response of the ocean to surface forcing is to aid in the design and interpretation of observations of the MOC. A substantial portfolio of observations targeting the Atlantic MOC is now taking shape. This includes: various activities under the ASOF programme aiming to measure fresh water fluxes between the Arctic and Atlantic (see Dickson and Boscolo, 2002); the basin scale hydrographic programme (http://clivar-search.cms.udel.edu/hydro/hydro_table.asp); a series of Labrador Sea/Grand Banks moored arrays (IfM Kiel, Schott et al.); transport measurements in the Florida straits; the MOVE array at 16°N (IfM Kiel, Send et al.); and the tropical Atlantic surveys conducted by research labs in the USA, France and Germany. In addition there are a number of proposed efforts including an array of three sections to monitor the communication of deep MOC anomalies along the shelf between Grand Banks and Cape Cod (Hughes, Marshall, Williams); a line at 39°N (WHOI, Toole et al.); a proposed array across 26°N (SOC, Marotzke et al.) which, together with the ongoing efforts should provide data from which a time series of MOC observations could be constructed. However, it might be best to include satellite data of sea surface height and temperature; *in situ* data from the PIRATA array, XBT's and the emerging ARGO profiles (see also http://www.clivar.org/organization/atlantic/IMPL/index.htm) to obtain a basin wide synthesis using a variety of methods including 4 dimensional data assimilation (Stammer et al., 2002). In the South Atlantic the observational data base is thinner, and as a result, our knowledge of the role of the South Atlantic in the coupled climate system is less certain. Efforts are underway to identify the climate variability in the region and the broad scale and targeted ocean observations needed to increase our understanding. A workshop is planned for early 2003 to initiate this activity.

In summary CLIVAR is well underway in the Atlantic sector. A significant number of national and international observational, modelling and synthesis programmes exist in support of CLIVAR objectives.

References

Dengg, J., and C. Böning, 2002: Effects of Denmark Strait Overflow on the large-scale circulation in a numerical model of the North Atlantic, *J. Phys. Oceanogr.*, to be submitted.

Dickson, R., and R. Boscolo, 2002: The Arctic-Subarctic Ocean Flux Study (ASOF): Rational, Scope and Methods. *CLIVAR Exchanges*, 25, 64.

Dong, B.-W., and R.T. Sutton, 2002: Adjustment of the coupled ocean-atmosphere system to a sudden change in thermohaline circulation. *Geophys. Res. Lett.*, submitted.

Garzoli, S., 2001: Workshop on tropical Atlantic variability. *CLIVAR Exchanges*, **22**, 33-35.

IPCC, 2001: Climate Change 2001: The Scientific Basis. In: *Contribution of Working Group I to the Third Assessment Report of the Intergovernmental Panel on Climate Change*, Houghton, J.T., Y. Ding, D.J. Griggs, M. Noguer, P. van der Linden, X. Dai and K. Maskell, Eds., Cambridge University Press, Cambridge, UK.

Johnson, H.L., and D.P. Marshall, 2002: Localization of abrupt change in the North Atlantic thermohaline circulation. *Geophys. Res. Lett.*, **29**, in press, 10.1029/2001GL014140.

Landsea, C.W., R.A. Pielke, Jr., A.M. Mestas-Nunez, and J.A. Knaff, 1999: Atlantic basin hurricanes: indices of climate change. Climatic Change, **42**, 89-129.

Stammer, D., C. Wunsch, I. Fukumori, and J. Marshall, 2002: State estimation improves prospects for ocean research. *EOS, Transactions American Geophysical Union*, Vol. 83, No. 27, p. 289, 294-295.

Visbeck, M., J.W. Hurrell, and Y. Kushnir, 2001: First International Conference on the North Atlantic Oscillation (NAO): Lessons and Challenges for CLIVAR. *CLIVAR Exchanges*, **19**, 24-25.

Benchmarks for Atlantic Ocean Circulation

Robert L. Molinari, Roberta Lusic, Silvia L. Garzoli, Molly O. Baringer and Gustavo Goni

NOAA/AOML, Miami, FL, USA
corresponding e-mail: bob.molinari@noaa.gov

Oceanographers frequently decompose the total oceanic circulation into two components: a wind-driven component existing primarily in the horizontal plane and a thermohaline-driven component existing primarily in the vertical plane (also called the meridional overturning circulation, MOC). Although this decomposition is a simplification of the dynamics of the motion in the ocean (the two components are not separable in the complete equations of motion), it provides a framework for describing responses of the ocean to different surface forcing functions. Numerical modelling, paleoclimate and observational studies indicate that both the wind-driven and thermohaline circulation can play an important role in longer-term (greater than decadal) climate variability. The U.S. National Oceanic and Atmospheric Administration addresses both components to satisfy its missions of detecting, attributing and forecasting long-term climate change. We contribute to NOAA's mission by developing and providing observational benchmarks (i.e., indices) for various components of the wind-driven circulation (hereinafter WDC) and MOC in the Atlantic Ocean.

Many early NOAA programmes (e.g. STACS, ACCP) were searching for indices of critical North Atlantic WDC and MOC features to monitor. Although not originally NOAA programmes, other studies have considered the contribution of southern hemisphere features to the MOC. For continuity of the upper layer limb of the MOC, exchanges are required: from the Indian Ocean to the South Atlantic; across the South Atlantic; and across the equator. The inter-ocean exchange takes place through the Benguela/Agulhas system, south of South Africa. The Agulhas Current at its retroflection sheds energetic rings that carry salt and warm water into the South Atlantic. Satellite altimetric measurements have been calibrated to provide estimates of the transport of the Agulhas Current and the separated rings. The extension of the Benguela Current brings the Indian Ocean waters to the central South Atlantic as it flows northwestward in the South Atlantic subtropical gyre.

The pathways of the upper limb MOC transport are then complicated by the wind-driven circulation features along the western boundary and the interior tropical Atlantic (i.e., equatorial upwelling, off-equatorial down welling, zonal currents), that provide obstacles for this limb to move from the South Atlantic to the North Atlantic. Currently, there is insufficient understanding and data to identify these pathways precisely. However numerical models do provide some initial guidance. Using an eddy-resolving numerical circulation model, Fratantoni et al. (2000) concluded that 14 Sv of upper limb MOC flow is partitioned among three pathways connecting the equatorial and tropical wind-driven gyre: a frictional western boundary current accounting for 6.8 Sv; a diapycnal pathway involving wind-forced equatorial upwelling and interior Ekman transport, 4.2 Sv; and North Brazil Current (NBC) rings shed at the NBC retroflection, 3 Sv. The results of an AOML, university observational programme indicate that previous estimates both in the numbers of rings per year and in their contribution to hemispheric exchanges were low. Based on the results of this work, a monitoring strategy is being developed to monitor ring formation and propagation.

Both the intensity of the subtropical gyre and a component of the warm upper level poleward flow in the North Atlantic are being monitored by submarine cable observations in the Straits of Florida. Similarly, the characteristics of the cold deep return flow are being tracked by research vessel transects across the DWBC east of the Bahamas. In the North Atlantic Ocean, time-series of both the upper layer temperature structure within the subtropical gyre and total water column changes across the basin are being maintained.

The recent history of these and other components of the MOC and WDC motions are characterized by data collected over the past 10 to 50 years. These benchmarks are designed to serve several purposes. Independently these benchmarks serve as indices for (1) the intensity of various components of the MOC and WDC, thereby providing alerts for dramatic changes in these features and (2) verification of the ability of GCM's to simulate the ocean's role in climate variability. Collectively, when assimilated into GCM's they will provide global benchmarks for detection and attribution of climate change. All the benchmarks presently available are shown in Fig. 1 (page 1). We will now describe a few of these indices; where sufficient data are available we provide a description of the characteristics of various scales of variability.

1. Agulhas Current

Monitoring both the Agulhas transport into the South Atlantic in the upper kilometre of the ocean and the number of rings shed at its retroflection provides a means of detecting any substantial changes in inter-ocean water exchanges. After calibrating the observations with an array of inverted (IES) echo sounds, satellite altimetry has been used to estimate inter-ocean exchange between the Indian and Atlantic Oceans and has been maintained since 1993. The time-series for this transport is shown in Fig. 2. In addition, ring shedding events can be identified.

Agulhas Current and ring shedding characteristics

After turning to the west, the circulation of this current turns or retroflects back to the east between 15 and 25°E (Fig. 2, upper panel). The net westward baroclinic transport across a TOPEX/POSEIDON groundtrack (light grey line in the top panel of Fig. 2) is estimated using altimetry-derived sea height anomaly and historical hydrographic data within a two-layer reduced gravity scheme.

- *Mean annual transport and number of rings shed:* The mean annual transport of the Aguhlas Current from the coast to 40°S above the 10°C isotherm is 15.7 ± 1.5 Sv, with a maximum of 23 ± 1.5 Sv in 1997 and a minimum of 13 ± 1.5 Sv in 1993. The number of rings shed at the retroflection is between 4 and 7 per year and the transport of the rings varies between 0.8 and 2.4 Sv.
- *Interannual signal*: Strong interannual variability in the transport time series is primarily related to ring shedding (Fig. 2, center panel).
- *Annual signal*: The altimeter-derived Agulhas transport shows no apparent seasonal signal (Garzoli and Goni, 2000), contrary to previous numerical model results (Matano et al., 1998).

2. North Brazil Current

The North Brazil Current is a western boundary current in the tropical Atlantic that transports upper ocean waters across the equator. Particularly during summer and fall, the NBC retroflects from the coast at 6° to 7°N and feeds the North Equatorial Countercurrent and North Equatorial Undercurrent. During this retroflection phase large anticyclonic rings are shed. These features then move northwestward toward the Caribbean Sea, roughly paralleling the South American coastline. As part of the NBC Ring study, an analysis of altimetric data was made (Goni and Johns, 2001). Using a two-layer reduced gravity model, sea height anomaly was converted into upper layer thickness. The thickness maps are used to infer the NBC rings formation and propagation. Analysis of the historical altimetric record indicates that ring shedding is nearly a factor of two greater than previously estimated even though the altimeter does not track all the rings formed at the retroflection, (Garzoli et al., 2002).

North Brazil Current rings characteristics

- *Transport resulting from mean annual ring shedding:* The estimated yearly mass transported by rings is 9 Sv.
- *Interannual variability:* The available time series of ring shedding derived from the altimeter is shown in Fig. 3.
- *Annual cycle:* There are insufficient data to determine if there is an annual signal in ring generations. However, the analysis of the IES data obtained during the North Brazil Current ring experiment (Garzoli et al., 2002) indicates that there is no seasonality.

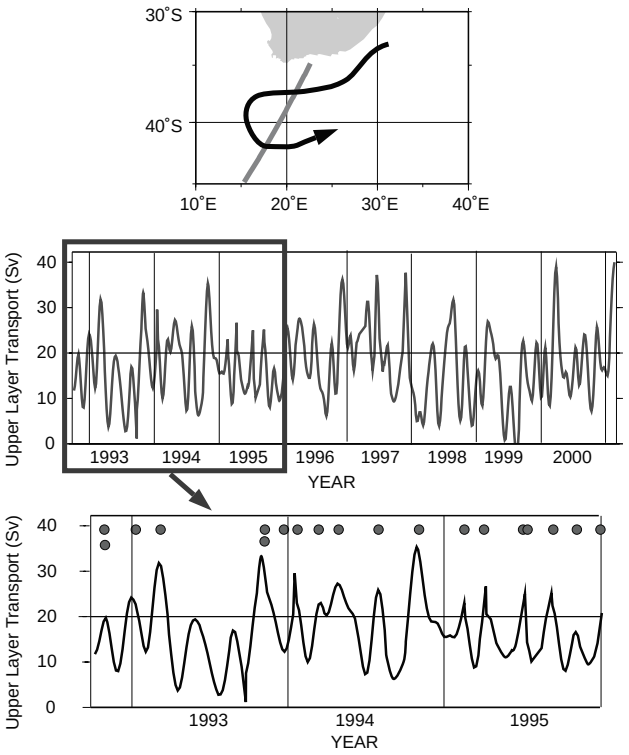

Fig. 2: (top) Schematic of the Agulhas Current retroflection. (center) Baroclinic transport from the surface to the 10°C isotherm across a selected TOPEX/Poseidon altimeter ground track from the coast to 40°S. (light grey line in top panel). (centre) Baroclinic transport between 1993 and 1995 showing a strong correspondence between ring shedding (circles) and maximum transport values (bottom).

3. Florida Current Transport

The Florida Current (FC) is the western boundary current for the subtropical gyre of the North Atlantic. In addition, to transporting water masses originating in the northern hemisphere, the FC advects water from the southern hemisphere that has crossed both the equator and the North Atlantic's tropical/subtropical gyre boundary. Ultimately, a portion of the FC transport becomes entrained in the subpolar gyre where it contributes to the formation of the deeper water masses. Beginning in the early 1980's, submarine cable observations of voltage differences across the Straits have been calibrated with direct current data to estimate FC transport.

Florida Current characteristics

- *Mean annual transport*: The mean annual transport of the Florida Current at 27°N over the cable record is 32 Sv. Earlier data collected at 26°N during the late 1960's early 1970's observed a mean annual transport of 30 Sv (Niiler and Richardson, 1973). Johns et al., (1999) computed a mean annual transport through the NW Providence Channel (located between the two transport sections) of about 1 to 2 Sv. Thus over the past 30+-years the mean annual transport of the Florida Current appears stable.

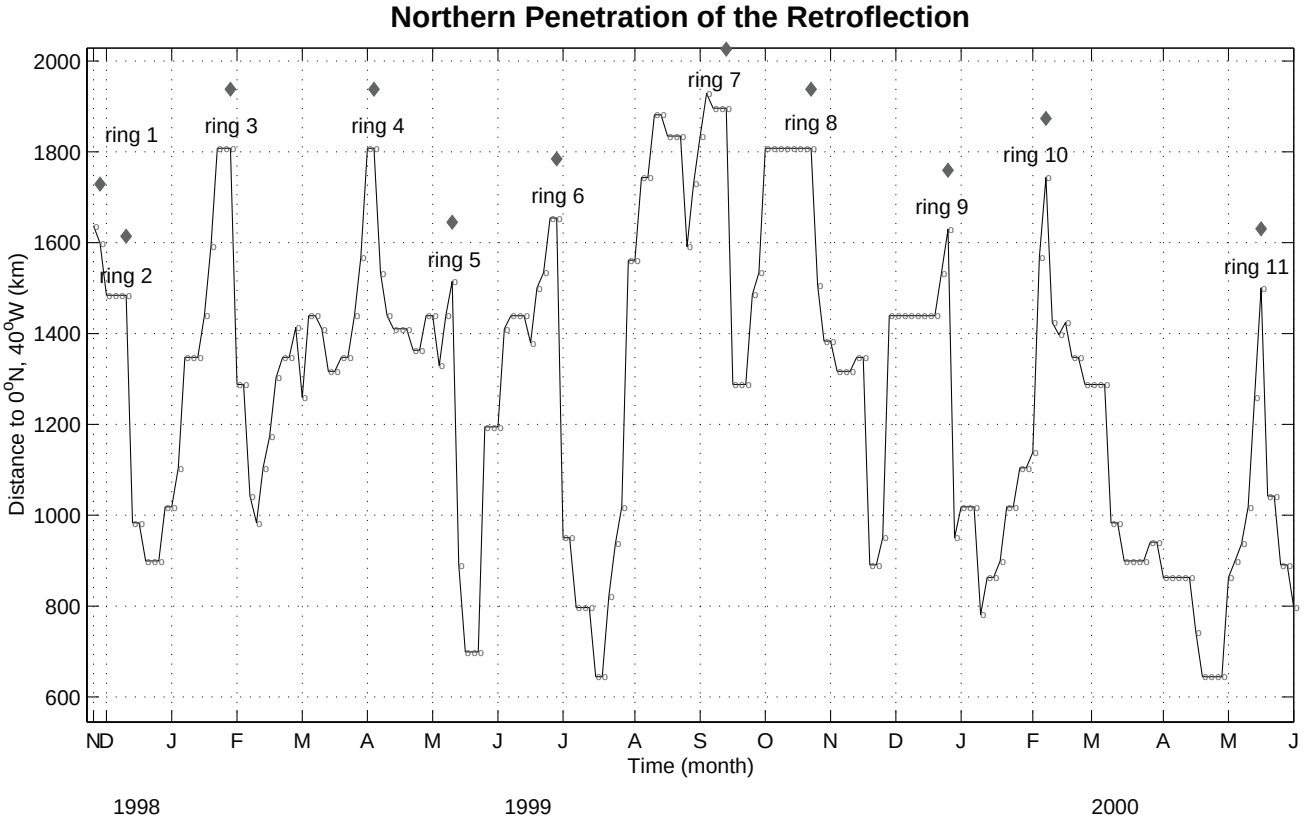

Fig. 3: Time series of the latitude of penetration of the NBC retroflection estimated from synoptic dynamic height maps. It is measured as the distance (in km) between the northern most point of the retroflection and an arbitrary point in space (0°N 40°W). Diamonds indicate the time of a ring shedding. The northward motion can be considered as the motion of the northward penetration (30km/day). The southward motion is only a resetting of the index. As the ring separates, the retroflection reforms further south.

- *Decadal signals*: A smoothed version of the 20-year time-series is shown in Figure 4. On decadal time-scales, the variability is less than 4 Sv (10-15% of the mean annual signal). This signal in FC transport is visually correlated with a NAO-index with similar time-scales (Fig. 4).
- *Annual signal:* Using the 1960/1970's data, (Niiler and Richardson, 1973) estimated an annual signal for FC transport. Largest transports were in the summer and minimum, in the fall. The amplitude of the annual signal was about 3 SV. However, (Behringer and Larsen, 2001) found a larger semi-annual component in the more recent transport data than observed in the earlier records.

4. Lower Layer

The Deep Western Boundary Current (DWBC) provides the main conduit for waters formed in the subpolar and polar Atlantic to the South Atlantic and then on to the other ocean basins. As surface forcing functions change in the formation regions for the DWBC water masses, the characteristics of the water masses will vary downstream. Tracking these changes provides a benchmark for evaluating model simulations of the advective times from the formation regions. For example, a water mass formed in the Labrador Sea (LSW) is advected in the DWBC to 26.5°N, east of Abaco Island, the Bahamas. Time series of the characteristics of LSW at Abaco provide a benchmark for present day advective time-scales from source to subtropical western boundary.

Lower layer characteristics

***Decadal Signal*:** Temperature and salinity characteristics at the depth of LSW in the DWBC at 26.5°N are shown in Fig. 5 (page 35). Late-90 cooling and freshening can be correlated to changes in the characteristics of LSW at its formation region. The comparison indicates the arrival of LSW at Abaco some 8 to 10 years after formation in the Labrador basin. These advective times are somewhat shorter than previously hypothesized but consistent with other observations obtained in the central subtropical and eastern mid-latitude Atlantic (Molinari et al., 1998).

References

Baringer, M.O., and J.C. Larsen, 2001: Sixteen years of Florida Current transport at 27°N. *Geophys. Res. Lett.*, **28**, 3179-3182.

Fratantoni, D.M., W.E. Johns, T.L. Townsend, and H.E. Hurlburt, 2000. Low-Latitude Circulation and Mass Transport Pathways in a Model of the Tropical Atlantic Ocean. *J. Phys. Oceanogr.*, **30** (8), 1944-1966.

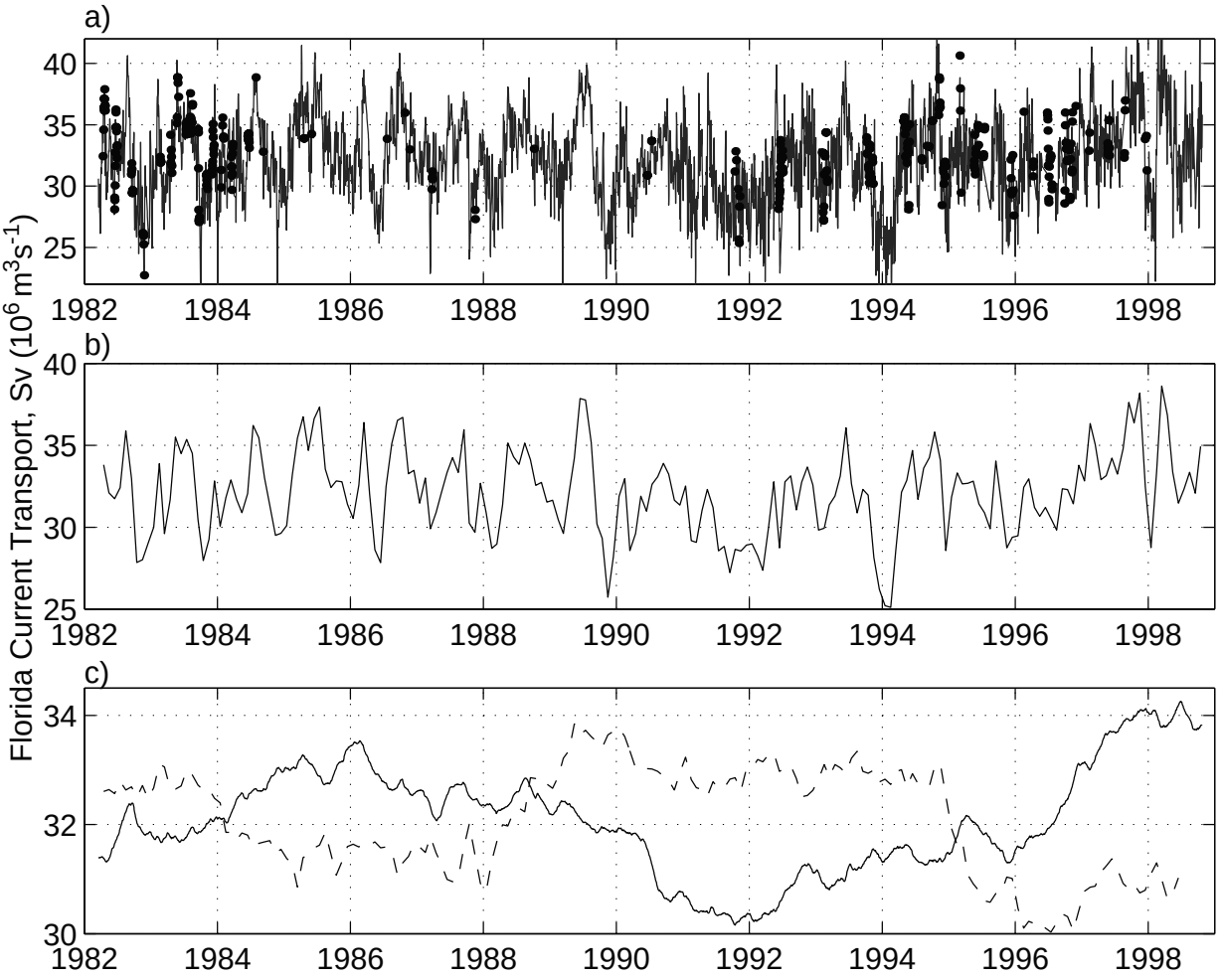

Fig. 4: Time series of Florida Current transport inferred from the cable voltages including (a) the daily transport values, (b) the monthly average transport, and (c) the two year running means of the daily transport values (solid line). Panel (c) also includes a monthly mean NAO index (Hurrell, 1995) (dashed line). Panel (a) includes in situ observations of Florida Current transport obtained on small boat cruises (solid circles).

Garzoli, S.L., Q. Yao, and A. Ffield, 2002: North Brazil Current rings and the variability in the latitude of retroflection. In: *Interhemispheric Water Exchange in the Atlantic Ocean*, G. Goni and P. Malanotte-Rizzoli (Eds.), Elsevier Science, submitted.

Garzoli, S.L., and G. Goni, 2000: Combining altimeter observations and oceanographic data for ocean circulation studies. In: *Satellites, Oceanography and Society*, Halpern, D., (ed.) Elsevier Science B. V., 79 -97.

Goni G., and W.E. Johns, 2001: A Census of North Brazil Current Rings Observed from TOPEX/POSEIDON Altimetry: 1992 – 1998. *Geophys. Res. Lett.*, **28**, 1-4.

Hurrell, J.L., 1995: Decadal Trends in the North Atlantic Oscillation: Regional Temperatures and Precipitation. *Science*, **269**, 676.

Johns, E., W.D. Wilson, and R.L. Molinari, 1999: Direct observations of velocity and transport in the passages between the Intra-Americas Sea and the Atlantic Ocean, 1984-1996. *J. Geophys. Res.*, **104**, 25805-25820.

Matano, R.P., C.G. Simionato, W.P. de Ruijiter, P.L. van Leeuween, P.T. Strub, D.B. Chelton, and M.G. Schlax, 1998: Seasonal variability in the Agulhas retroflection region. *Geophys. Res. Lett.*, **25**, 4361-4364.

Molinari, R.L., R.A. Fine, W.D. Wilson, R.G. Curry, J. Abell, and M.S. McCartney, 1998: The arrival of recently formed Labrador Sea Water in the Deep Western Boundary Current at 26.5ºN. *Geophys. Res. Lett.*, **25**, 2249–2252.

Niiler, P.P., and W.S. Richardson, 1973: Seasonal variability of the Florida Current. *J. Mar. Res.*, **31**, 144-166.

Inter-ocean Fluxes south of Africa in an Eddy-permitting Model

Juliet Hermes[1], Chris J.C. Reason[1], Johann R.E. Lutjeharms[1], and Arne Biastoch[2]
[1]EGS and Oceanography Departments, University of Cape Town, Rondebosch, South Africa
[2]Institut für Meereskunde, Universität Kiel Kiel, Germany
corresponding e-mail: jhermes@physci.uct.ac.za

Indian-Atlantic ocean water exchange south of Africa is an important component of the global thermohaline circulation. Evidence exists that variability in these exchanges, on both meso- and longer time scales, may significantly influence weather and climate patterns in southern Africa (e.g., Walker, 1990; Reason and Mulenga, 1999; Rouault et al., 2002). Observational estimates of the rate of mass and heat exchange between these oceans have varied and it has been difficult to verify these in any reliable manner. Results to date have been comprehensively reviewed by De Ruijter et al. (1999). Model based diagnostics of the inter-ocean fluxes are essential. As a first step in this direction, a model designed especially for the Agulhas system has been used in this initial study of the inter-ocean volume and heat fluxes and their seasonal to interannual variability (more details can be found in Reason et al., 2002).

Results were obtained from a 12 yr post spin up integration of the regional eddy permitting model, Agape of Biastoch and Krauß (1999) (more details can be found on http://www.ifm.uni-kiel.de/fb/fb1/tm/research/woce/agulhas/agape.html). The heat and volume fluxes are calculated from 5 year statistics after the spin-up.

The annual mean heat transport and net surface heat flux along various sections are plotted in Fig. 1.

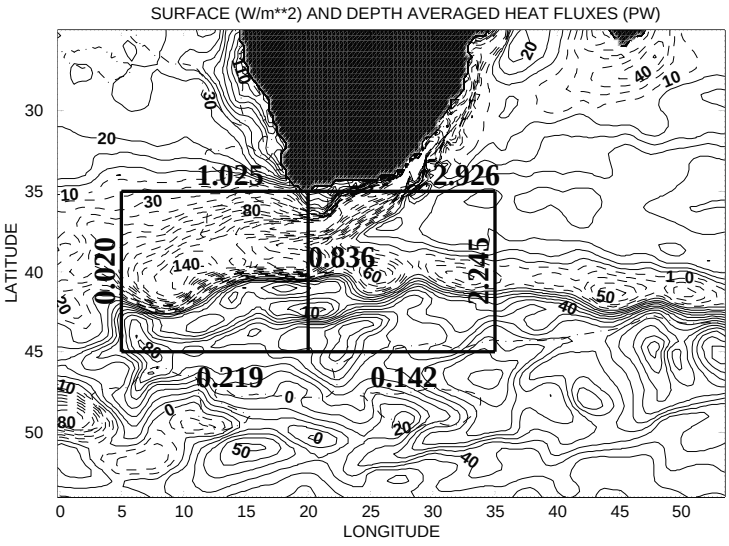

Fig. 1: The annual mean total heat transport (PW) and net surface heat flux (contour interval 10 Wm^{-2}) averaged over years 31-35 of the model integration.

There is a net westward transport through 20°E of 0.84 PW (Fig. 1) but this ranges from 1.3 PW westwards during the spring of year 32 to only about 0.35-0.5 PW west during each summer/autumn (Fig. 2). Even though the volume transport is sometimes eastwards, the net heat transport is always west into the SE Atlantic, due to the Agulhas Current water being much warmer than the water further south along this section. At 5°E the Agulhas transport is returned by the retroflection so that there is an eastward transport of 0.02 PW on the annual mean. However, eastward transport only occurs in summer and autumn, during winter and spring this transport is westwards. The model estimate of 1.03 PW flowing north along 35°S is larger than previous hydrographic estimates (0.02-0.47 PW – Gordon (1985)) and model calculations (0.51 PW – Thompson et al. (1997) and 0.6 PW – Semtner and Chervin (1992)), but these models omitted factors such as the Indonesian Throughflow and the Mozambique Channel flow.

In terms of the volume transport, the annual mean transport into the SE Atlantic is around 2.9 Sv through 20°E and about 15.5 Sv through 35°S. Much of this flow re-circulates so that only about 0.3 Sv escapes into the SE Atlantic west of 5°E. Substantial variability does occur on monthly through to interannual time scales as shown in Figs. 2 and 3. In terms of volume flux, although the mean annual transport through 20°E is always to the west, it can vary with as much as 12 Sv flowing east from the SE Atlantic into the South Indian ocean during the summer of year 34 to almost 16 Sv west into the SE Atlantic during the winters of years 31 and 34. This corresponds to an annual mean heat transport of 0.84 PW going westward through 20°E (Fig 2a), but ranging from as much as 1.3 PW west into the SE Atlantic during spring of year 32 to only about 0.35-0.5 PW west during each summer/autumn (Fig. 2b). Note that figure 3a and b cover the latitude band of Fig. 2 in two separate parts.

The fluxes discussed above refer to both the eddy component and the mean current (including Agulhas rings). Estimates of the eddy variability (not rings) were made and reveal that along the section at 20°E there is a net west transport into the South Atlantic of 0.12 PW, as compared to the total westwards transport integrated along this section of 0.84 PW. These results suggest that in the model it is eddy variability associated with the southern Agulhas, and not rings, which significantly contribute to the heat transport into the South Atlantic.

Time series and spectra of the heat and volume transports at various locations in the region, obtained from years 31-43 of the integration were calculated and are shown in Fig. 3 a-c. Fig. 3a (sec-

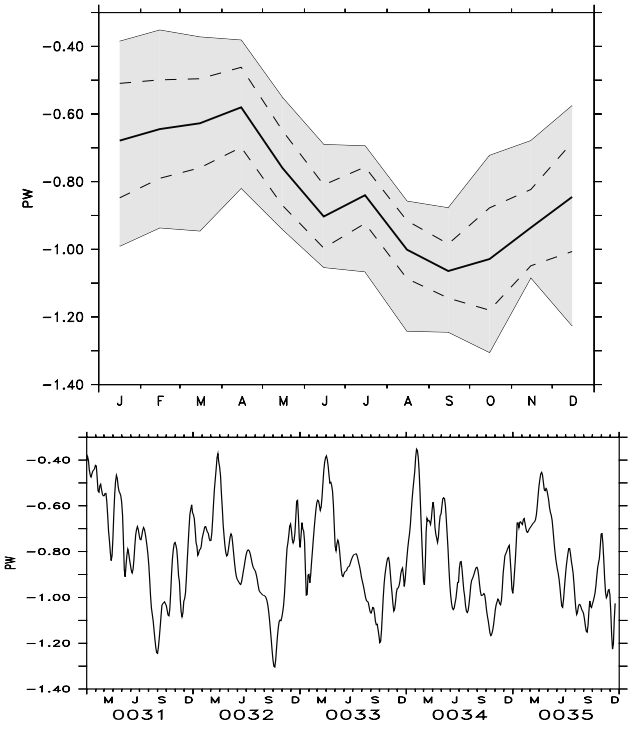

Fig. 2: Upper panel: Monthly mean heat transport (PW) (bold line) along 20°E between 45-35°S together with the maximum (upper line) and minimum (lower line) values and one standard deviation above and below the mean (stippled lines). Lower Panel: time series of this transport for years 31-35 of the integration.

tion of Agulhas Current) displays a peak at around 3 months, this is most likely to be associated with Agulhas ring shedding which occurs on this timescale. The semi-annual signal seen in Fig. 3b appears to be a feature of the Agulhas and Agulhas Return Current. Spectral energy at this timescale does not show up on the transports averaged along other sections (e.g. at 5°E). Whether this signal is derived from the Southern Hemisphere semi-annual oscillation in mid- to high latitude winds and surface pressure, or from that in the South Equatorial and East Madagascar Currents (Matano et al., 2002) is yet to be determined. Fig. 3c displays significant events that occur in the 5°E section that do not occur in the upstream sections. These result from seasonal variability in the longitudinal position of the Agulhas retroflection zone, which directly influences this section and leads to the dominating 12 month spectral peak. Meridional shifts also occur, contributing to the shifts in transport sign.

The model variability refers to only that generated internally through ocean processes since the monthly forcing is repeated each year. How the ocean variability might change when forced with the full spectrum of atmospheric variability is yet to be investigated. However, these initial results support suggestions from previous work that the southern Agulhas Current region is highly variable on meso-, seasonal and interannual timescales and they provide motivation for more thorough studies of this South Atlantic-Indian ocean exchange.

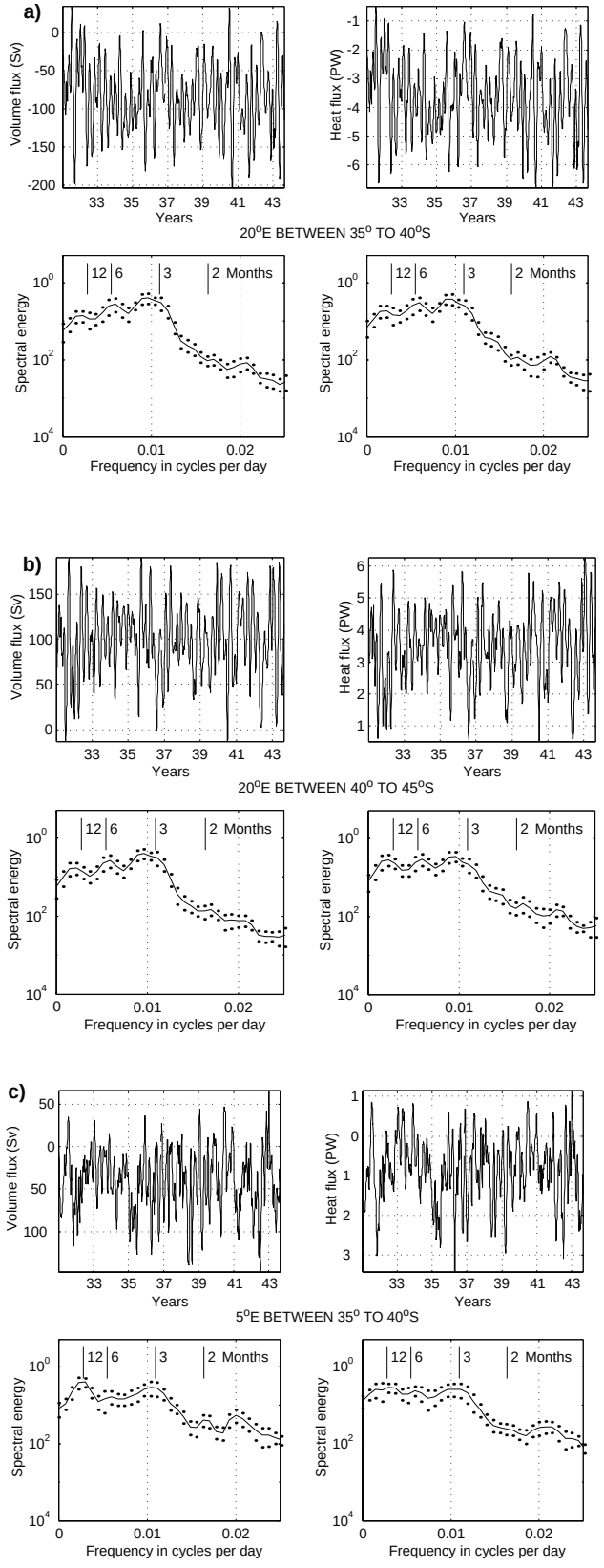

Fig. 3: Time series and normalised spectra of total heat and volume fluxes from years 31-43 of the model integration at (a) 20°E between 35 and 40°S, (b) 20°E between 40 and 45°S and (c) 5°E between 35 and 40°S. The diamonds indicate the 95 % confidence interval.

Acknowledgements

This research forms part of the author's PhD and has been supported by the Water Research Commission.

References

Biastoch, A., and W. Krauß, 1999: The role of mesoscale eddies in the source regions of the Agulhas Current. *J. Phys. Oceanogr.*, **29**, 2303-2317.

De Ruijter, W.P.M., A. Biastoch, S.S. Drijfhout, J.R.E. Lutjeharms, R.P. Matano, T. Pichevin, P.J. van Leeuwen, and W. Weijer, 1999: Indian-Atlantic inter-ocean exchange: dynamics, estimation and impact. *J. Geophys. Res.*, **104**, 20885-20911.

Gordon, A.L., 1985: Indian-Atlantic transfer of thermocline water at the Agulhas retroflection. *Science*, **227**, 1030-1033.

Matano, R.P., E.J. Beier, P.T. Strub, and R. Tokmakian, 2002: Large-scale forcing of the Agulhas variability: the seasonal cycle. *J. Phys. Oceanogr.*, **32** (4), 1228-1241.

Reason, C.J.C., J.R.E. Lutjeharms, J. Hermes, A. Biastoch, and R.E. Roman, 2002: Inter-ocean fluxes south of Africa in an eddy-permitting model. *Deep-Sea Res.*, in press.

Reason, C.J.C., and H. Mulenga 1999: Relationships between South African rainfall and SST anomalies in the Southwest Indian Ocean. *Int. J. Climatol.*, **19** (15), 1651-1673.

Rouault, M., S.A. White, C.J. C.Reason, J.R.E. Lutjeharms, and I. Jobard, 2002: Ocean-atmosphere interaction in the Agulhas Current and a South African Extreme weather event. *Weather and Forecasting*, **17** (4), 655-669.

Semtner Jr., A.J., and R.M. Chervin, 1992: Ocean general circulation from a global eddy-resolving model. *J. Geophys. Res.*, **97**, 5493-5550.

Thomson, S.R., D.P. Stevens, and K. Döös, 1997: The importance of interocean exchange south of Africa in a numerical model. *J. Geophys. Res.*, **102** (C2), 3303-3315.

Walker, N.D., 1990: Links between South African summer rainfall and temperature variability of the Agulhas and Benguela Current systems. *J. Geophys. Res.*, **95**, 3297-3319.

On the Leading Modes of Sea Surface Temperature Variability in the South Atlantic Ocean

Virginia Palastanga[1], Carolina S.Vera[1] and Alberto R. Piola[1,2]

[1] CIMA/Dept. of Atmospheric and Ocean Sciences, U. Buenos Aires-CONICET. Buenos Aires, Argentina

[2]Departamento Oceanografía, Servicio de Hidrografía Naval, Buenos Aires, Argentina

corresponding e-mail: carolina@at.fcen.uba.ar

Introduction

The variability of the sea surface temperature (SST) in the south Atlantic is not as well understood yet as in the North Atlantic. This in part is due to the fact that the data coverage in the South Atlantic is rather poor, especially south of 35°S. Because the South Atlantic plays a key role in the energy transport towards the North Atlantic and influences the climate over South America, a better understanding of the basin-scale SST variability is required. Several studies (Paegle and Mo, 2002, and references therein) have diagnosed strong links between rainfall variability over South America and SST conditions in the South Atlantic. Recently, Robertson et al. (2002) examined the atmospheric response to oceanic anomalies in the tropics and subtropics of the South Atlantic based on AGCM simulations and found strong, statistically significant signals on the atmospheric low-level circulation and precipitation on interannual time scales.

The availability of gridded SST datasets, which combine in situ observations with satellite data, have motivated the study of the main patterns of South Atlantic SST variability (Venegas et al., 1997 and 1998; Sterl and Hazeleger, 2002; Robertson et al., 2002; among others). However, the structure and variability of the leading modes are still controversial. The controversy arises around the existence of a tropical dipole structure and of a South Atlantic monopole. The disagreements might be explained by differences in the datasets, filtering techniques as well in the methods of climate pattern detection. Here we present a brief discussion of the leading modes of SST variability in the South Atlantic based on empirical orthogonal function (EOF) analyses of the observed SST anomalies. We show that the EOF analysis performed in time domain (T-EOF) is an efficient tool to isolate the SST leading patterns without requiring additional filtering. In contrast with the patterns based on EOF analyses performed in spatial domains (S-EOF), the T-EOF patterns emerge even using different time periods and different spatial domains.

Data and methods

The study area covers the South Atlantic between 50°S and the equator and between 70°W and 20°E. We use monthly mean SST fields from the NCEP-NCAR

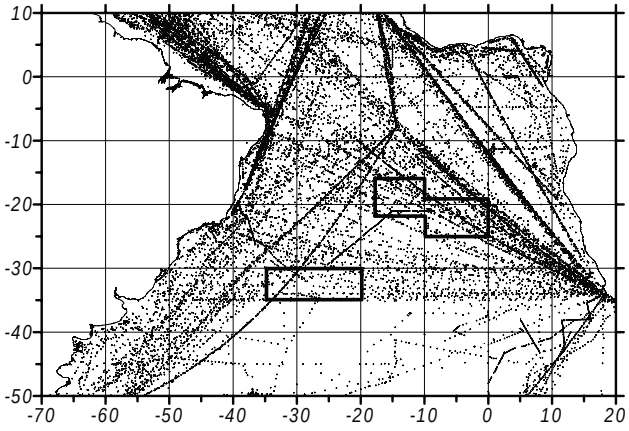

Fig 1: In situ SST observations available in the South Atlantic for the period 1990-2000. Boxes are defined in the text.

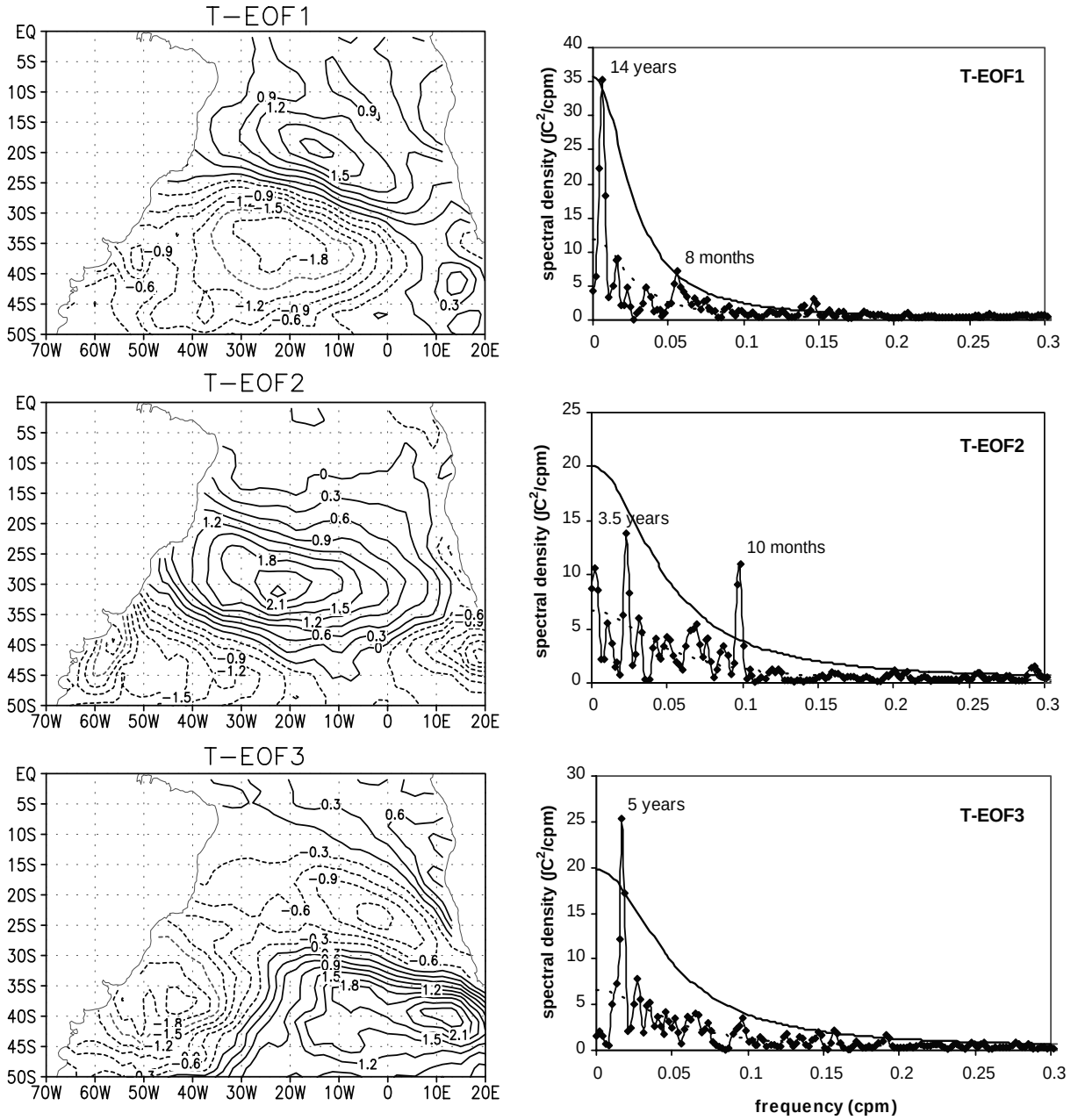

Fig. 2: (Left panels) principal components of the first three modes of the T-EOF analysis for the period 1972-2000. Contour interval is 0.3°C. (Right panels) spectra of the first three T-EOFs including expected red noise spectra (stippled) and 95% confident bands.

reanalysis (Kalnay et al., 1996). Prior to 1982, this dataset includes the 2.3b version of the Global Sea Ice and Sea Surface Temperature dataset (GISST) (Rayner et al., 1996). After that time, SSTs correspond to the Reynolds dataset that combines in situ and satellite data through an optimum interpolation analysis (Reynolds and Smith, 1994). Comparisons between GISST and Reynolds datasets showed that the GISST data exhibit spurious variability at mid and high latitudes of the South Atlantic, probably due to the poor performance of the interpolation method on very sparse data regions (Hurrell and Trenberth, 1999). Other datasets like the Comprehensive Ocean-Atmosphere Data Set (COADS) are also strongly affected by the lack of information south of 35°S (Fig. 1). Therefore, we study the period between 1 January 1972 and 31 December 2000, thus restricting the number of years without satellite information.

To determine the leading patterns of SST variability, the EOF analysis was performed in two different ways: i) S-EOFs are obtained from the EOF analysis computed in spatial domain. They represent spatial patterns while the corresponding principal components are time series; ii) T-EOFs are time series resulting from an EOF analysis in the time domain and the corresponding principal components are spatial fields. The latter seems to be more efficient in distributing the temporal variance in a few significant modes.

Leading SST patterns

The first three dominant SST patterns derived from the T-EOF analysis are displayed in Fig. 2, these patterns explain 19%, 10% and 8.5% of the variance respectively. T-EOF1 displays the typical north-south oriented dipole with dominant variability on interdecadal time scales. This pattern is recognized as the leading mode of SST variability in the South Atlantic and it is further discussed in the next section. T-EOF2 is characterized by a strong centre at around 20°W, 30°S and two centres of opposite-sign located south of Africa and along the South American coast, respectively. This is the only leading mode exhibiting a significant spectral peak on subannual time scales. These high-frequency SST variability centres are located over the most energetic regions of oceanic meso-scale variability in the South Atlantic, the Brazil-Malvinas confluence and the Agulhas retroflection (Chelton et al., 1990) . T-EOF3 exhibits an east-west dipole pattern at mid latitudes with significant variability at interannual time scales. This mode presents a large correlation with ENSO, being highest when the ENSO index leads T-EOF3 by 6 months.

S-EOFs computed for the same time period and domain (not shown) were computed. Only the leading S-EOF mode agrees with the corresponding T-EOFs, S-EOF1 exhibits a dipole structure similar to T-EOF1 and it resembles the pattern found in other studies which also computed S-EOFs based on different datasets and time periods (Robertson et al., 2002 and references therein). The leading S-EOF shows variability in interdecadal and interannual time scales. This explains why to obtain the interdecadal signal in previous studies it was necessary to low-pass filter the SST anomalies (Venegas et al., 1997, Sterl and Hazeleger, 2002, among others).

Our results show that the EOF analysis performed in the time domain is useful to isolate the interdecadal variability, without filtering and also to determine leading modes associated with independent spectral peaks.

The South Atlantic dipole

The dipolar structure that characterizes the leading mode of SST variability in the South Atlantic is a very robust pattern. The VARIMAX rotation method was applied to compute rotated EOFs based on both S-EOFs and T-EOFs and the dipole structure remained as the leading mode. To evaluate the existence of the dipole in the dataset for the pre-satellite period, a complementary study was carried out. We wish to determine the impact of the reduced data coverage in the mid-latitude South Atlantic on the dipole representation. The leading T-EOF for the period 1964-1981 shows the expected dipole structure at interdecadal time scales although the spectral peak is found around 18 years (Fig. 3a). However, the leading S-EOF mode for the same period is characterized by a monopole pattern extending over the entire domain, with dominant interannual variability (Fig. 3b), while the interdecadal dipole pattern appears as the second leading mode. Venegas et al. (1997) obtained the same two first modes applying the S-EOF analysis to the COADS dataset. Moreover, Dommenget and Latif (2000) identified a similar leading monopole pattern over the tropical Atlantic. The existence of the South Atlantic monopole is questionable, as it seems to be influenced by the inhomogeneous distribution of in-situ observations in the South Atlantic (Fig. 1). In contrast, the uneven data configuration does not appear to significantly affect the results of the T-EOF analysis.

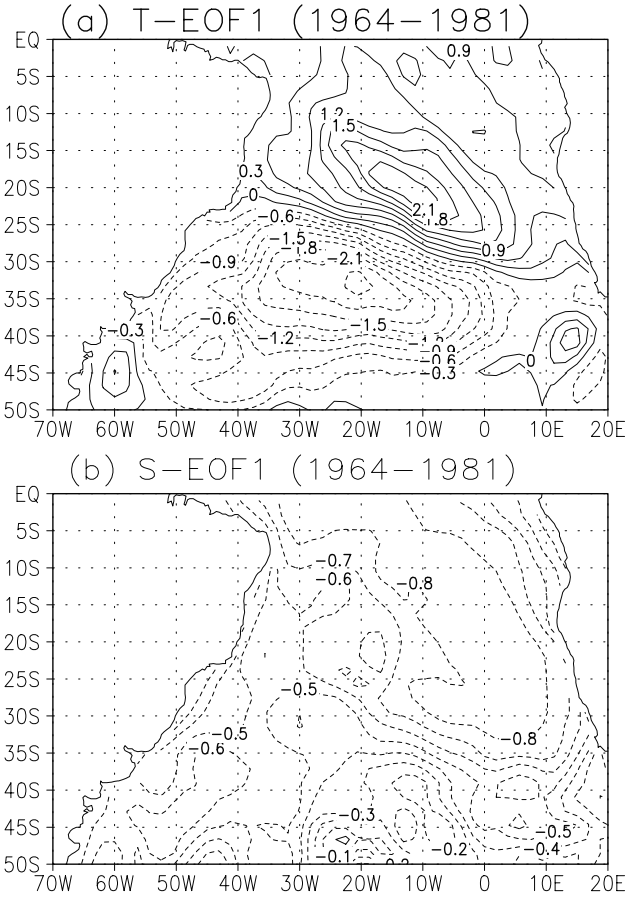

Fig. 3: Leading modes for the 1964-1981 period based on (a) T- EOF and (b) S-EOF, analysis respectively. Contour interval is (a) 0.3°C and (b) 0.1.

It is noticeable that the tropical action center of the South Atlantic dipole covers the region which some studies identified as the tropical South Atlantic mode (Dommenget and Latif, 2000 and references therein). Although a leading dipole pattern across the equator emerges from an S-EOF analysis performed over the tropical Atlantic, Mestas-Nuñez and Enfield (1999), Dommenget and Latif (2000), and others, have questioned its existence and concluded that the centres of action across the equator present almost independent variability.

To test the performance of EOF analysis in the time domain in determining the Atlantic tropical dipole structure, T-EOF analysis was made between 30°S and 30°N.

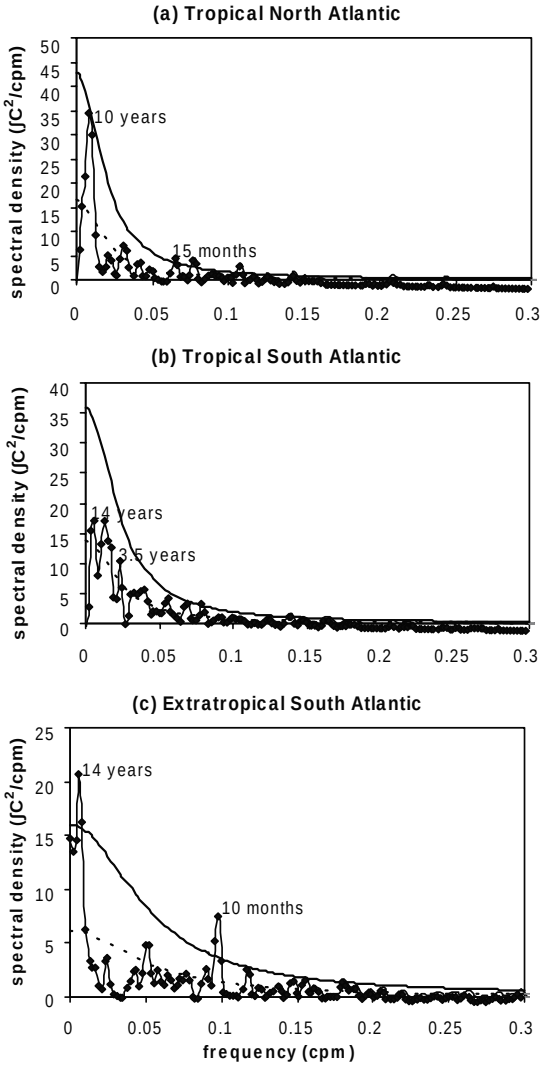

Fig. 4: Spectra of the SST time series for (a) tropical North Atlantic center, (b) Tropical South Atlantic center and (c) Extratropical South Atlantic center. Expected red noise spectra (stippled) and 95% confidence lines are included.

Both the unrotated and rotated leading T-EOF resemble the dipole pattern across the equator with marginally significant variability on interdecadal time-scales.

In addition, for the period 1972-2000, we analysed the SST anomaly time-series in the three main centres of action found in the Atlantic basin. Two regions were selected in the South Atlantic (Fig. 1), which correspond to the tropical and extra-tropical centres found in T-EOF1 (Fig. 2). A third region was selected in the North Atlantic, over the centre of the tropical dipole. The latter is bounded by 35ºW-19ºW, 22ºN-15ºN (not shown).

The tropical North Atlantic variability exhibits a peak at around 10 years, which is close to the 95% confidence level. The South Atlantic regions show the maximum variability at around 14 years. However, only the spectral amplitude for the extra-tropical region is significant at the 95% confidence level (Fig. 4).

While Dommenget and Latif (2000) have shown that SST anomalies at the two tropical centres are not significantly correlated, Sterl and Hazeleger (2002) found significant correlation between the SST anomalies of the two South Atlantic centres. In order to explore whether there is any frequency range for which SSTs in the three regions are significantly correlated, we computed the cross spectra, phase and coherence between each of the SST anomaly time series. The cross spectrum between the SST anomalies representing the South Atlantic dipole shows a well-defined, significant peak at around 14 years. These observations suggest that the dipolar structure is a real physical mode of South Atlantic SST variability.

The SST cross spectrum for the cross-equatorial centres of action shows a marginally significant peak at around 14 years. Fig. 4 shows that although the tropical South Atlantic SSTs exhibits variability at around that period, the tropical North Atlantic SSTs do not. Therefore, in agreement with Mestas-Nuñez and Enfield (1999), Dommenget and Latif (2000), and references therein, the tropical Atlantic dipole does not appear to be a physical pattern of the SST variability at interannual time scales.

References

Chelton, D.B., M.G. Schlax, D.L. Witter, and J.G. Richman, 1990: Geosat altimeter observations of the surface circulation of the southern ocean. *J. Geophys. Res.,* **95**, 17877-17903.

Dommenget, D., and M. Latif, 2000: Interannual to decadal variability in the Tropical Atlantic. *J. Climate.,* **13**, 777-792.

Kalnay, E., M. Kanamitsu, R. Kistler, W. Collins, D. Deaven, L. Gandin, M. Iredell, S. Saha, G. White, J. Woollen, Y. Zhu, A. Leetmaa, B. Reynolds, M. Chelliah, W. Ebisuzaki, W. Higgins, J. Janowiak, K.C. Mo, C. Ropelewski, J. Wang, Roy Jenne, and D. Joseph, 1996: The NCEP/NCAR 40-year reanalysis project. *Bull. Amer. Meteor. Soc*., **77**, 437-471.

Hurrell, J.W., and K.E.Trenberth, 1999: Global sea surface temperature analyses: Multiple problems and their implications for Climate Analysis, Modeling and Reanalysis. *Bull. Amer. Meteor. Soc*, **80**, 2661-2678.

Mestas-Nuñez, A.M., and D.B. Enfield, 1999: Rotated global modes of non-ENSO sea surface temperature variability. *J. Climate,* **12**, 2734-2746.

Paegle, J.N., and K.C. Mo, 2002: Linkages between Summer Rainfall Variability over South America and Sea Surface Temperature Anomalies. *J. Climate*, **15**, 1389–1407.

Rayner, N.A., E.B. Horton, D.E. Parker, C.K. Folland, and R.B. Hackett, 1996: Version 2.2 of the Global Sea-Ice and Sea Surface Temperature Data Set, 1903-1994. *Clim. Res. Tech. Note* **74**, Meteorological Office, Bracknell, UK., 21 pp. plus figures.

Reynolds, R.W., and T.M. Smith, 1994: Improved global sea surface temperature analysis using optimum interpolation. *J. Climate*, **7**, 929-948.

Robertson, A.W., J.D. Farrara, and C.R. Mechoso, 2002: Simulations of the atmospheric response to South Atlantic sea surface temperature anomalies. *J. Climate*, submitted.

Sterl, A., and W. Hazeleger, 2001: Patterns and wmechanisms of air-sea interaction in the South Atlantic Ocean. *J. Climate*, submitted.

Venegas, S.A., L.A. Mysak, and D.N. Straub, 1997: Atmosphere-ocean coupled variability in the South Atlantic. *J. Climate*, **10**, 2904-2920.

Venegas, S.A., L.A. Mysak, and D.N. Straub, 1998: An interdecadal climate cycle in the South Atlantic and its links to other basins. *J. Geophys. Res.*, **103**, C11, 24723-24736.

Links between the Atlantic Ocean and South American Climate Variability

Andrew W. Robertson[1] and Carlos R. Mechoso[2]
[1]International Research Institute for Climate Prediction, Palisades, NY, USA
[2]Dept. of Atmospheric Sciences, University of California, Los Angeles, CA, USA
corresponding e-mail: awr@iri.columbia.edu

1. Introduction

Hopes for seasonal-to-interannual climate prediction over South America are currently largely pinned on the influence of the Pacific and Atlantic Oceans on the atmospheric circulation over the continent. Here we focus on the influence of the Atlantic anomalies on precipitation during the austral summer when the South American Monsoon System (SAMS) is active.

SAMS precipitation variability can be divided roughly into two components: (1) a near-equatorial one associated with the Atlantic Intertropical Convergence Zone (ITCZ) and convection over Amazonia, and (2) a subtropical one associated with the South Atlantic Convergence Zone (SACZ) and related circulation features over the Pampas and SE South America. Each of these components involves a maritime atmospheric convergence zone together with continental convection, thus linking climate variability of the Atlantic Ocean with that over South America. This short article highlights selected aspects of the linkages between interannual climate variability over the Atlantic and South America, and thus underscores the synergy between the climate programmes centred on each one. Our emphasis is on societally important hydrological aspects: droughts and river flows.

2. Equatorial variability

The influence of equatorial Atlantic sea surface temperatures (SSTs) on droughts over NE Brazil is well documented (Hastenrath and Heller, 1977; Moura and Shukla, 1981; Mechoso and Lyons, 1988; Mechoso et al., 1990): droughts occur when the southward seasonal migration of the ITCZ to its southernmost position in March–April is reduced due to anomalously warm (cold) SST anomalies over the tropical North (South) Atlantic, as well as to the direct Walker Cell-like influence of ENSO. The complex way in which ENSO interacts with the tropical Atlantic is not yet well understood. It has recently been proposed that the meridional gradient of SST between the tropical North Atlantic (TNA) and the tropical South Atlantic (TSA) acts as a preconditioner on the direct ENSO impact on NE Brazil rainfall (Giannini et al., 2001). While most studies have focused on rainfall variability over NE Brazil, recent work suggests potentially useful one-year-ahead predictability of river flow in the Oros river, based on an empirical model with Niño-3, TSA and TNA SSTs as predictors (De Souza Filho and Lall, 2002).

The relationship between NE Brazil rainfall and the Atlantic Ocean appears rather confined to coastal regions, and a major challenge is to identify useful predictable relationships between the broader-scale SAMS and the Atlantic. A major limitation to progress is the lack of long reliable records of precipitation. Riverflow records provide a valuable climate dataset, particularly for the Paraná-Paraguay rivers. These have their sources near 15°S and flow southward to the Plata estuary and have reliable records since the early 1900s. As shown in Fig. 1, these records contain a statistically significant cycle at about 8 years (Robertson and Mechoso, 1998) whose period and phase closely match the near decadal cycle present in the North Atlantic Oscillation (NAO) (Robertson, 2001); each accounts for about 15% of the interannual variance. This covariability between the boreal winter NAO and the austral summer SAMS is intriguing. When SSTs are correlated with the 8-yr riverflow cycle, the typical NAO tripole signature in SST becomes clear (Fig. 2, page 35). The cold SST anomalies over the TNA that accompany enhanced river flows and a positive NAO suggest that an enhancement of the

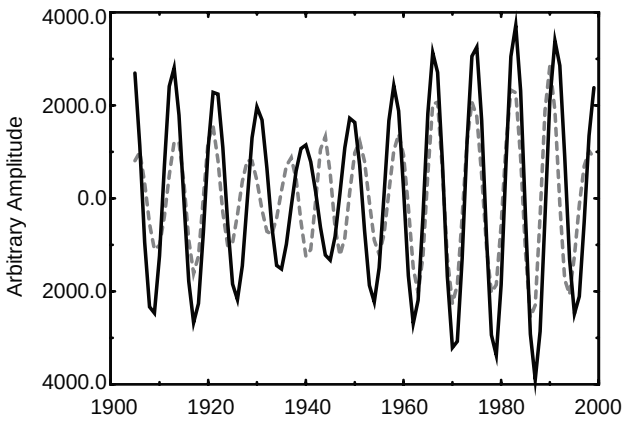

Fig. 1: Leading oscillatory component of NAO (stippled, grey) and Paraná river (at Corrientes, black) timeseries, computed using Singular Spectrum Analysis (SSA) for each case with a window of 30 years. December–March averages.

strength of the NE Trade winds over the tropical Atlantic may flux additional moisture into South America, which is then advected southward by the South American low-level jet, another component of SAMS. The NCEP/NCAR reanalysis data does provide some support for this conjecture (Nogues-Paegle et al., 2000), but the atmospheric record is too short and incomplete to distinguish this scenario from the alternatives, namely that a common forcing is simply reflected in both series or, indeed, that the Southern Hemisphere is forcing the North (Robertson et al., 2000).

3. Subtropical Variability

Variability of the SACZ dominates the atmospheric circulation over SE South America between about 20-40°S during austral summer. Most basically, the SACZ exists in association with the southward transport of moisture from the tropics around the western margin of the subtropical anticyclone over the South Atlantic (Kodama, 1993). Fig. 3 (page 35) shows the leading interannual principal component of upper-tropospheric Reanalysis winds, regressed onto (a) 850-hPa winds and 500-hPa omega vertical velocity, and (b) SST. This leading mode of circulation variability consists of an isolated Rossby wave with a dipole in the vertical motion field that reflects interannual changes in the intensity of the SACZ and "compensating" descent over the Pampas to the southwest (Robertson and Mechoso, 2000). Note that the low-level wind anomalies are such as to reinforce the vertical motion anomalies through low-level advection of heat and moisture.

This mode of variability is highly correlated with dipolar SST anomalies over the South Atlantic (Fig. 3b), with *cold* anomalies in the subtropics tending to accompany an intensified SACZ. Similar findings have been reported by Barros et al. (2000), while Diaz et al. (1998) have shown that interannual rainfall variability over Uruguay is correlated with a similar pattern of SST anomalies during austral summer. Since Uruguay lies under the southern pole of the omega dipole in Fig. 3a, dryer conditions are correlated with the SST pattern in Fig. 3b.

Fig. 3 does not show the SST-omega relationship that we would expect for subtropical SST anomalies forcing the accompanying variations in the SACZ. One could argue that the SACZ variations are forcing variations in the SST below, with enhanced cloudiness leading to cold anomalies. However, the covariability with SST is complex, and surface fluxes of heat computed from the Reanalysis data do not show a coherent relationship.

Fig. 4 (page 36) shows the response of the UCLA atmospheric general circulation model to prescribing the SST anomaly in Fig. 3b. A statistically significant response is found in low-level circulation and precipitation. The GCM is able to capture the same broad circulation anomaly pattern seen in Fig. 3, but is of the opposite polarity to the observed one. This circulation pattern does extend into the continent, although statistically significant rainfall anomalies are largely over the ocean. Quite similar findings are also reported by Barreiro et al. (2002) from an ensemble of long simulations with the CCM3 model. The implication of these GCM studies is that atmospheric predictability associated SST anomalies over the subtropical South Atlantic is low.

4. Conclusions

The main linkages we have highlighted between the Atlantic Ocean and climate variability over South America, illustrated in Fig. 5 (page 36) are:

- Changes in ITCZ position and intensity, affecting continental convection through large-scale ascent and low-level moisture advection by the NE Trades. Influence of changes in cross-equatorial SST gradient, resulting from local and remote (ENSO, NAO) processes. NAO influence seen at 8-yr period.
- Changes in SACZ position and intensity, reflected in SST anomalies over the SW Atlantic. Large intrinsic interannual variability of the SACZ, modulated by ENSO, imprinted on Atlantic SST. Potential role for South Atlantic processes through changes in the strength and position of the subtropical anticyclone, or changes in ocean currents in the Brazil-Malvinas confluence region. Common spectral peak near 17 years.

An issue of concern for a better understanding of Atlantic-South American climatic linkages is the relative insensitivity of GCM-simulated rainfall anomalies over the continent that arise from interannual Atlantic SST anomalies. It is unclear to what extent this insensitivity is real, or whether it stems from inadequacies in the models over land.

5. References

Barreiro, M., P. Chang, and R. Saravanan, 2002: Variability of the South Atlantic Convergence zone simulated by an atmospheric general circulation model. *J. Climate,* **15**, 745-763.

Barros V., M. Gonzalez, B. Liebmann, and I. Camilloni, 2000: Influence of the South Atlantic convergence zone and South Atlantic Sea surface temperature on interannual summer rainfall variability in Southeastern South America. *Theor. Appl. Climatol.*, **67**, 123-133.

Diaz, A.F., C.D. Studzinski, and C.R. Mechoso, 1998: Relationships between precipitation anomalies in Uruguay and Southern Brazil and sea surface temperatures in the Pacific and Atlantic oceans. *J. Climate,* **11**, 251-271.

De Souza Filho, F.A., and U. Lall, 2002: Seasonal to interannual ensemble streamflow forecasts for Ceara, Brazil: Applications of a multivariate semi-parametric algorithm. *Water Resources Res.*, in press.

Giannini, A., J.C.H. Chiang, M.A. Cane, Y. Kushnir, and R. Seager, 2001: The ENSO teleconnection to the tropical Atlantic Ocean: Contributions of the remote and local SSTs to rainfall variability in the tropical Americas. *J. Climate*, **14**, 4530-4544.

Hastenrath, S., and L. Heller, 1977: Dynamics of climate hazards in Northeast Brazil. *Quart. J. Roy. Meteor. Soc.*, **103**, 77-92.

Kodama, Y.-M., 1993: Large-scale common features of subtropical precipitation zones (the Baiu frontal zone, the SPCZ, the SACZ) Part II: Conditions of the circulations for generating the STCZs. *J. Meteor. Soc. Japan*, **71**, 581-610.

Mechoso, C.R., and S.W. Lyons, 1988: On the atmospheric response to SST anomalies associated with the Atlantic warm event during 1984. *J. Climate*, **1**, 422-428.

Mechoso, C.R., S.W. Lyons, and J.A. Spahr, 1990: The impact of sea surface temperature anomalies on the rainfall over northeast Brazil. *J. Climate*, **3**, 812-826

Moura, A.D., and J. Shukla, 1981: On the dynamics of droughts in Northeast Brazil: Observations, theory and numerical experiments with a general circulation model. *J. Atmos. Sci.*, **38**, 2653-2675.

Nogues-Paegle, J., A.W. Robertson, C.R. Mechoso, 2000: Relationship between the North Atlantic Oscillation and river flow regimes of South America. Proc. 25th Climate Diagnostics and Prediction Workshop, Palisades, NY, 23-27 October, 2000, 323-326.

Robertson, A.W., 2001: On the influence of ocean-atmosphere interaction on the Arctic Oscillation in two general circulation models. *J. Climate*, **14**, 3240-3254.

Robertson, A.W., and C.R. Mechoso, 1998: Interannual and decadal cycles in river flows of southeastern South America. *J. Climate*, **11**, 2570-2581.

Robertson, A.W., and C.R. Mechoso, 2000: Interannual and interdecadal variability of the South Atlantic convergence zone. *Mon. Wea. Rev.*, **128**, 2947-2957.

Robertson, A.W., C.R. Mechoso, and Y.-J. Kim, 2000: The influence of Atlantic sea surface tempearature on the North Atlantic Oscillation. *J. Climate*, **13**, 122-138

Observing the Tropical Instability Waves in the Atlantic Ocean

Markus Jochum[1], Paola Malanotte-Rizzoli[1], Antonio Busalacchi[2], and Nelson Hogg[3]
[1]Massachusetts Institute of Technology, Earth, Atmospheric and Planetary Sciences, Cambridge, MA, USA
[2]Earth System Science Interdisciplinary Center, University of Maryland, College Park, MD, USA
[3]Woods Hole Oceanographic Institution Woods Hole, MA, USA
corresponding e-mail: mjochum@mit.edu

Introduction

Tropical Instability Waves (TIW) have first been observed by Legeckis (1977); they can been detected in the Pacific and Atlantic Oceans by their associated SST anomalies (see Fig. 1, page 36) and are generated in the equatorial mixed layer by shear instabilities of the equatorial current system. Their period is between 20 and 40 days and their wavelength is of the order of 1000km (Legeckis (1977) and Weisberg and Weingartner (1988)). Hansen and Paul (1984) and Bryden and Brady (1989) show that the equatorward heat flux of the TIW exceeds the atmospheric heat flux at the equator. Thus, the position and strength of the equatorial cold tongue is sensitive to the structure of the TIW.

More recently, Masina et al. (1999) analyzed the dynamics of the TIW and showed that they can radiate energy from the surface into the deep ocean. Chelton et al. (2001) discuss how the TIW affect the coupling between the ocean and the atmosphere in the eastern Pacific. For the Atlantic, Foltz et al. (2002) analyzed their associated crossequatorial mass transport, and Jochum (2002) showed in an idealized numerical study that the TIW drive the Tsuchiya Jets, a pair of equatorial subthermocline countercurrents.

Although the TIW seem to be of critical importance to the equatorial dynamics, they are only poorly observed. Most of what is known about their properties is inferred from numerical models and to our knowledge no systematic study of their observed off-equatorial subsurface structure has yet been done. This report describes a research strategy for the Atlantic Ocean TIW to evaluate the subsurface structure of the TIW and their contribution to the equatorward heat flux, the oceanic variability and the mean circulation.

The Observations

The proposed work is based on the existing PIRATA mooring array and its recently proposed extension. The PIRATA array consists of a set of 11 ATLAS buoys along the equator and along 38°W and 10°W and two equatorial ADCP moorings at 23°W and 10°W. The proposed extension includes one subsurface and two surface moorings along 20°W. The assumptions that enter the following discussion are based on an idealized numerical simulation of the tropical Atlantic and have to be verified with the help of more realistic models. However, we believe that the qualitative aspects of our numerical study are robust and can help to assess the feasibility of an observational programme. There are three important questions for the understanding of the TIW and their associated heat flux, all of which can be answered with data of the programmes above:

- What is the subsurface structure of the TIW and its associated free waves, and how much energy is radiated into the deep ocean by these waves?
  Masina et al.'s (1999) results, as well as ours, suggest that the TIW induces Yanai waves with an eastward and downward group velocity and first meridional mode Rossby waves with a westward and downward group velocity. This is a fairly robust re-

sult because within the time and length scales of the TIW these are the only available free waves. The two already operational equatorial ADCPs at 23°W and 10°W are sufficient to decompose the velocity signal into the relevant modes and determine the distribution of energy between them. Furthermore, in connection with satellite based altimetry these ADCPs allow to establish a connection between the easily observable surface expression of the TIW and their subsurface structure.

- Are the Tsuchiya Jets indeed maintained against friction by the Eliassen-Palm flux of the TIW as suggested by Jochum (2002)?
  The work of Jochum (2002) implies that the dominant balance in the core of the Tsuchiya Jet is between frictional shear stress and vertical divergence of meridional eddy heat flux ($k_z\, u_{zz} \approx (1/(T_z)) \bullet \overline{(v'T')}_z$). The proposed current meter mooring at 20°W/5°S would in principle be able to verify this hypothesis. There are only two practical concerns: A priori the location of the jets core is not known, and the time series that is needed to obtain a statistically significant mean for $v'T'$ might be unreasonably long. The numerical results, however, suggest that throughout most of the year a single meridional velocity section is an excellent indicator for the position of the Tsuchiya Jet core. An exception is the summer, where at 20°W the Tsuchiya Jet is masked by seasonal Rossby waves. The model also suggests that a one year time series of temperature and velocity is sufficient to estimate $v'T'$ with an accuracy of 30% at a confidence level of 90%.
- What is the TIW's contribution to the meridional heat flux and its divergence south of the equator?
  While the equatorial ADCP at 23°W and the subsurface mooring at 20°W/5°S are in principle able to provide the required data, the model results suggests that at 150m depth at the equator at least a two year time series is required to estimate the meridional eddy heat flux with an accuracy of 30%. This is much longer than at 5°S because of the much stronger seasonal cycle at the equator. The experience of Bryden and Brady (1989) in the equatorial Pacific also suggest that one year is a minimum duration for an equatorial mooring to obtain heat fluxes that are significantly different from zero. Thus, it is desirable to deploy the subsurface mooring at 5°S and the ADCP at the equator for a duration of 2 years to enhance the PIRATA observations with an estimate of the eddy heat flux which is expected to be several times larger than the ocean-atmosphere heat exchange (Bryden and Brady (1989)).

Although PIRATA has not been designed to analyze TIW, it is possible to answer the three questions above within the already existing PIRATA programme and its proposed extension; but the design of the programmes allows to determine only the basic structure of the TIW. It is not possible with the current design to determine the eddy momentum flux divergence of the TIW and it is difficult to determine their eddy heat flux divergence, both of which are of major importance for the equatorial circulation (Hansen and Paul (1984) and Bryden and Brady (1989)). It takes, however, only minor additions to PIRATA to correct for this. Since all the studies that the authors are aware of show that in the central equatorial Atlantic the zonal divergences of heat and momentum transport are negligible, only two additional subsurface moorings at 20°W, one between the equator and 5°S and one south of 5°S, would provide the unique opportunity to determine the complete momentum and heat budget south of the equator.

Acknowledgments

The computations have been performed at NCAR facilities in Boulder, CO. This research was funded with NOAA grant No.: NA16GP1576.

References

Bryden, H.L., and E.C. Brady, 1989: Eddy momentum and heat fluxes and their effects on the circulation of the equatorial Pacific ocean. *J. Mar. Res*., **47**, 55-79.

Chelton, D.B., S.K. Esbensen, M.G. Schlax, N. Thum, M.H. Freilich, F.J. Wentz, C.L. Gentemann, M.J. McPhaden, and P.S. Schopf, 2001: Observations of coupling between surface wind stress and sea surface temperature in the eastern Tropical Pacific. *J. Climate*, **14**, 1479-1498.

Foltz, G., J.A. Carton, and E. Chassignet, 2002: Vortices in the tropical Atlantic Ocean. *Unpublished manuscript*.

Hansen, D.V., and C.A. Paul, 1984: Genesis and effects of long waves in the equatorial Pacific. *J. Geophys. Res*., **89**, 10431-10440.

Jochum, M., 2002: On the pathways of the return flow of the meridional overturning circulation in the tropical Atlantic. Ph.D. thesis, Massachusetts Institute of Technology, Cambridge, USA.

Legeckis, R., 1977: Long waves in the eastern equatorial Pacific ocean: A view from a geostationary satellite. *Science*, **197**, 1179-1181.

Masina, S., S.G.H. Philander, and A.B.G. Bush, 1999: An analysis of tropical instability waves in a numerical model of the Pacific Ocean - 2. Generation and energetics of the waves. *J. Geophys.Res*., **104**, 29613-29635.

Weisberg, R.H., and T.J. Weingartner, 1988: Instability Waves in the equatorial Atlantic Ocean. *J. Phys. Oceanogr*., **18**, 1641-1657.

Searching for the Role of ENSO in Tropical Atlantic Variability using a Coupled GCM[&]

Lixin Wu, Qiong Zhang, and Zhengyu Liu
Center for Climatic Research
University of Wisconsin-Madison, Madison, WI, USA
corresponding e-mail: lixinwu@facstaff.wisc.edu

1. Introduction

Sea surface temperature (SST) in the tropical Atlantic ocean exhibits distinct variability at interannual and decadal timescales (e.g. Nobre and Shukla, 1996). One of the key questions about tropical Atlantic variability (TAV) concerns its origins. Some studies suggest that local ocean-atmosphere interaction plays a dominant role in the generation of TAV (e.g. Chang et al., 1997). Other studies, however, suggest that the TAV may be triggered by the Pacific ENSO (e.g. Curtis and Hastenrath, 1995; Enfield and Mayer, 1997; Saravanan and Chang, 2000; Chiang et al., 2000; Mo and Hakkiken, 2001), and/or by the North Atlantic Oscillation (e.g. Xie and Tanimoto, 1998; Grötzner et al., 1998; Yang, 1999). A recent study suggests that SST variability in the North Tropical Atlantic (NTA) is largely a response to remote ENSO and NAO forcing while the role of local ocean-atmosphere coupling and oceanic dynamics is negligible (Czaja et al., 2002). These studies have focused mostly on the analysis of climate variability in observations or model control simulations, and, therefore, it is difficult to isolate the direct cause of the variability, because the climate is already the final product of complex feedbacks.

In this letter, the role of ENSO in the generation of TAV is assessed in a set of coupled ocean-atmosphere sensitivity experiments using a partial coupling (PC) approach. We will show that ENSO predominantly dictates the temporal evolution of TAV at interannual timescales, and can enhance SST variability in both the South and North Tropical as well as the Equatorial Atlantic substantially. However, the influence of this remote forcing is strongly associated with local ocean-atmosphere feedback and will be much less effective if this feedback is absent.

2. TAV and ENSO: The Control Experiment

We used the Fast Ocean-Atmosphere Model (FOAM1.0) for the simulations (Jacob, 1997). The AGCM is the fully parallel version of the NCAR CCM2 (R15), with the atmospheric physics replaced by those of CCM3; the OGCM is developed following the GFDL MOM with a horizontal resolution of 2.8°-longitude, 1.4°-latitude, 16 vertical levels. Without flux adjustment, the model has been integrated for 850 years, and exhibits a stable mean climate (Jacob, 1997). Here we used the last 350-years of monthly data for analysis.

Both ENSO and TAV are reasonably reproduced in the FOAM control simulation (CTRL) (Liu et al., 2000; Liu and Wu, 2000). Over the Pacific, the leading EOF mode captures the major features of the observed ENSO; the area-weighted pattern correlation between the model and observed EOFs of ENSO is 0.82 (Fig. 1 of Liu et al., 2000). The power spectrum of the Niño3 SST index shows a dominant interannual peak at about 4-years (Fig. 1a1). Overall, FOAM simulates a reasonable ENSO variability, with a realistic time-scale and an amplitude of about 75% of the observed ENSO. Over the tropical Atlantic, the leading two EOFs show a pattern with a uniform polarity and a dipole-like pattern flanking the equator, respectively; the leading two rotated EOFs, however, show a South Tropical Atlantic (STA) and a North Tropical Atlantic (NTA) mode, separately (Liu and Wu, 2000). There is also an Equatorial Atlantic (EQA) mode in the model (not shown), which is analogous to the ENSO in the equatorial Pacific (Zebiak, 1993; Latif and Grötzner, 2000). All three of these modes exhibit significant interannual variability with timescales around 4-years, as shown by the power spectrum of the EQA, NTA and STA SST indices, respectively (Fig. 1b1, c1, d1). There is also some decadal to multidecadal variability, but we focus on the interannual timescales.

The TAV seems to be associated with ENSO in the model. The squared coherence spectrum of the Niño3 SST with the NTA, EQA and STA SSTs shows that these three tropical Atlantic modes are highly correlated with ENSO at interannual time scales (~ 4-yr) (Fig. 2) with a lag of 3, 6 and 4 months, respectively (not shown). The correlation of SST, surface wind stress and surface heat flux in the tropical Atlantic against the Niño3 SST during the boreal spring season (FMA: February-March-April) further displays the linkage between ENSO and TAV (Fig. 3) (the lagged correlation of SST for the FMA season with the DJF Niño3 SST index remains broadly similar). The SST correlation reproduces major features of observations as noted by Enfield and Mayer (1997), with broad warming in both the NTA and STA, although the warming in the STA is somewhat stronger in the model than the observations. The surface wind anomalies are characterized by anomalous southwest trades in the NTA, easterlies in the central equatorial Atlantic and southeast trades in the STA. The warming in the northwestern tropical Atlantic seems to be directly caused by an enhancement of downward heat flux due to the weakening of the northeast trades. In the equatorial Atlantic, the ocean gains heat from the atmosphere although the equatorial easterly wind is enhanced, and warming appears with a lag of 6 months after ENSO. This suggests the potential role of equatorial oceanic dynamics on the generation of local SST variations. In the model, the delayed response (6 months) of the EQA SST to ENSO seems to be caused by equatorial wave dynamics as pro-

[&] CCR contribution number 808

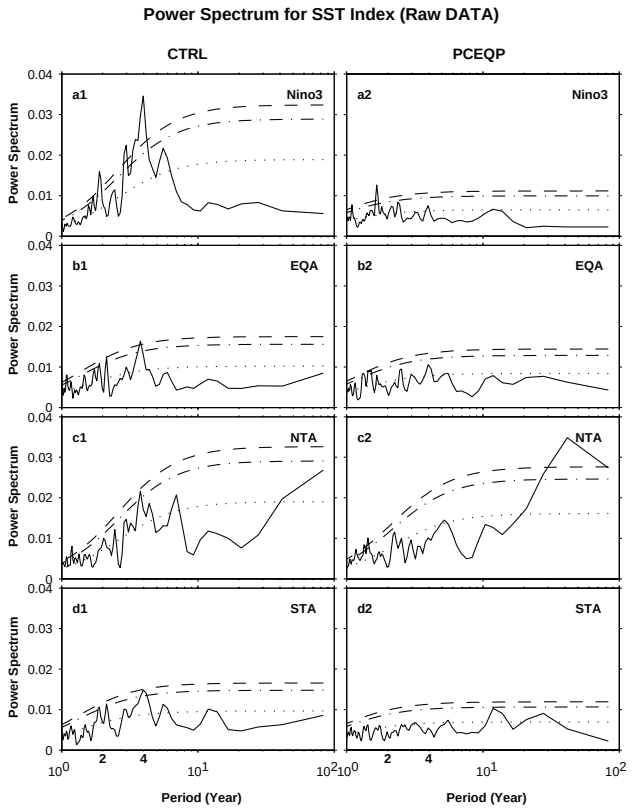

Fig. 1: Power spectrum of the Niño3, NTA, EQA and STA SST indices (see Table 1 for a definition of the regions covered by Nino3, NTA, EQA and STA) in CTRL (a1-d1) and PCEQP (a2-d2). Levels of 50 (dot), 90 (dot-dash) and 95% (dash) statistical confidence are indicated. All indices are unfiltered monthly data of 350-years model integration. The time series is detrended and the average seasonal cycle is removed. Periods less than one year are not shown. The spectrum is obtained by a multitaper spectral method (Mann and Lees, 1996).

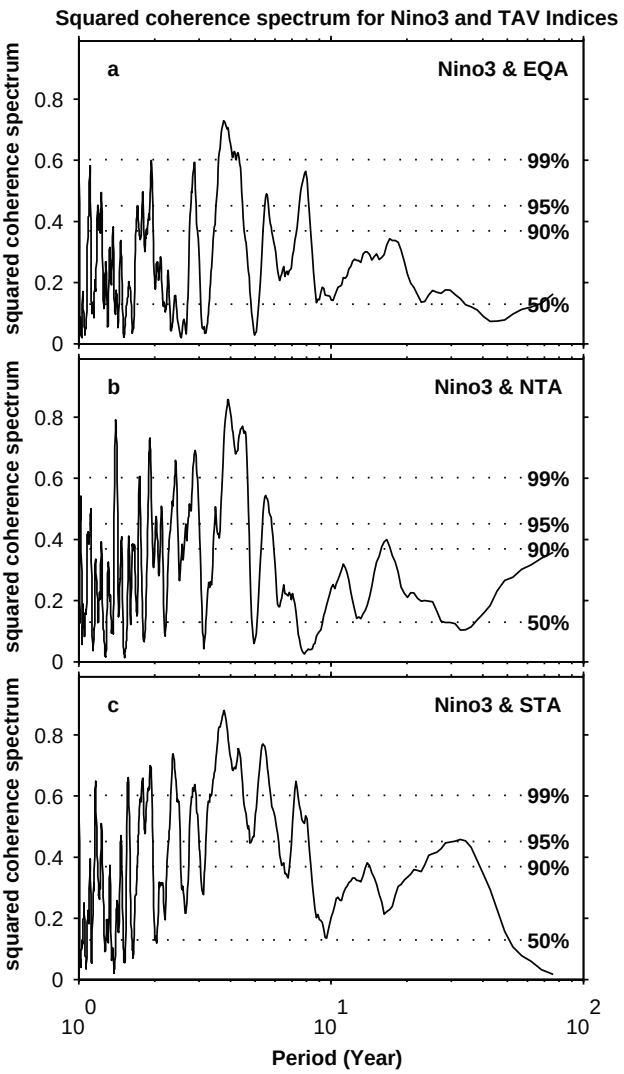

Fig. 2: Squared coherence spectrum between the NINO3 and TAV SST indices in the EQA (upper), NTA (middle), and STA (lower) in CTRL with confidence limits as shown.

posed by Latif and Grötzner (2000). The anomalous easterly deepens the thermocline in the western equatorial Atlantic, which propagates slowly eastward and affects SSTs in the eastern equatorial Atlantic. In the STA, the warming seems to be associated with oceanic processes since the increased surface heat loss associated with stronger winds would decrease SST, as noted in the observations (Venegas et al., 1997). For example, anomalous southeasterlies in the STA can bring more heat from the equator to the subtropics via anomalous poleward surface Ekman flow, resulting in warming in the subtropics within only a few months of the warming in the eastern equatorial Pacific (EQP).

The remote influence of ENSO on TAV seems to be mediated by atmospheric processes through the Pacific North American (PNA) teleconnection that produces a negative pressure anomaly over the western subtropical Atlantic, and the Pacific South American wave train that influences the South Atlantic (not shown). The El Niño signal in the tropical Atlantic surface pressure is

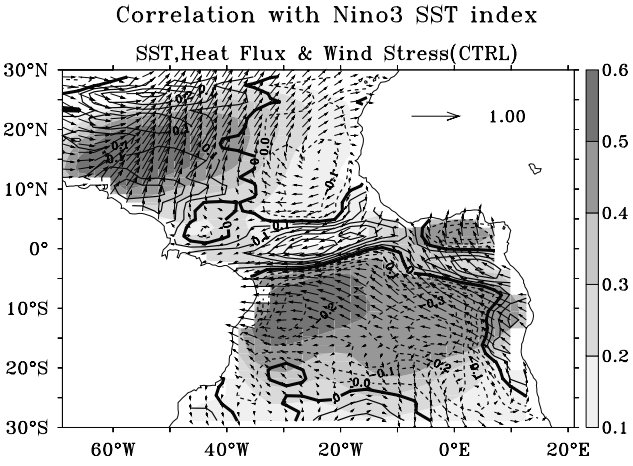

Fig. 3: Correlation of SST(shading), downward net surface heat flux (contour) and wind stress (vectors) with the Niño3 SST index during the boreal spring season (February-March-April) in CTRL. The 95% significance level for the correlation between the heat flux and the Niño3 SST index is about 0.11.

Table 1: Variance of SST indices (°C)²

	Interannual (< 8 year)			
	Niño3	NTA	EQA	STA
CTRL	0.205	0.037	0.037	0.028
PC-EQP	0.013	0.023	0.026	0.012

Niño3: (150°W, 90°W)x(5°S, 5°N);
NTA: (70°W, 20°W)x(5°N, 20°N);
EQA: (50°W, 10°E)x(5°S, 5°N);
STA: (40°W, 10°E)x(5°S, 20°S).

dominated by a positive pressure anomaly reflecting the anomalous Walker circulation (e.g. Covey and Hastenrath, 1978) (not shown). Overall, the model captures the major features of ENSO influence on the tropical Atlantic sector, and these features are broadly consistent with previous observational and modelling studies (e.g. Enfield and Mayer, 1997; Saravanan and Chang, 2000).

While the above analysis provides some insight into the influence of ENSO on the TAV, it doesn't answer the question whether the TAV is directly forced by ENSO or not, because the climates in the fully coupled GCMs are the product of complex interactions involving feedbacks that are not easily separated. In the following, we use the partial coupling strategy to assess more quantitatively the potential role of ENSO in the generation of TAV.

3. The Role of ENSO on TAV: The Partial-Coupling Experiment

To assess the role of ENSO on the generation of TAV, we performed a PC experiment, denoted PC-EQP, in which ENSO is removed from the coupled ocean-atmosphere system. In the model, the annual cycle of SST of the CTRL run is prescribed to force the atmosphere in the equatorial Pacific (within 20° of the equator); elsewhere the air-sea coupling remains active as in CTRL. A similar experiment was also performed by Huang et al. (2001) using the COLA coupled GCM model. In spite of differences in the models, the major conclusions drawn from the PC experiments with these two models are consistent (personal communication).

Without air-sea coupling in the equatorial Pacific, ENSO virtually vanishes in PC-EQP (Fig. 1a2; Table 1). The suppression of SST variability in the equatorial Pacific reduces SST variability in the NTA, EQA and STA regions significantly as summarized in Table 1. Without ENSO, SST interannual variability is reduced by 37%, 30% and 55% in the NTA, EQA and STA, respectively (Table 1). In addition to the reduction of SST variance, the temporal evolution of SST in these three regions also undergoes dramatic changes. Similar to the equatorial Pacific in PC-EQP, SSTs in the NTA, EQA and STA regions do not show any distinct variability at interannual timescales, which is in sharp contrast to the CTRL (Fig. 1 b2-d2 vs. Fig. 1b1-d1). This suggests that the temporal evolution of the TAV, particularly the variability at interannual timescales, is largely dictated by ENSO. In contrast to interannual variability, the temporal evolution of the TAV at decadal timescales seems to be suppressed by the tropical Pacific SST variability. It should be noted that the influence of ENSO in the STA regions in our model is somewhat stronger than in other previous studies. Recent studies suggest that ENSO can excite the Pacific South American wave train to contribute the variations of the STA SSTs through local heat flux changes and oceanic dynamics (Mo and Hakkinen, 2001). In our model, this wave train is visible in the regression of 200 hPa wind against the Niño3 SST (not shown).

ENSO may also affect air-sea coupled feedback over the tropical Atlantic. Observational evidence suggest a positive correlation between SST and net down-

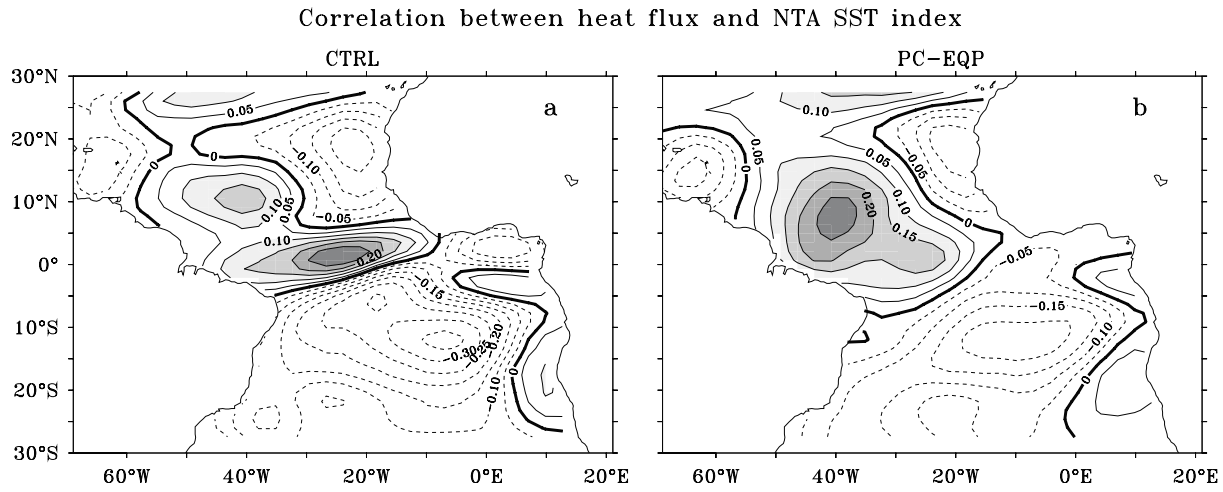

Fig. 4: Correlation of downward net surface heat flux with the NTA ((70°W, 20°W) x (5°N, 20°N)) SST index during the boreal spring season (February-March-April). (a) CTRL; (b) PC-EQP. The shaded area means the correlations are above the 95% confidence level.

ward heat flux in the NTA, especially during the boreal spring season (Chang et al., 1997). Recent studies show this positive feedback occurs only in the deep tropics (Saravanan and Chang, 2000; Chang et al., 2000; Chiang et al., 2002). To quantify the influence of ENSO forcing on the local correlation between surface heat flux and SST, we correlate the surface heat flux with the local NTA SST index. For the CTRL run, the correlation of the downward heat flux during the boreal spring season with the NTA SST index is positive in the deep Tropics, equatorward of 15°, but negative in the eastern NTA off the coast of West Saharan Africa and most of the STA (Fig. 4a). In the absence of the equatorial Pacific forcing, the correlation and hence the positive feedback over the equatorial region is weakened dramatically, while in the western tropical Atlantic warm pool region remains significant (Fig. 4b). This suggests that ENSO can contribute to positive correlation between SST anomalies and surface heat flux in the deep tropics of the Atlantic during boreal spring season, but is not a necessary condition for the generation of the positive feedback. This is consistent with the previous AGCM study by Saravanan and Chang (2000).

The positive ocean-atmosphere feedback in the NTA may intensify the influence of ENSO forcing over that domain. Without air-sea coupling in the NTA, the variance of the NTA SST is reduced dramatically by 80% even though ENSO is present, and none of the leading rotated EOFs shows a coherent NTA mode (Wu and Liu, 2002). This suggests that both remote forcing and local ocean-atmosphere interaction are needed for a full development of the NTA mode, supporting the view drawn from previous AGCM studies (Chang et al., 2000; Saravanan and Chang, 2000).

4. Summary

Aided by the partial coupling approach, our coupled GCM study shows that ENSO predominantly dictates the temporal evolution of TAV at interannual timescales, and can enhance SST variance in the NTA, EQA and STA substantially. In the NTA, ENSO-induced warming is caused by surface heat flux associated with weakening of the northeast trades, in the EQA and perhaps the STA the changes are associated with oceanic processes.

ENSO also contributes to the positive correlation between SST and downward surface heat flux in the NTA during the boreal spring season, but is not a necessary condition. Our model shows that local ocean-atmosphere coupling is critical for a full development of TAV.

Taking together with our previous modelling study of remote NAO forcing on TAV (Wu and Liu, 2002), we conclude that in the NTA, about 60% of SST variance can be explained as a result of remote ENSO (about 30%) and NAO (about 30%) forcing in conjunction with local ocean-atmosphere coupled feedback; in the EQA and STA about 30 to 50% of SST variance can be explained by ENSO, while the influence of NAO forcing is negligible.

Acknowledgment

This work is supported by NASA, NOAA and DOE. All the computations were performed at NCSA. We would like to thank Dr. John Kutzbach for his useful comments and generous editorial help, and Pat Behling for processing data and graphics.

References

Chang, P., L. Ji, and H. Li, 1997: A decadal climate variation in the tropical Atlantic Ocean from thermodynamic air-sea interactions. *Nature*, **385**, 516-518.

Chang, P., R. Saravanan, L. Ji, and G.C. Hegerl, 2000: The effect of local sea surface temperature on atmosphere circulation over the tropical Atlantic sector. *J. Climate*, **13**, 2195-2216.

Chiang, J.C.H., Y. Kushnir, and S.E. Zebiak, 2000: Interdecadal changes in eastern Pacific ITCZ variability and its influences on the Atlantic ITCZ. *Geophys. Res. Lett.*, **27**, 3687-3690.

Chiang, J.C.H., Y. Kushnir, and A. Giannini, 2002: Deconstructing Atlantic Intertropical Convergence Zone variability: Influence of the local cross-equatorial sea surface temperature gradient and remote forcing from the eastern equatorial Pacific. *J. Geophys. Res.*, **107**, in press.

Covey, D., and S. Hastenrath, 1978: The Pacific El Niño Phenomenon in the Atlantic Sector. *Mon. Wea. Rev.*, **106**, 1280-1287.

Curtis, S., and S. Hastenrath, 1995: Forcing of anomalous SST evolution in the tropical Atlantic during Pacific warm events. *J. Geophys. Res.*, **100**, 15835-15847.

Czaja, A., P. van der Vaart, and J. Marshall, 2002: A diagnostic study of the role of remote forcing in Tropical Atlantic Variability. *J. Climate*, submitted.

Enfield, D.B., and D.A. Mayer, 1997: Tropical Atlantic Sea surface temperature variability and its relation to the El Niño-Southern Oscillation. *J. Geophys. Res.*, **102**, 929-945.

Grötzner, A., M. Latif, and T.P. Barnett, 1998: A decadal climate cycle in the North Atlantic Ocean as simulated by the ECHO coupled GCM. *J. Climate*, **11**, 831-847.

Huang, B., Z. Pan, and P.S. Schopf, 2001: The interannual variability in the Tropical Atlantic Ocean simulated by a regionally coupled ocean-atmosphere GCM. U.S. CLIVAR Atlantic workshop, June 12-14, Boulder, Colorado.

Jacob, R., 1997: Low frequency variability in a simulated atmosphere ocean system. Ph.D. thesis, University of Wisconsin-Madison.

Latif, M., and A. Grötzner , 2000: The equatorial Atlantic oscillation and its response to ENSO. *Climate Dynamics*, **16**, 213-218.

Liu, Z., J. Kutzbach, and L. Wu, 2000: Modeling climatic shift of El Nino variability in the Holocene. *Geophys. Res. Lett.*, **27**, 2265-2268.

Liu, Z., and L. Wu, 2000: Tropical Atlantic Oscillation in a coupled GCM. *Atmos. Sci. Lett.*, **1**, 26-36.

Mann, M., and J. Lees, 1996: Robust estimation of background noise and signal detection in climate time series. *Clim. Change*, **33**, 409-445.

Mo, K.C., and S. Hakkiken, 2001: Interannual variability in the

tropical Atlantic and linkages to the Pacific. *J. Climate*, **14**, 2740-2762.

Nobre, C., and J. Shukla, 1996: Variations of sea surface temperature, wind stress, and rainfall over the tropical Atlantic and South America. *J. Climate*, **9**, 2464-2479.

Saravanan, R., and P. Chang, 2000: Interaction between Tropical Atlantic Variability and El Niño-Southern Oscillation. *J. Climate*, **13**, 2177-2194.

Venegas, S., L. Mysak, and D. Straub, 1997: Atmopshere-ocean coupled variability in the South Atlantic. *J. Climate,* **10**, 2904-2920.

Wu, L., and Z. Liu, 2002: Is Tropical Atlantic Variability driven by the North Atlantic Oscillation? *Geophys. Res. Lett.*, **29**, in press.

Xie, S., and Y. Tanimoto, 1998: A pan-Atlantic decadal climate oscillation. *Geophys. Res. Lett.*, **25**, 2185-2188.

Yang., J, 1999: A linkage between decadal climate variations in the Labrador Sea and the tropical Atlantic Ocean. *Geophys. Res. Lett.*, **26**, 1023-1026.

Zebiak, S.E., 1993: Air-sea interaction in the equatorial Atlantic region. *J. Climate*, **6**, 1567-1586.

Coupled Ocean-Atmosphere Variability in the Tropical Atlantic Ocean

Bohua Huang, Paul S. Schopf, and Jagadish Shukla
Center for Ocean-Land-Atmosphere Studies
Calverton, MD, USA
corresponding e-mail: huangb@cola.iges.org

A rotated empirical orthogonal function (REOF) analysis of the observed seasonal mean sea surface temperature (SST) anomalies for 1950-1998 from the tropical Atlantic basin shows that there are three important patterns of variability (Fig. 1):

1. Southern Tropical Atlantic (STA) Pattern (Fig.1a): The SST fluctuations are centred near the Angola coast and expand toward the equator into the Gulf of Guinea.

2. Northern Tropical Atlantic (NTA) Pattern (Fig.1b): This pattern is characterized by SST anomalies centred near the African coast in the northern tropical Atlantic Ocean.

3. Southern Subtropical Atlantic (SSA) Pattern (Fig.1c): The SST fluctuations are in the open ocean of the subtropical South Atlantic.

Both the STA and NTA have been shown as leading tropical Atlantic modes in many previous studies (see, e.g., Enfield and Mayer, 1997; Dommenget and Latif, 2000), which contribute to the fluctuation of the equatorial SST meridional gradient. The SST gradient then affects the position of the inter-tropical convergence zone (ITCZ) and rainfall over the ocean and its adjacent regions (Nobre and Shukla, 1996). The STA is also associated with the anomalous events in the Gulf of Guinea and near the Angola coast (Hirst and Hastenrath, 1983; Huang et al., 1995). The SSA has been demonstrated to be the dominant SST fluctuation in the subtropical South Atlantic Ocean (Venegas et al., 1997). Previous studies also demonstrated that regional air-sea coupling (e.g., Zebiak, 1993; Chang et al., 1997) and remote forcing factors, such as the El Niño/Southern Oscillation (ENSO), play roles in forming some of these SST patterns (e.g., Nobre and Shukla, 1996; Enfield and Mayer, 1997; Saravanan and Chang, 2000; Czaja et al., 2002). The scientific question, then, is whether these SST patterns are externally forced or can be generated as intrinsic modes of the tropical Atlantic ocean-atmosphere processes.

To answer these questions, we have analysed the Atlantic Ocean variability simulated by a coupled ocean-atmosphere model, in which ocean-atmosphere coupling is included only within the Atlantic Ocean between 30°S-65°N. Therefore, one major potential remote-forcing factor to the tropical Atlantic, the ENSO, is suppressed. The oceanic and atmospheric components of the coupled GCM, referred to as the OGCM and the AGCM respectively hereafter, are described in more detail by Huang et al. (2002). In the coupled region, all surface fluxes simulated by the AGCM and the SST simulated by the OGCM are supplied, each to the other component, at daily intervals. Over the uncoupled portion of the global domain, the SST is prescribed for the AGCM and the surface wind stress is prescribed for the OGCM with observed monthly climatological data. A 10°-wide zone in the South Atlantic Ocean within 30°S-40°S is used to blend the coupled and uncoupled portions of the domain. The coupled run has been conducted for 200 years. The output from the last 110 years is used in this analysis.

Our results show that the leading SST patterns shown in Fig. 1 can be reproduced quite realistically by this regionally coupled model (Fig. 2). In particular, the model NTA and SSA patterns (Fig. 2b, c) have amplitudes comparable to their observed counterparts (Fig. 1b, c) and explain a significant amount of the total variance. This seems to suggest that these patterns can be produced by air-sea coupling within the Atlantic Ocean or by the oceanic responses to atmospheric internal forcing, in which there was no external SST forcing.

The model STA pattern (Fig. 2a), however, is weaker in its strength, especially to the north of 10°S, and explains much less variance, than it does in the observations (Fig. 1a). Since the observed STA pattern implies air-sea interactions sensitive to the equatorial wind in the western and central Atlantic (Hirst and Hastenrath, 1983; Zebiak, 1993), its weak amplitude in the coupled model suggests that these equatorial processes are not adequately simulated. We suspect that this situation is related to a warm mean SST bias to the south of the equa-

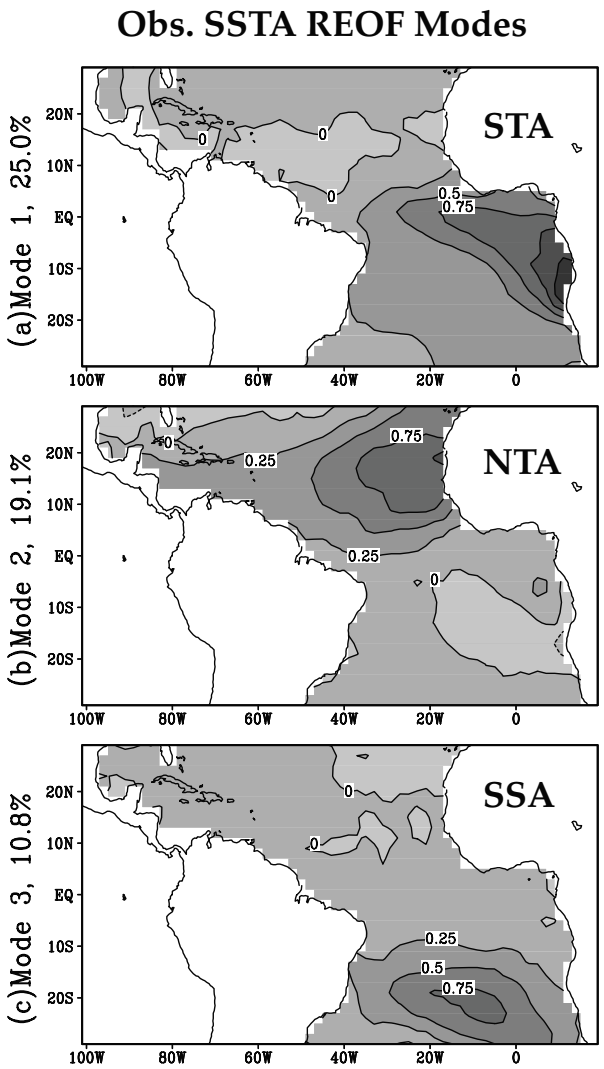

Fig. 1: The spatial patterns of the (a) 1st, (b) 2nd, and (c) 3rd REOF modes of the seasonal mean SST anomalies for 1950-1998. The SST data are from U.S. Climate Prediction Center's analysis. The magnitude of the patterns corresponds to two times of the standard deviation of the normalized time series. The contour interval is 0.25°C.

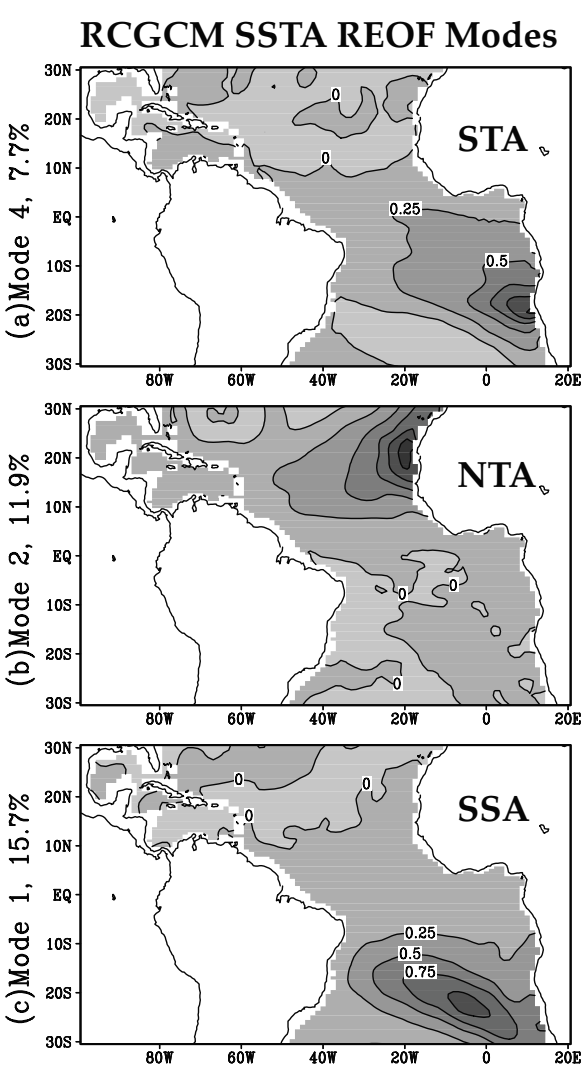

Fig. 2: The spatial patterns of the (a) 4th, (b) 2nd, and (c) 1st REOF modes of the seasonal mean SST anomalies from the 110-year regional coupled GCM simulation. The magnitude of the patterns corresponds to two times of the standard deviation of the normalized time series. The contour interval is 0.25°C.

tor. The bias then is related to the fact that in the coupled model the ITCZ has two preferred locations. From boreal summer to fall, the ITCZ is located to the north of the equator. However, it shifts to the south of the equator from January to May. During these months, it tends to block the southeast trade winds from reaching the equatorial zone.

The effect of this systematic error on the SST variability can be seen in the structure of the standard deviation of SST anomalies in the model (Fig. 3b). Although the model reproduced the main features of the observed variability (Fig. 3a), its major difference from the observations is a zonal belt of minimum standard deviation (less than 0.3°C) between 5°-15°S. This zone largely cuts off the link between the fluctuations near the Angola coast and those within the equatorial wave-guide and splits them into two separate modes. In reality, however, they are closely connected (Fig. 3a, see also, Hirst and Hastenrath, 1983). As a result, the model STA pattern is significantly weakened. Our composite analysis based on time series of the STA modes shows that, unlike the observations, the model STA pattern is much less correlated with the equatorial winds in the central and western equatorial Atlantic.

Our further analysis suggests that anomalous events associated with both the NTA and the SSA are mainly associated with the anomalous surface heat fluxes caused by the changing trade winds. The wind changes, in turn, are associated with the fluctuations of the subtropical anticyclones in the atmosphere, which, apart from regional air-sea interactions within the tropical Atlantic, are also connected with the extra-tropical varia-

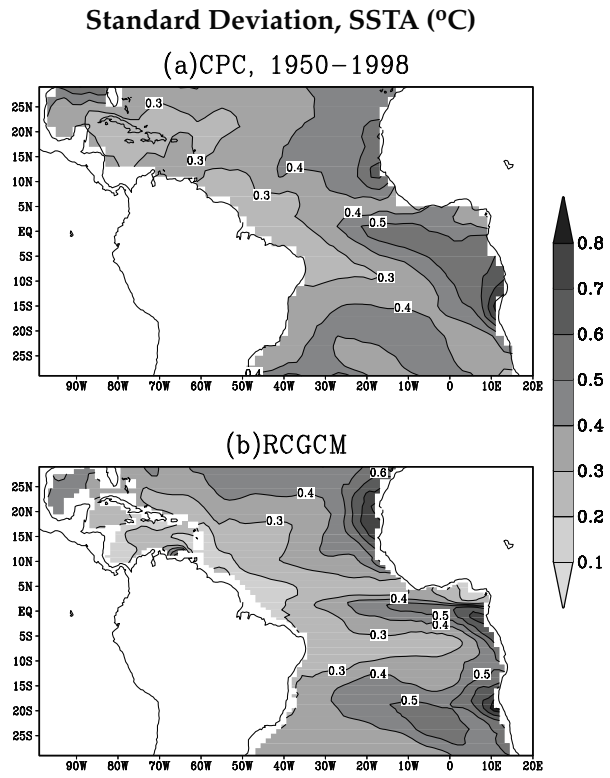

Fig. 3: The spatial structure of the standard deviation of the seasonal mean SST anomalies from (a) U.S. Climate Prediction Center's Analysis for 1950-1998 and (b) 110-year simulation of the regional coupled GCM. The contour interval is 0.1ºC. The SST anomalies are seasonally averaged data.

tions. For NTA, they seem to be related to the North Atlantic Oscillation while low-frequency Rossby waves (Hoskins and Karoly, 1981) propagating from the west may also play a role. For SSA, there is a significant connection to the Antarctic Oscillation (Gong and Wang, 1999). Since climatological SST is prescribed outside the Atlantic domain and in the global southern extra-tropical oceans, some anomalous atmospheric signals from the global atmospheric internal variability (Straus and Shukla, 2002) might propagate into the coupled Atlantic domain. However, the local coupled processes may further modify these signals. For instance, after the SST anomalies are initiated by these forcings, regional air-sea processes seem to expand these anomalies further toward the equator on a seasonal time scale.

In a previous study using the regional coupled model forced with observed SST in 1950-1998 over the uncoupled domain, Huang et al. (2002) found significant ENSO influences on the NTA, which is similar to the observed ENSO-NTA relationship (Enfield and Mayer, 1997). The present experiment suggests that the spatial pattern of NTA is mainly determined by ocean-atmosphere coupling within the Atlantic Ocean. The main effect of ENSO may be primarily to modulate the temporal evolution of the NTA through influencing atmospheric planetary waves propagating into the basin.

These results on NTA and SSA are largely consistent with those derived by Dommenget and Latif (2000) based on annual mean SST data from several globally coupled ocean-atmosphere general circulation models (CGCM). In fact, the two leading REOF modes of our model simulation, the SSA (Fig. 2c) and NTA (Fig. 2b), are very similar to the two leading modes from the models Dommenget and Latif (2000) have shown. However, our interpretation and explanation of the patterns in the southern ocean are different. In model simulations reported by Dommenget and Latif (2000), a pattern similar to the observed SSA is found as a leading mode for all the models. They further noticed that this model mode is strongly affected by subtropical atmospheric fluctuations. However, Dommenget and Latif (2000) have interpreted that mode to be a simulation of the observed STA and concluded that STA is mainly caused by forcings from the subtropics. Therefore, they suggested that the main patterns in both hemispheres resemble local oceanic responses to atmospheric fluctuations from the subtropics, with air-sea feedback and ocean dynamics having little effect in the tropics. Our conclusion in this respect is different from Dommenget and Latif (2000). Based on our results, the contribution of the regional air-sea coupling and oceanic dynamics may still be significant, especially for STA, even though it is underestimated due to the systematic errors of the present coupled ocean-atmosphere general circulation models.

Acknowledgments

This study is supported by grants (NA96GP0446 and NA169PI570) from National Oceanic and Atmospheric Administration's CLIVAR Atlantic Program. We would like to thank Mr. Z. Pan for programming assistance and Dr. J.L. Kinter III for useful discussions.

References

Chang, P., L. Ji, and H. Li, 1997: A decadal climate variation in the tropical Atlantic Ocean from thermodynamic air-sea interactions. *Nature*, **385**, 516-518.

Czaja, A., P. van der Vaart, and J. Marshall, 2002: A diagnostic study of the role of remote forcing in tropical Atlantic variability. *J. Climate*, submitted.

Dommenget, D., and M. Latif, 2000: Interannual and decadal variability in the tropical Atlantic. *J. Climate*, **13**, 777-792.

Enfield, D.B., and D.A. Mayer, 1997: Tropical Atlantic sea surface temperature variability and its relation to El Niño-Southern Oscillation. *J. Geophys. Res.*, **102**, 929-945.

Gong, D., and S. Wang, 1999: Definition of Antarctic oscillation index. *Geophys. Res. Lett.*, **26**, 459-462.

Hirst, A., and S. Hastenrath, 1983: Atmosphere-ocean mechanisms of climate anomalies in Angola-tropical Atlantic sector. *J. Phys. Oceanogr.*, **13**, 1146-1157.

Hoskins, B.J., and D.J. Karoly, 1981: The steady linear response of a spherical atmosphere to thermal and orographic forcing. *J. Atmos. Sci.*, **38**, 1178-1196.

Huang, B., P.S. Schopf, and Z. Pan, 2002: The ENSO effect on the tropical Atlantic variability: A regionally coupled model study. *Geophys. Res. Lett.*, in press.

Huang, B., J.A. Carton, and J. Shukla, 1995: A numerical simulation of the variability in the tropical Atlantic Ocean, 1980-88. *J. Phys. Oceanogr.*, **25**, 835-854.

Nobre, P., and J. Shukla, 1996: Variations of sea surface temperature, wind stress, and rainfall over the tropical Atlantic and South America. *J. Climate*, **9**, 2464-2479.

Saravanan, R., and P. Chang, 2000: Interaction between tropical Atlantic variability and El Niño-Southern Oscillation. *J. Climate*, **13**, 2177-2194.

Straus, D.M., and J. Shukla, 2002: Does ENSO force the PNA? *J. Climate*, in press.

Venegas, S.A., L.A. Mysak, and D. Straub, 1997: Atmosphere-ocean coupled variability in the South Atlantic. *J. Climate*, **10**, 2904-2920.

Zebiak, S.E., 1993: Air-sea interaction in the equatorial Atlantic region. *J. Climate*, **8**, 1567-1586.

Interior Ocean Pycnocline Transports in the Atlantic Subtropical Cells

Dongxiao Zhang[1,2], Michael J. McPhaden[2], and William E. Johns[3]
[1]Joint Institute for the Study of the Atmosphere and Ocean, University of Washington, Seattle, WA, USA
[2]NOAA/Pacific Marine and Environmental Laboratory, Seattle, WA, USA
[3]Rosenstiel School of Marine and Atmospheric Science, University of Miami, Miami, FL, USA
corresponding e-mail: zhang@pmel.noaa.gov

1. Introduction

Subtropical Cells (STCs) are shallow meridional overturning cells that transport water subducted in the subtropics during the winter season to the tropics, where it is upwelled to the surface. The upwelled water is modified by air-sea heat exchange and then advected back to the subtropics by poleward Ekman flows in the surface layer to complete the STC. The STCs in the Pacific have been extensively studied both observationally and theoretically (e.g., McCreary and Lu, 1994; Liu et al., 1994; and Johnson and McPhaden, 1999), and several recent studies suggest STCs may play a role in regulating the low frequency climate variability involving tropical Pacific SST (Gu and Philander, 1997; Kleeman et al., 1999; McPhaden and Zhang, 2002). Unlike the STCs in the Pacific, fewer studies have been conducted on the STCs in the Atlantic, though several modelling papers (Fratantoni et al., 2000; Inui et al., 2002; Lazar et al.,. 2002; Malanotte-Rizzoli et al., 2000; Harper, 2000; Jochum and Malanotte-Rizzoli, 2001) have recently appeared. These studies suggested strong dependence of the strength and mean pathways of STCs on model configurations and climatological forcings. Differences between the model simulations may also be attributed to differences in how the large scale Thermohaline Circulation (THC) is simulated in the models. Here we form a high resolution hydrographic climatology for the Atlantic to describe the subsurface limb of STCs, which connect the tropical-extratropical Atlantic in the pycnocline. The primary data set is a combination of the World Ocean Database (Conkright et al., 1999) from the National Oceanographic Data Center (NODC), new hydrographic data collected during the World Ocean Circulation Experiment (WOCE), and data collected during cruises to service Pilot Research Moored Array in the Tropical Atlantic (PIRATA) moorings. A total of 86,131 casts with both temperature and salinity measurements in the Atlantic between 40° S and 50° N reach a depth of at least 1200 m, which is the reference level we use for our geostrophic velocity estimates. The number of casts available for defining water mass properties at shallower levels is considerably greater (e.g. 166,941 casts reach at least 300 m). By decade, the number of available cast ranges between about 7,000 - 30,000 to 1200 m and 13,000 - 53,000 to 300 m, with maximum sampling taking place in the 1970's and 80's.

2. Flow on Isopycnal Surfaces in the Pycnocline

Flow in the Atlantic STCs is concentrated on isopycnal surfaces that outcrop and are ventilated in the subtropics. Temperature, salinity, geostrophic streamlines, and potential vorticity (N^2f/g, where N is the buoyancy frequency, f is Coriolis parameter, and g is gravitational acceleration) are calculated on these isopycnal surfaces and averaged from 1950-2000. Calculations are performed using the Hydrobase analysis package (Curry, 1996), which implements isopycnal averaging to grid individual profiles along their density surfaces into bins on a 0.25° latitude x 0.25° longitude grid. The resulting bin-averaged profiles are then mapped onto 0.5° x 0.5° grid using objective analysis with zonal and meridional de-correlation scales set at 5° longitude x 2° latitude. To illustrate the basic structure of STCs, we show the fields of planetary potential vorticity (PV) and salinity on the 25.4 σ_θ isopycnal surface (roughly equivalent to 20°C) in the upper pycnocline (Fig. 1a, b, page 37). The PV field is characterized by the high PV ridge extending from the eastern boundary near 15° N to the western part of the basin near 10° N, almost reaching the western boundary. This PV ridge underlies the Inter-tropical Convergence Zone (ITCZ) where wind stress curl pumps the pycnocline up toward the surface and vertically compresses density surfaces. Also shown are the wintertime outcrop lines of this surface in both the Northern and Southern Hemisphere. Assuming that PV is approximately conserved along trajectories, water subducted in the Northern Hemisphere subtropics on this density surface would have to take a convoluted pathway around the western rim of this PV ridge to get to the equatorial region (McCreary and Lu, 1994). In contrast, the PV field in the Southern Hemisphere is more uniform, allowing for a more direct interior pathway between the subtrop-

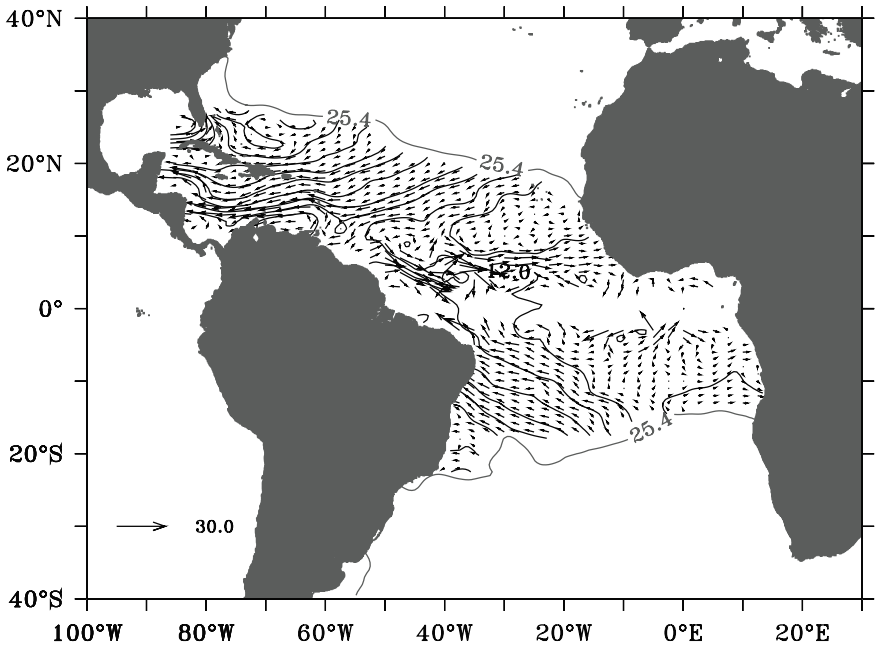

Fig. 2: Geostrophic velocities in cm s^{-1} and streamlines (referenced to 1200 m) on the isopycnal surface σ_θ = 25.4 kg m^{-3}.

ics and the equator. The salinity field of Fig. 1b is characterized by low salinity tropical waters sandwiched between the Salinity Maximum Waters in the North and South Subtropical Atlantic. A salinity front, roughly along the axis of North Equatorial Current (NEC), originates near Cape Verde and extends to the South American shelf near 5°N, separating the most saline subtropical water from the low salinity tropical water. The southward bending of the 36.2 salinity contour near 7° N, 50° W suggests an intrusion of northern subtropical water into the tropics. In the Southern Hemisphere, a similar front extends from the northern rim of the South Atlantic subtropical gyre to Cape San Roque (near 6°S, 35° W), roughly along the axis of South Equatorial Current (SEC). The high salinity of southern subtropical origin is seen to penetrate across the equator along the North Brazil shelf via the North Brazil Current (NBC) and North Brazil Undercurrent (NBUC). The high salinity tongue associated with the Equatorial Undercurrent (EUC) extends eastward along the equator, drawing in saline waters from both the north and south between 40° W and the western boundary. An indication of a weak high salinity tongue is also seen along ~ 5°N, associated with the North Equatorial Countercurrent/North Equatorial Undercurrent (NECC/NEUC) system, which receives water from both the NEC and the NBC retroflection, as well as the northern branch of the South Equatorial Current (nSEC) (Schott et al., 1998; Bourles et al., 1999). The mean STC pathways are shown by the geostrophic streamlines and velocity vectors along the isopycnal surface 25.4 kg m^{-3} in Fig. 2. The reference level is chosen to be 1200 m, where meridional velocity is close to zero and is the boundary between the northward flowing Antarctic Intermediate Water (AAIW) and southward flowing North Atlantic Deep Water (NADW). Velocity calculations stop within 2° of the equator, where geostrophy becomes tenuous and cross-streamline flow is more likely to occur. In the Northern Hemisphere, flow reaching the equator originates in the area confined between 22° -32° W and 18° - 22° N. The flow sweeps around the PV ridge along 10° N and in the western basin between 40° W and 55° W, where there appears to be a concentration of equatorward flow. In the South Atlantic, flow reaching the equator originates in a larger domain from 5° W-30° W along the outcrop line. The pathways are spread over a wide window, which at 6° S extends from 10° W to the western boundary. A large part of the interior flow converges on the western boundary south of Cape San Roque (~ 6° S) and presumably turns northward in the NBUC toward the equator.

3. Mean Transport of Equatorward Flow in the Interior Pycnocline

To quantify the strength of STC interior pathways, we calculate the equatorward transport in the pycnocline across 10° N and 6° S. The 10° N zonal section is chosen because it lies along the potential vorticity ridge, across which a portion of the NEC turns southward into the NECC in the western basin. The reason for choosing 6° S is because it is at the tip of Cape San Roque, and SEC water that reaches the South American coast south of this cape flows into the western boundary current. To determine the total meridional transport we must add an Ekman contribution to the geostrophic flow. According to the observational studies on Ekman layer transports and mixed layer depth (e.g., Chereskin and Roemmich, 1991) we assume an Ekman transport distribution with 3/4 of the transport in the mixed layer and 1/4 of the transport extending into the thermocline to a distance equal to one half of the mixed layer depth. The Ekman transport is calculated from ensemble mean of various wind products (ERS, ECMWF, NECP, COADS, and Servain winds). Fig. 3a and b illustrate the total volume transport (Ekman + geostrophic) distribution across 6° S and 10° N in isopycnal layers, excluding the mixed

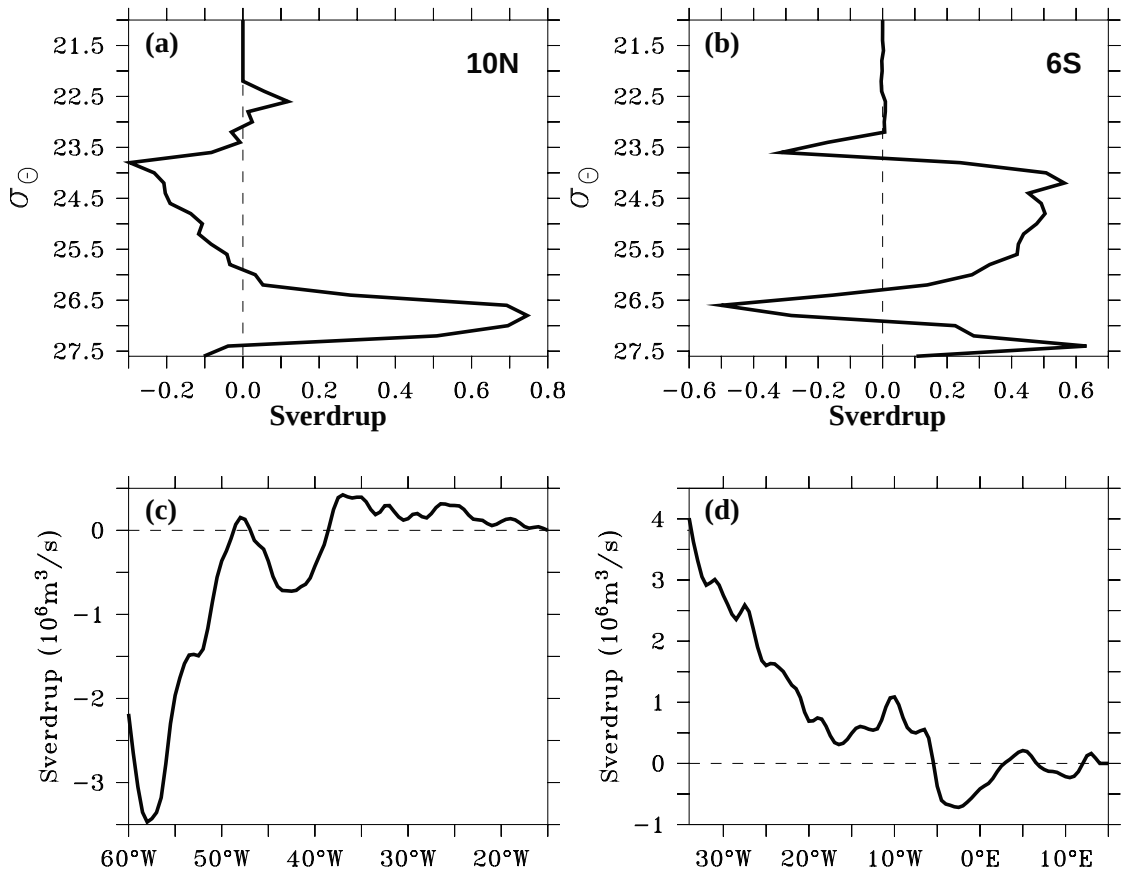

Fig. 3: Net meridional volume transport (Sv) excluding the mixed layer in isopycnal layers from the African coast to 60° W across 10° N (a) and to 34° W across 6° S (b); Meridional volume transport (Sv) in the pycnocline layers with net equatorward transport (23.4-26.0 σ_θ at 10° N and 23.6-26.4 σ_θ at 6° S) zonally accumulated from the African coast westward along 10° N (c) and 6° S (d).

layer. The interior equatorward transport in the pycnocline is between 23.2-26.0 σ_θ at 10°N and between 23.6-26.4 σ_θ at 6° S. In this paper we refer to this layer of equatorward flow as the "pycnocline layer". The poleward transport in the overlying layers is due to the stronger poleward Ekman transport than the equatorward geostrophic transport, and we will henceforth refer to this as the "surface layer". At 10° N, poleward transport below the pycnocline layer, between about 26.0-27.4 σ_θ, corresponds to the interior pathway of the THC in the South Atlantic Central Water (SACW) layers (Arhan et al. 1998). At 6° S, the southward transport between 26.4-26.8 σ_θ is the result of the strong interior recirculation of SACW. The 26.4 σ_θ surface is also the deepest on which water can be subducted along the path of the SEC and Benguela Current off the coast of South Africa. Fig. 3c and d show the cumulative transport across 10° N and 6° S in the layers with net equatorward interior flow in the pycnocline (Fig.3a and b), integrated westward from the eastern boundary. At 10° N, the strongest equatorward flow occurs near 40° W and between 51°-55° W. These two regions are separated by a cyclonic recirculation cell (Fig. 2) located between 44°-51° W. At 6° S, the cumulative equatorward transport increases steadily from 15° W toward the western boundary. The net transport across 10° N between the eastern boundary and 55° W, defined as the northern hemisphere STC interior transport, is 2.0±0.7 Sv. The net transport across 6° S between the eastern boundary and 33° W (2° longitude off the Cape San Roque) is defined as the southern STC interior transport and is estimated to be 4.0±0.5 Sv. Errors are derived from Monte Carlo simulations by randomly using subsets of available data along the two sections.

4. Summary and Discussion

The pathways of subducted water in the Southern Hemisphere to the EUC are relatively direct and include a western boundary route through the NBUC/NBC and NBC retroflection, and a wide interior route across 6° S between the western boundary and 10° W. Serpentine pathways towards the equator in the Northern Hemisphere are suggested by potential vorticity, salinity, isopycnal depth distributions, as well as by the geostrophic current fields. The pathways are confined in the western basin between 40° W-55° W. The pycnocline flow in the STC is 2.0±0.7 Sv southward across the high PV ridge along 10° N in the interior of the Northern Hemisphere, and 4.0±0.5 Sv northward across 6° S in the interior of the Southern Hemisphere. The data coverage does not allow for a direct estimate of the STC transport in the western boundary. However, from a mass balance study of the upper tropical Atlantic, Zhang et al. (2002) estimated the STC transport in the western boundary to be 3.0 Sv southward across 10° N and 6.0 Sv northward across 6° S. Ac-

cording to their analysis, 21 Sv of pycnocline water upwells into the surface layer of tropical Atlantic. The STCs account for 70% or 15 Sv of this upwelling, with another 6 Sv associated with the surface return flow of the THC. Interannual and decadal time scale fluctuations in these circulation cells, and their relation to SST variability, are presently under investigation.

Acknowledgments:

This work was supported by the NOAA Tropical Atlantic Climate Variability Program.

References:

Arhan, M., H. Mercier, B. Bourles, and Y. Gouriou, 1998: Hydrographic sections across the Atlantic at 7°30N and 4°30S. *Deep-Sea Res.*, **45**, 829–872.

Bourles, B., R.L. Molinari, E. Johns, W.D. Wilson, and K.D. Leaman, 1999: Upper layer currents in the western tropical North Atlantic (1989-1991). *J. Geophys, Res.*, **104**, 1361–1375.

Chereskin, T.K., and D. Roemmich, 1991: A comparison of measured and wind-derived Ekman transport at 11°N in the Atlantic Ocean. *J. Phys. Oceanogr.*, **21**, 869–878.

Conkright, M.E., S. Levitus, T. O'Brien, T.P. Boyer, C. Stephens, D. Johnson, O. Baranova, J. Antonov, R. Gelfeld, J. Rochester, and C. Forgy, 1999: World Ocean Database 1998 Version 2.0, National Oceanographic Data Center Internal Report 14, National Oceanographic Data Center, National Oceanic and Atmospheric Administration, Silver Spring, MD.

Curry, R.G., 1996: Hydrobase - A database of hydrographic stations and tools for climatological analysis, Woods Hole Oceanog. Inst. Tech. Rep., WHOI-96-01, 44 pp.

Fratantoni, D.M., W.E. Johns, T.L. Townsend, and H.E. Hurlburt, 2000: Low latitude circulation and mass transport pathways in a model of the tropical Atlantic Ocean. *J. Phys. Oceanogr.*, **30**, 1944–1966.

Gu, D.-F., and S.G.H. Philander, 1997: Interdecadal climate fluctuations that depend on exchanges between the tropical and extratropics. *Science*, **275**, 805–807.

Harper, S., 2000: Thermocline ventilation and pathways of tropical-subtropical water mass exchange. *Tellus*, **52A**, 330–345.

Inui, T., A. Lazar, P. Malanotte-Rizzoli, and A. Busalacchi, 2002: Wind stress effects on the Atlantic subtropical-tropical circulation. *J. Phys. Oceanogr.*, submitted.

Johnson, G.C., and M.J. McPhaden, 1999: Interior pycnocline flow from the subtropical to the equatorial Pacific Ocean. *J. Phys. Oceanogr.*, **29**, 3073-3089.

Jochum, M., and P. Malanotte-Rizzoli, 2001: Influence of the meridional overturning circulation on tropical-subtropical pathways. *J. Phys. Oceanogr.*, **31**, 1313–1323.

Kleeman, R., J.P. McCreary, and B.A. Kinger, 1999. A mechanism for generating ENSO decadal variability. *Geophys. Res. Lett.*, **26**, 1743–1746.

Lazar, A., T. Inui, A.J. Busalacchi, P. Malanotte-Rizzoli, and L. Wang, 2002: Seasonality of the ventilation of the tropical Atlantic thermocline. *J. Geophys. Res.*, submitted.

Liu, Z., S.G.H. Philander, and R.C. Pakanowski, 1994: A GCM study of tropical-subtropical upper-ocean water exchange. *J. Phys. Oceanogr.*, **24**, 2606–2623.

Malanotte-Rizzoli, P., K. Hedstrom, H. Arango, and D. Haidvogel, 2000: Water mass pathways between the subtropical and tropical ocean in a climatological simulation of the North Atlantic ocean circulation. *Dyn. Atmos. Oceans*, **32**, 331–371.

McCreary, J.P., and P. Lu, 1994: On the interaction between the subtropical and equatorial ocean circulation: subtropical cell. *J. Phys. Oceanogr.*, **24**, 466–497.

McPhaden, M.J., and D. Zhang, 2002: Slowdown of the meridional overturning circulation in the upper Pacific Ocean. *Nature,* **415**, 603–608.

Schott, F.A., J. Fischer, and L. Stramma, 1998: Transports and pathways of the upper-layer circulation in the western tropical Atlantic. *J. Phys. Oceanogr.*, **28**, 1904–1928.

Zhang, D., M.J. McPhaden, and W.E. Johns, 2002: Observational evidence for flow between the Subtropical and Tropical Atlantic: the Atlantic Subtropical Cells. *J. Phys. Oceanogr.*, submitted.

Monitoring the Atlantic Meridional Overturning Circulation at 16°N

Uwe Send[1], Torsten Kanzow[1], Walter Zenk[1], and Monika Rhein[2]
[1]Institut für Meereskunde an der Universität Kiel, Kiel, Germany
[2]Universität Bremen, Bremen, Germany
corresponding email: usend@ifm.uni-kiel.de

1. Introduction

The Atlantic MOC (meridional overturning circulation) is considered an important element of the climate system. Low-frequency fluctuations of the former are thought to have a large impact on the latter. Such fluctuations are common features in models, yet direct observational proof is missing; even the mean strength of the MOC is not well known. In the North Atlantic the southward transport of the DWBC has been shown to vary with latitude: South of Grand Banks 13 Sv (Pickard and Smethie, 1998), east of Abaco 40 Sv (Lee at al., 1996) and near the Equator 19-29 Sv (Schott et al., 1993; Fischer and Schott, 1997; Rhein et al., 1995) have been found. These variations are commonly explained via local recirculation in the Atlantic interior.

Thus, reasonable statements about MOC strength and its temporal variability can only be made from observations that zonally integrate the meridional transports on the basin scale. Here, preliminary analyses of the Feb. 2000 to Jan. 2002 observations from the Meridional Overturning Variability Experiment (MOVE) will be presented. The scientific aim of MOVE, a component of the German CLIVAR programme, is to acquire multiyear time series of variations of the meridional transport and the hydrographic conditions of the NADW (cold limb of MOC) and to interpret these in terms of forcing factors of the MOC. Present funding is available until 2005.

2. Experiment design

The experimental strategy makes use of horizontally integrating geostrophic end-point moorings. This allows monitoring of transport fluctuations on the basin scale with a limited number of moorings. Thus it is well suited for observing large scale phenomena. Further, our simulations have shown that the use of modern equipment and an optimized experiment design reduce the uncertainties sufficiently (Kanzow, 2000). However, as the amplitudes of horizontal density and bottom pressure differences are fairly small, the sensors and instrument depths have to be calibrated with great care (e.g. a pressure equivalent of 1 mm corresponds to a transport of 1 Sv). The MOVE moored array is located at 16°N (Fig. 1, right panel) monitoring deep transports through the 1000 km section between the Lesser Antilles and the Mid-Atlantic Ridge. Among the reasons to choose that region were its relatively flat bottom and steep continental slope (Fig. 1, left panel) as well as the sufficient distance from the equator to apply geostrophy. Three moorings (M1-M3), each covering the depth range of 1200-5000m, are equipped with density sensors to calculate the dynamic height transport, while external fluctuations are obtained using precise bottom pressure recorders. Finally, an extra current meter mooring (M4) on the western boundary slope captures that part of the DWBC which passes inshore of the geostrophic array. The data set further incorporates moored direct current measurements on each of the moorings, hydrographic / LADCP sections along 16°N as well as RAFOS floats trajectories in the upper NADW range.

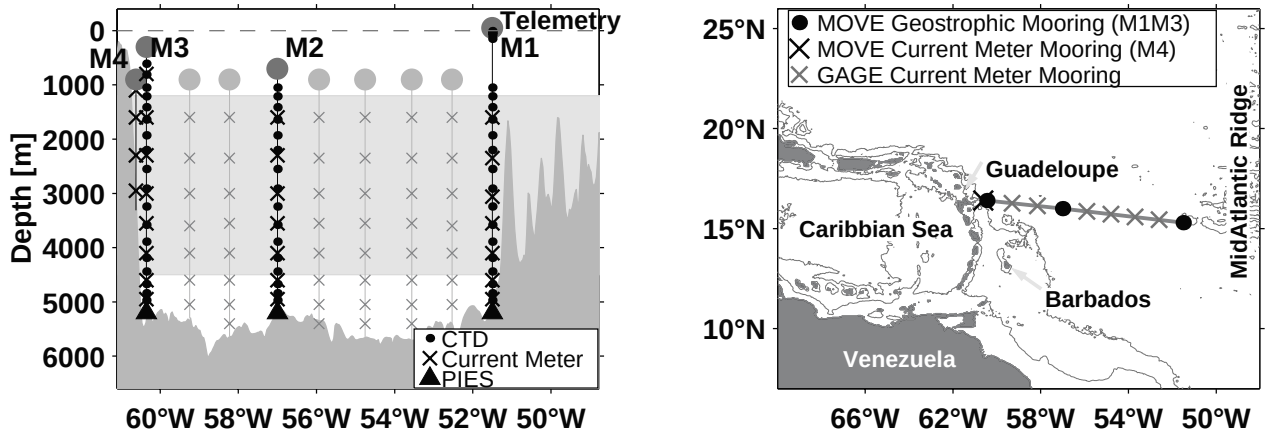

Fig. 1: Left panel: The MOVE array between Lesser Antilles and Mid-Atlantic Ridge consisting of 3 mixed geostrophic / current meter moorings (M1-M3) and one boundary current meter mooring (M4). MOVE was merged with GAGE (Guyana Abyssal Gyre Experiment, WHOI, Jan 2000 - April 2002), whose six current meter moorings are also shown. The NADW range is shaded in light grey. Right panel: Location of the MOVE array, which zonally intergrates across the whole western basin of the North Atlantic the meridional transports of the cold limb of the MOC.

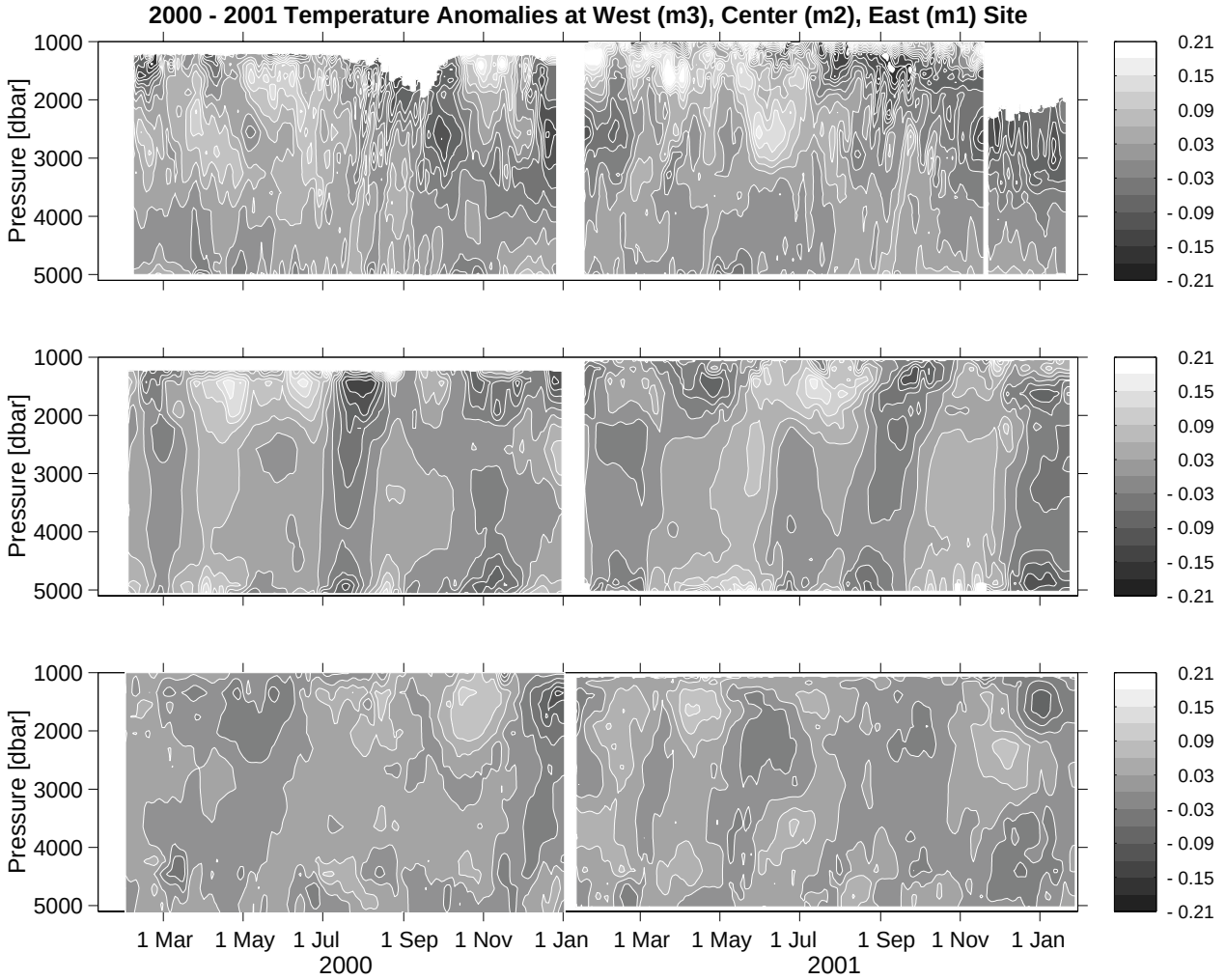

Fig. 2: Temperature anomalies from the west (M3), center (M2) and east (M1) geostrophic moorings (top, middle and bottom panel, respectively) from Feb. 2000 - Feb. 2002. Gaps in Jan. 2001 are due to the annual mooring turn-around. Missing data in upper NADW range at site M3 after mid of Nov. 2001 were caused by mooring breakage.

3. Measurements

Apart from small data losses, like deep M3 mooring subduction around Sept. 2000 or M3 mooring breakage in Nov. 2001 (Fig. 2), the measurements are very successful and of excellent quality. The 2 year time series of temperature anomalies (and salinity, not shown here) at the three geostrophic sites exhibit interesting features (Fig. 2): At the western boundary (M3) highly variable conditions with fluctuations on a weekly scale are visible. Also, in both years the coldest anomalies occur in autumn and winter. They go along with strong southward currents (Fig. 3, bottom). Because of this variability a longer term trend towards freshening and cooling as suggested by Molinari et al. (1998) could not yet be detected, a longer time series would be needed. The sites M2 and M3 exhibit temperature fluctuations on a monthly scale with those of M2 being of much more barotropic nature. Those are likely to be caused by Rossby waves which meridionally shift the background stratification past the mooring sites. The more baroclinic temperature anomalies at M1 could be caused due to the vincinity of the Mid-Atlantic Ridge.

The meridional geostrophic transport fluctuations (Fig. 3, top) integrated across the whole section (M1-M3) yield fluctuations on a monthly scale at times larger than 10 Sv and also longer term variability. It is interesting to note that to some degree the direct boundary transport (Fig. 3, bottom) compensates this variability. This is a clear indication of a meandering DWBC which in turn shows the necessity of mooring M4 on the continental slope. The eastern (M1-M2) and western (M2-M3) contributions to the total M1-M3 geostrophic fluctuations are anticorrelated at monthly and higher frequency time scales. Thus, the zonal integration of meridional currents across the whole western basin significantly increases the signal to noise ratio for longer term signals of the MOC. As a first crude attempt to derive absolute transports from the first deployment period (Feb. 2000 - Jan. 2001), the geostrophic fluctuations were referenced using annual means of the current-meters of moorings M1-M3. Interestingly, we obtained a total (M1 to western boundary) mean transport of 12 Sv to the south, which decomposed to 17 Sv southward west of M2 opposed by 5 Sv to the north east of M2. This could be an indication of a deep interior recirculation pattern.

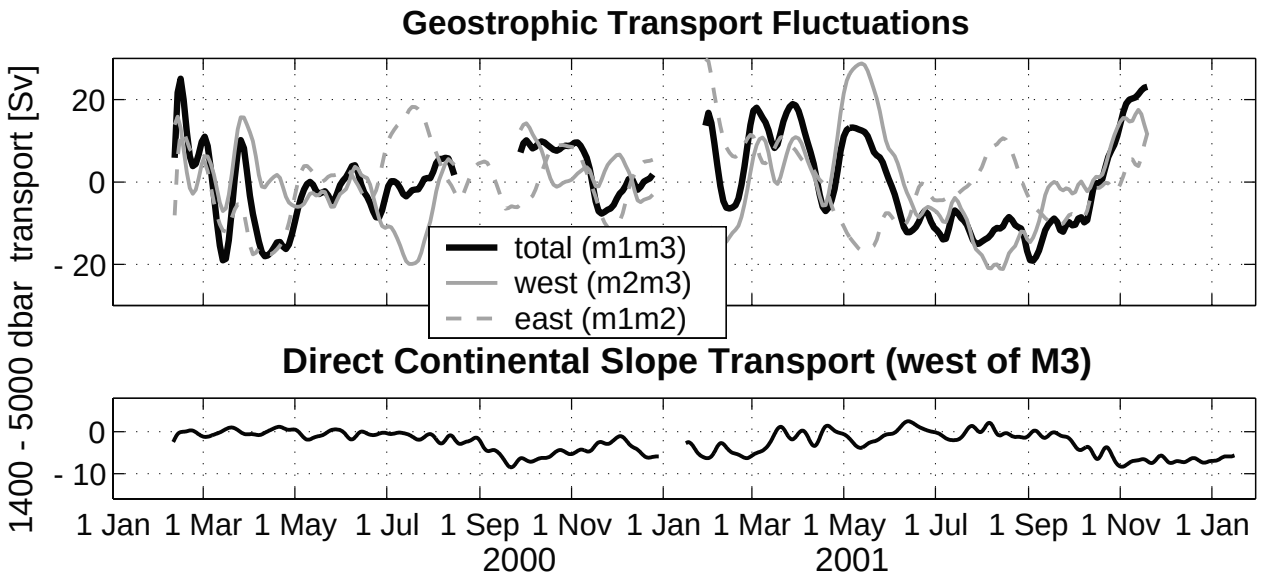

Fig. 3: Top panel: Meridional geostrophic transport fluctuations in the 1400-5000 dbar range. Those time series were obtained adding the dynamic height (internal) and the bottom pressure (external) transport contributions. Transports through the whole section (M1-M3, solid black), the western part (M2-M3, solid grey) and the eastern part (M1-M2, dashed grey) are displayed. Bottom panel: Current meter derived meridional transport along the continental slope (west of M3) in the 1400-5000 dbar range.

4. Conclusion and Outlook

The measurements available to date seem to confirm the monitoring strategy as well as the experiment design. Intense short-term variability has been documented, but the 2 year time series is still too short to reveal longer term trends in the hydrography and the transports. As a next step, different independent techniques will be applied to make the geostrophic transports fluctuations absolute. The mean will be referenced using the joint MOVE / GAGE current meters, float trajectories, LADCP sections and identification of long-term levels of no motion from water masses. The last, especially, will be accompanied by analyses of the high resolution Atlantic FLAME model (Dengg, 1999, http://www.ifm.uni- kiel.de/fb/fb1/tm/research/FLAME/index.html). Finally the origin of the transport variability will be explored. Here, the role the wind, topography as well as buoyancy forcing will be considered using FLAME and other models as well as observations. MOVE is funded until 2005 and a number of extensions have already been set in place in January 2002: The dynamic height component now covers the whole water column which allows us to couple the transport fluctuations to satellite SSH measurements. Further the section will be equipped with acoustic tomography systems to detect the integrated temperature fluctuations. Also the real-time telemetry (developed at IfM Kiel) of density data will be improved.

References:

Dengg, J., C. Böning, U. Ernst, R. Redler, and A. Beckmann, 1999: Effetcs of an improved model representation of Overflow Waters on the subpolar North Atlantic. Int. WOCE Newsletter, **37**, 10-15, Southampton, UK.

Fischer, J., and F.A. Schott, 1997: Seasonal transport variability of the deep western boundary current in the equatorial Atlantic. *J. Geophys. Res*., **102**, 27751-27769.

Kanzow, T., 2000, Integrale Erfassung langperiodischer Transporte: Simulation und Optimierung eines verankerten Systems. Diploma Thesis, Christian-Albrechts-Universität Kiel, Kiel.

Lee, T.N., W.E. Johns, R.J. Zantopp, and E.R. Fillenbaum, 1996: Moored observations of Western Boundary Current variability and thermocline circulation at 26.5ºN in the subtropical North Atlantic. *J. Phys. Oceanogr.*, **26**, 962-983.

Molinari, R.L, R.A. Fine, W.D. Wilson, R.G. Curry, J. Abell, and M. McCartney, 1998: The arrival of recently formed Labrador Sea Water in the Deep Western Boundary Current at 26.5ºN. *Geophys. Res. Lett*., **25**, 2249-2252.

Rhein, M., L. Stramma, and U. Send, 1995: The Atlantic Deep Western Boundary Current: Water masses and transports near the equator. *J. Geophys. Res*., **100**, 2441-2457.

Pickard, R.S., and W.M Smethie, 1998: Temporal evolution of the Deep Western Boundary Current where it enters the subtropical domain. *Deep-Sea Res. I*, **45**, 1053-1083.

Schott, F., J. Fischer, J. Reppin, and U. Send, 1993: On the mean and seasonal currents and transports at the western boundary of the equatorial Atlantic. *J. Geophys. Res*., **98**, 14401-14421.

Inter-annual to Decadal Variability of the Meridional Overturning Circulation of the Atlantic: A Comparison of the Response to Atmospheric Fluctuations in three Ocean Models

Jens-Olaf Beismann[1], Claus W. Böning[1], and Detlef Stammer[2]
[1] Institut für Meereskunde Kiel, Germany
[2] Scripps Institution of Oceanography, La Jolla, USA
corresponding e-mail: jobeismann@ifm.uni-kiel.de

Introduction

The northward transports of mass and heat in the Atlantic play an important role for both the global Meridional Overturning Circulation (MOC) and the European climate. Inter-annual and longer-term changes of oceanic meridional transports are therefore of major interest in climate research.

Because of the previous sparseness of observational data and the difficulties to directly observe basin-scale transports, fluctuations of the Atlantic MOC have mostly been studied using output from numerical models. Among others, Eden and Willebrand (2001; hereafter EW01), Gulev et al. (2002), and Häkkinen (1999) have analysed the oceanic response to atmospheric forcing fluctuations on inter-annual to decadal time scales. In a similar study, Beismann and Barnier (2002) investigate the robustness of their model solution to changes in the overflows of dense waters from the Nordic Seas into the subpolar North Atlantic. In all of the above mentioned studies the North Atlantic Oscillation (NAO) and associated changes in surface forcing are being held responsible for the bulk of the simulated low-frequency variability in the ocean. EW01 described the underlying mechanisms as a superposition of a fast, barotropic response to changes in the wind field over the North Atlantic and a delayed reaction to modifications in the surface heat fluxes over the Labrador Sea. During an NAO "plus" (minus) phase, the former reduces (enhances) the meridional overturning rate, whereas the latter tends to reinforce (weaken) the overturning.

Recently, changes in the ocean and especially in its overturning circulation have become a prominent subject in the planning and interpretation of long-term or repeated measurements such as the „Meridional Overturning Variability Experiment" (MOVE, cf. Kanzow, 2000, see also the paper by Send et al., this issue) at 16°N and a monitoring project at 26.5°N (Marotzke et al., 2002) in the Atlantic. Such an observational capability seems important given the fundamental role that the MOC seems to play in the meridional transport of heat and the potential of an abrupt change in its strength with significant climate implications. However, understanding variations in the MOC and their frequency dependence appears as a prerequisite for building an observational capacity for measuring decadal and longer-term changes in and over the North Atlantic.

Here we present preliminary results of a model intercomparison study with emphasis on the simulated low-frequency (periods > 1 year) variations in the MOC in several models and their relation to atmospheric forcing fluctuations. It appears that the models show the mechanisms for the interannual variability of the extratropical MOC fluctuations to be of similar nature as for seasonal variations: a direct response to wind forcing. Due to the linear adiabatic nature of this mechanism, different models driven by the same wind stress show very similar results. Baroclinic changes in the MOC appear to be more prominent only on decadal and longer time scales. Because of the barotropic nature of the deep response of the basin on inter-annual time scales, it is unlikely that it can be observed entirely by available instrumentation. Circulation models are required, both in prognostic and in assimilation mode, as an important element in studies of variations of the overturning circulation on seasonal to decadal time scales.

Models

In order to explain changes in the MOC and heat transports and as a means to obtain improved estimates of the lower frequency transport variations, we explore the robustness of the simulated variations in three different models, notably MOM (Pacanowski, 1995), OPA (Madec et al., 1998), and the MIT model (Marshall et al., 1997). The output from these models is used to investigate their response to similar NCEP forcing (Kalnay et al., 1996). Although their configuration varies between Atlantic-only setups and global runs, the experiments allow to study of the dependence of the overturning sensitivity in the North Atlantic Ocean on model parameters such as resolution, eddy mixing parameterizations, and topography. If robust patterns in the simulated responses exist on various space and time scales, they might provide clues with respect to their physical causes and the relation to wind or buoyancy forcing as well as to the respective roles of barotropic or baroclinic and local or remote responses.

The above three models are being investigated here mostly in a non-eddy resolving mode. All three models are primitive equation models with z-coordinates in the vertical, but they differ in their numerical details, such as grids, physical parameterizations etc. More specifically those runs encompass:

- An isotropic 1° OPA simulation (spatial resolution: 1°, $1° \cdot \cos\phi$; $\Delta\lambda$, $\Delta\phi$) from the CLIPPER project (Tréguier et al., 1999; http://www.ifremer.fr/lpo/clipper). This model has been forced by monthly mean values of wind stress, net heat flux, and net

continued on page 43

From Molinari et al.: Benchmarks for Atlantic Ocean Circulation (page 6)

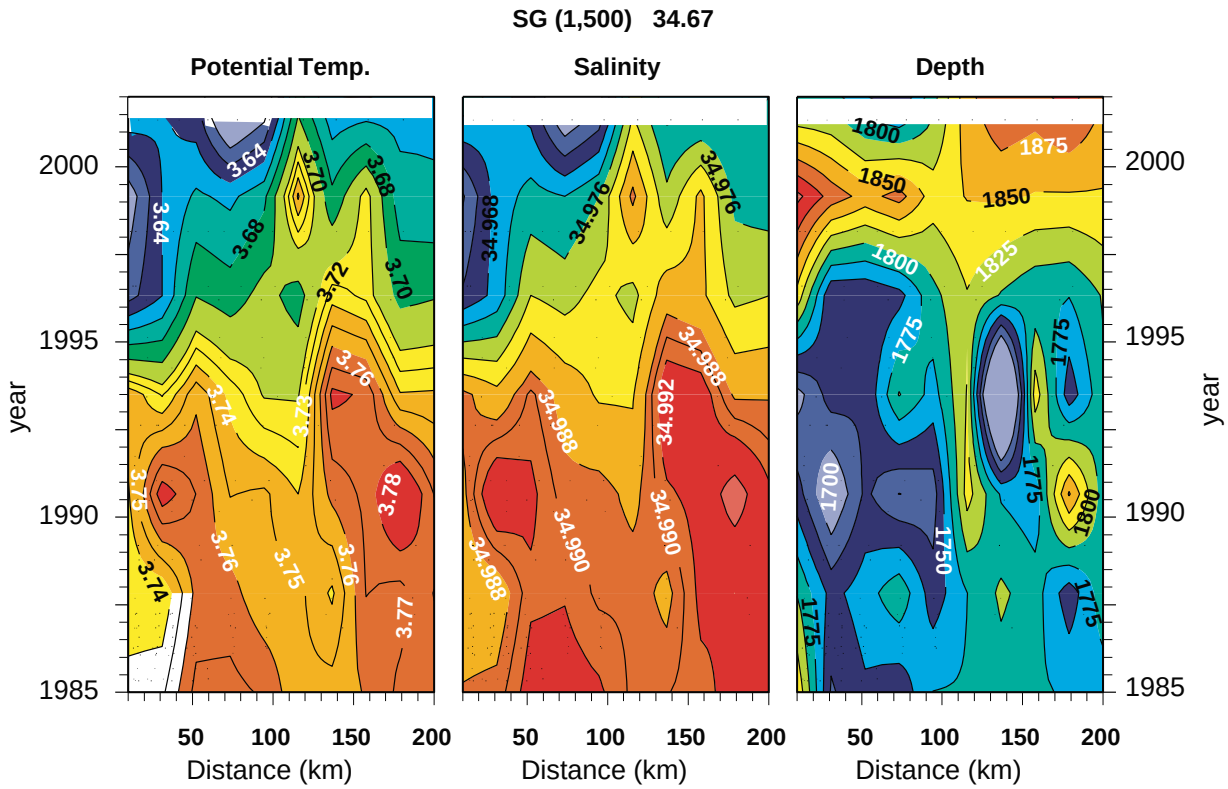

Fig. 5: Time series of T, S and depth along a density surface representing the Labrador Sea Water obtained from historical data collected east of Abaco Island, Bahamas. A pronounced cold, fresh pulse of Labrador Sea water appeared in 1995, less than eight years after it was produced in the Labrador Sea.

From Robertson and Mechoso: Links between the Atlantic Ocean and South American Climate Variability (page 16)

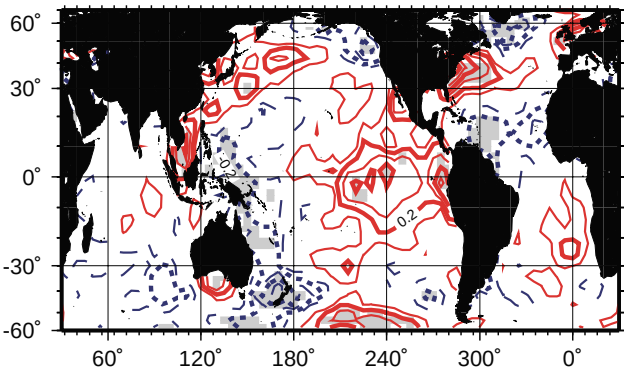

Fig. 2: Composites of GISST SST anomalies for one-sigma excursions of the 8-yr Corrientes oscillatory component in Fig. 1. Statistical significance at the 95% level indicated by shading; contour interval 0.1K.

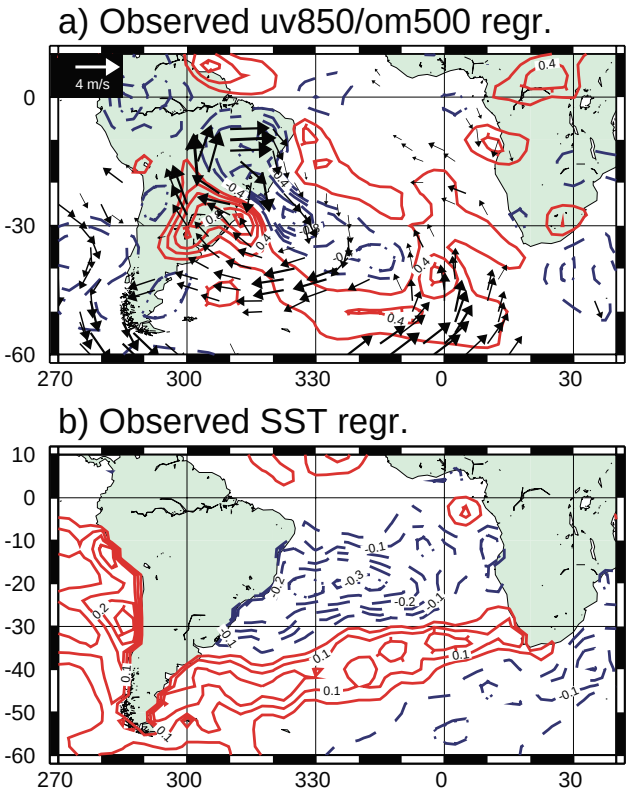

Fig. 3: Regression maps of the leading PC of 200-hPa JFM-averaged winds 1958–97 over southern South America from the NCEP-NCAR Reanalysis. (a) 850-hPa winds and 500-hPa omega, (b) GISST SST. Contour intervals are (a) 0.2 10^{-2} Pa s^{-1}, and (b) 0.05 K, with zero contour omitted.

From Robertson and Mechoso: Links between the Atlantic Ocean and South American Climate Variability (page 16)

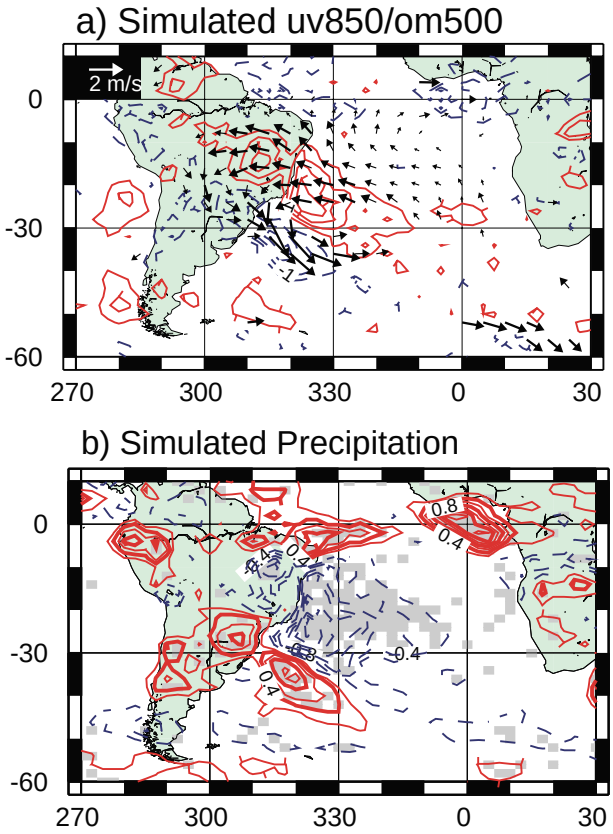

Fig. 4: GCM response (JFM average) to the SST anomaly pattern in Fig. 3b, with the latter scaled by a factor of three. (a) 850-hPa winds and 500-hPa omega (contours), and (b) precipation. The response is defined as the difference between an ensemble of 9 anomaly simulations are 20 control simulations. Shading indicates the 95% significance level, while in panel (a) only similarly significant vectors are plotted. Contour intervals are (a) 0.5 10^{-2} Pa s^{-1}, and (b) 0.2 mm day^{-1}; zero contours are omitted.

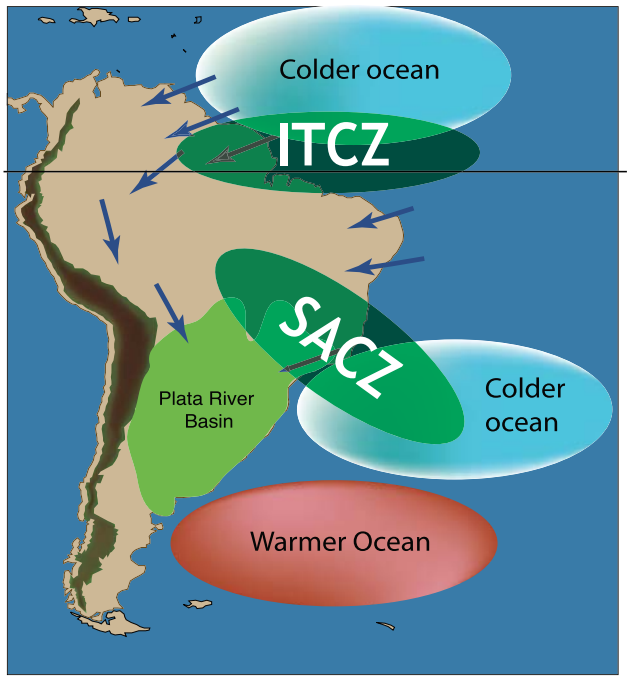

Fig. 5: A schematic of the main Atlantic-South American relationships discussed.

From Jochum et al.: Observing Tropical Instability Waves in the Atlantic Ocean (page 18)

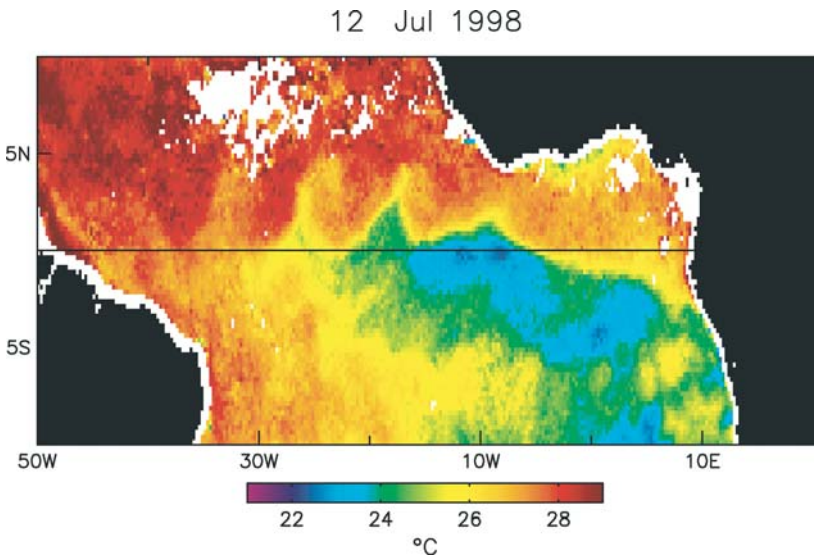

Fig. 1: The TIW are expressed in the SST by the four cusps of cold water along 2°N (courtesy of D. Chelton). The TIW are also present in the southern hemisphere but difficult to identify because of the weak thermal gradient there.

From Zhang et al.: Interior Pycnocline Transports in the Atlantic Subtropical Cells (page 27)

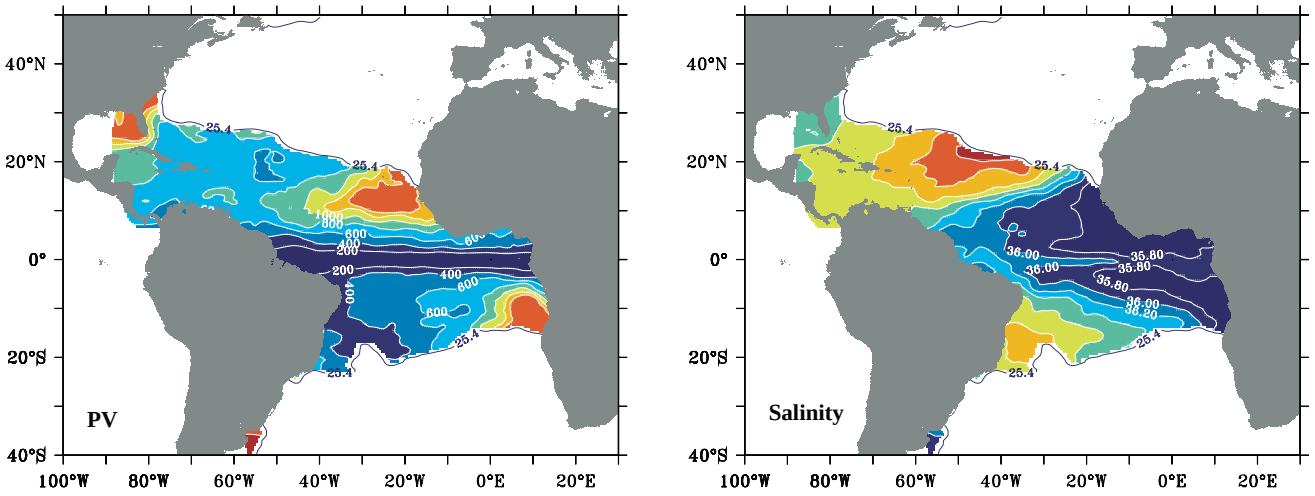

Fig. 1: (a, left) Absolute value of planetary potential vorticity (10^{-12} $m^{-1}s^{-1}$) and (b, right) salinity (PSU) on the isopycnal surface σ_θ = 25.4 kg m^{-3}. Outcrop lines (February and March in the Northern Hemisphere; August and September in the Southern Hemisphere) are shown by blue contours.

From Leffanue and Tomczak: Changes of Water Mass Properties observed in the Bermuda Time Series (BATS) (page 47)

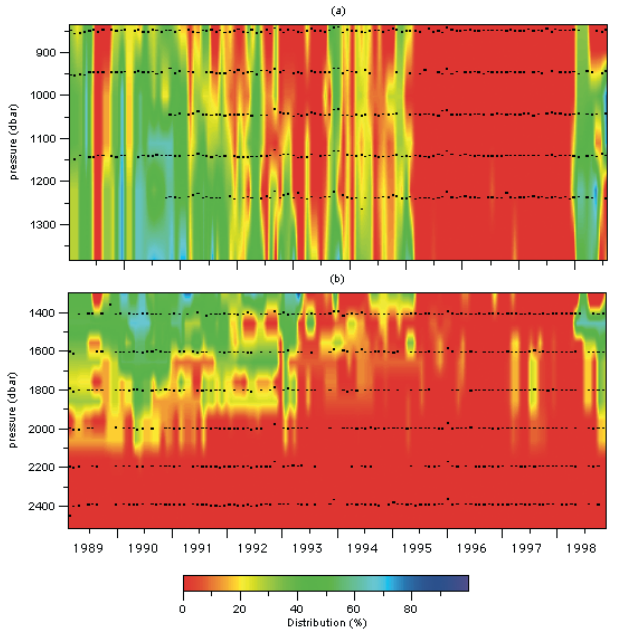

Fig. 1: Contribution (%) of Labrador Sea Water to the water column at the BATS study site. (a) depth range 900 – 1300m; (b) depth range 1400 – 2400m.

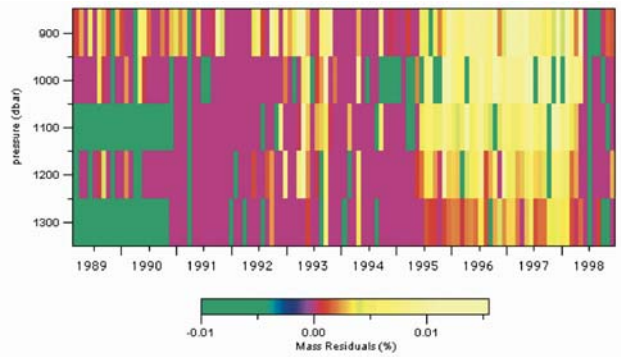

Fig. 2: Mass conservation residuals for depth range 900 – 1300m Green indicates no data.

From Hurrell and Folland: A change in Summer Atmospheric Circulation over the North Atlantic (page 52)

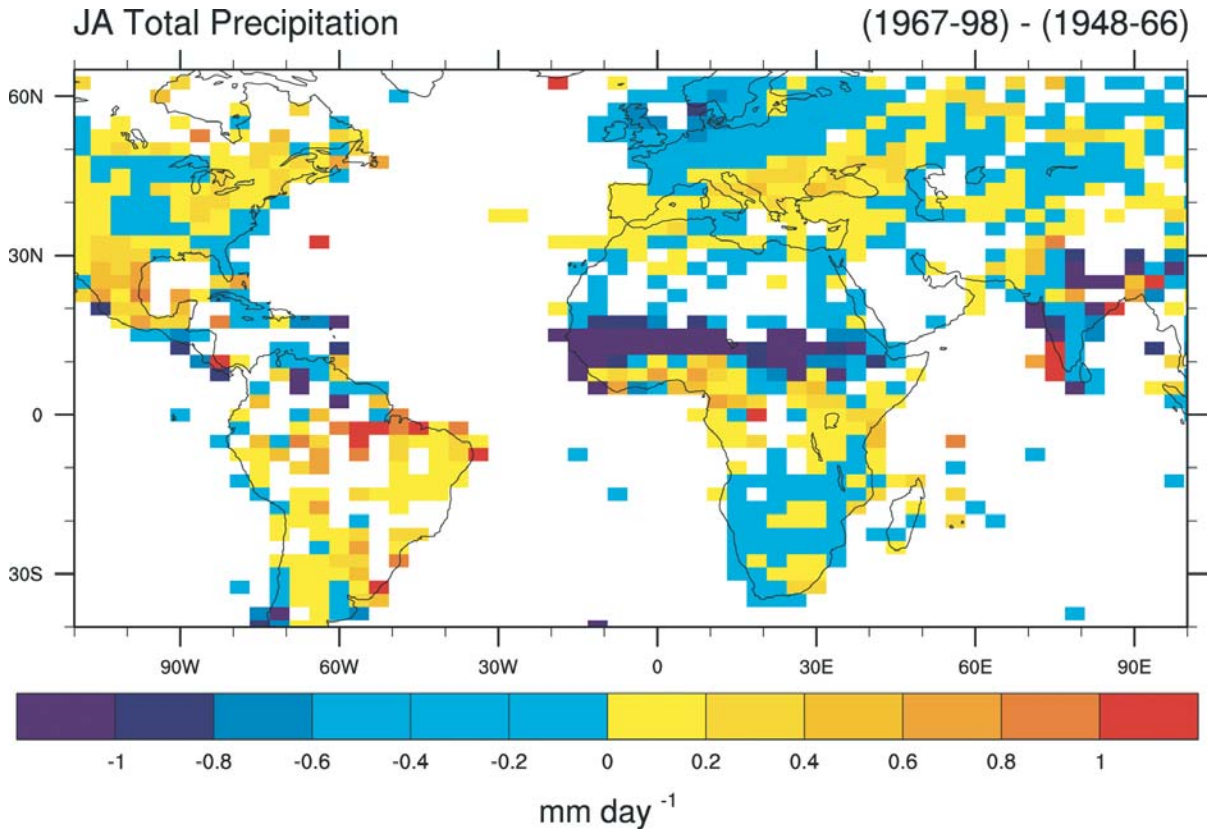

Fig. 3: The change in high summer (July-August) total precipitation (mm day^{-1}), 1967-1998 minus 1948-1966, estimated from land surface records ('g55wld0098.dat' constructed and supplied by Dr. Mike Hulme at the Climatic Research Unit, Univ. of East Anglia, Norwich, UK).

From Osborn: The winter North Atlantic Oscillation: roles of internal variability and greenhouse gas forcing (page 54)

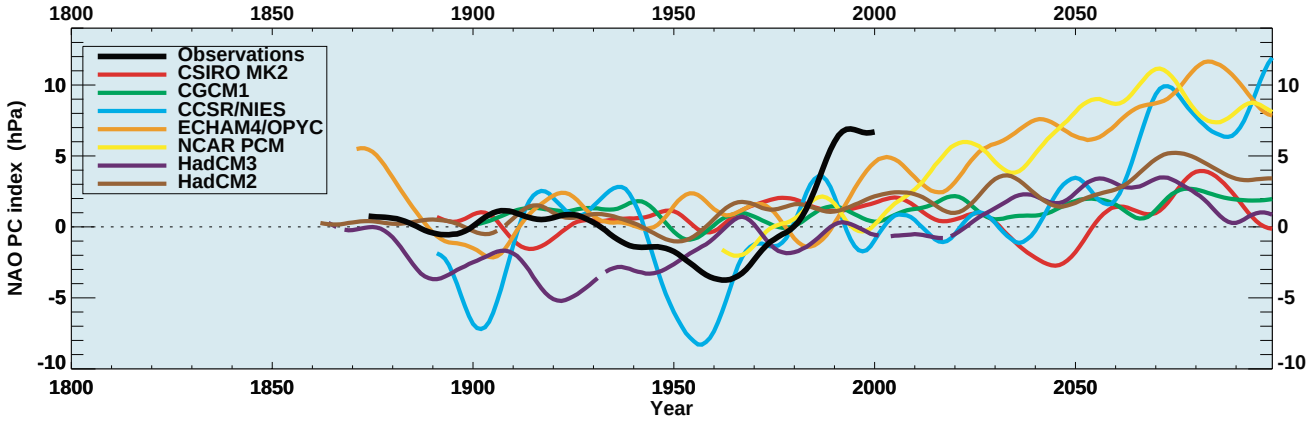

Fig. 4: Winter NAO indices (hPa) from observations (black) and from seven model simulations forced with increased carbon dioxide concentrations showing a shift towards positive NAO index that are consistent in sign though not in magnitude. All series have been smoothed by a 30-year low-pass filter.

From Fischer-Bruns et al.: Modelling the Late Maunder Minimum with a 3-dimensional OAGCM (page 58)

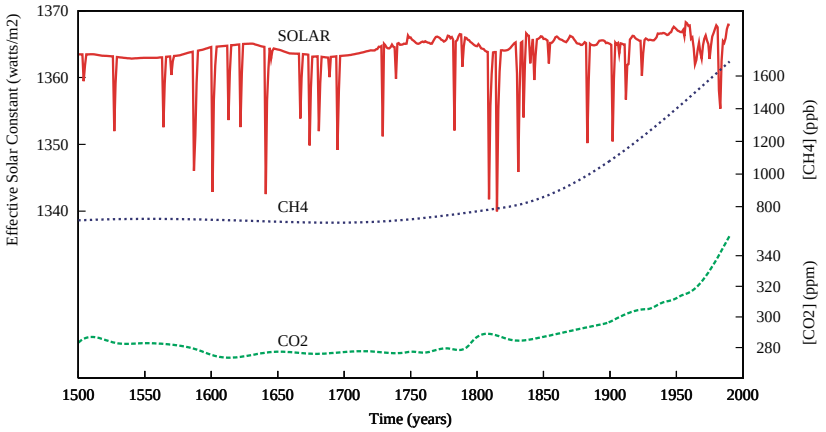

Fig. 1: Effective solar output (in W/m²) and concentrations of CO_2 and methane (CH_4) from 1500 to 2000 used to force the climate model.

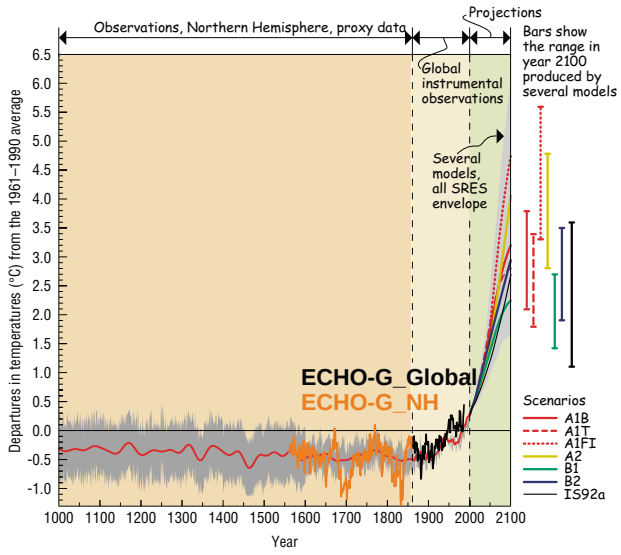

Fig. 2: Time series of mean temperature anomalies simulated in the 1550-1860 run for the NH (orange), for the whole globe from 1860 to 1990. These curves have been superimposed on the diagram of the IPCC synthesis report (Albritton et al., 2001) showing the temperature evolution according to Mann et al. (1998) and the projections up to the year 2100.

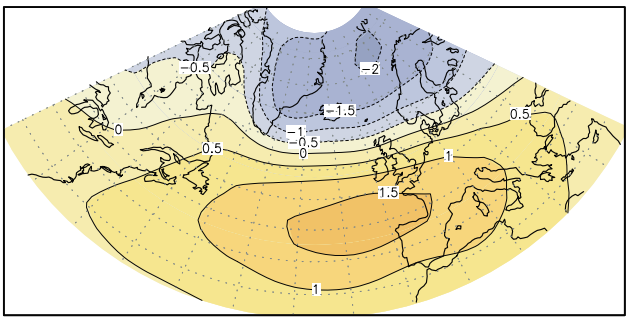

Fig. 4: Leading EOF of North Atlantic mean sea level pressure anomalies based on winter means (DJF) of the historic climate change simulation (1550-1990) explaining 38% of the total variance.

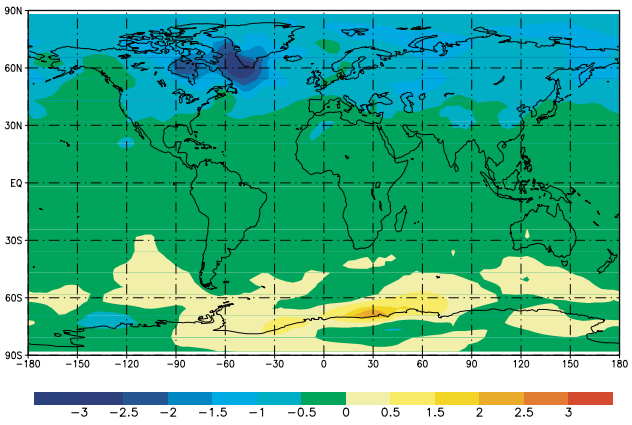

Fig. 3: Difference in annual mean near-surface air temperature, simulated during the Late Maunder Minimum event, 1675-1710, and the mean in 1550-1800 AD, in the forced simulation.

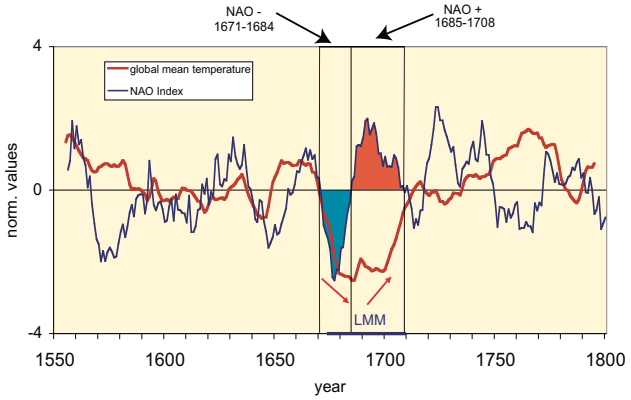

Fig. 5: Modeled annual global mean temperature and NAO index (1550-1800, normalized time series, 11 year moving average). In the LMM1 period (1671-1684, cooling phase) the NAO index is negative, in the LMM2 period (1685-1708, warming phase) the NAO index is positive.

From Karstensen et al.: Hydrographic and transient tracer response on atmospheric changes over the Nordic Seas (page 62)

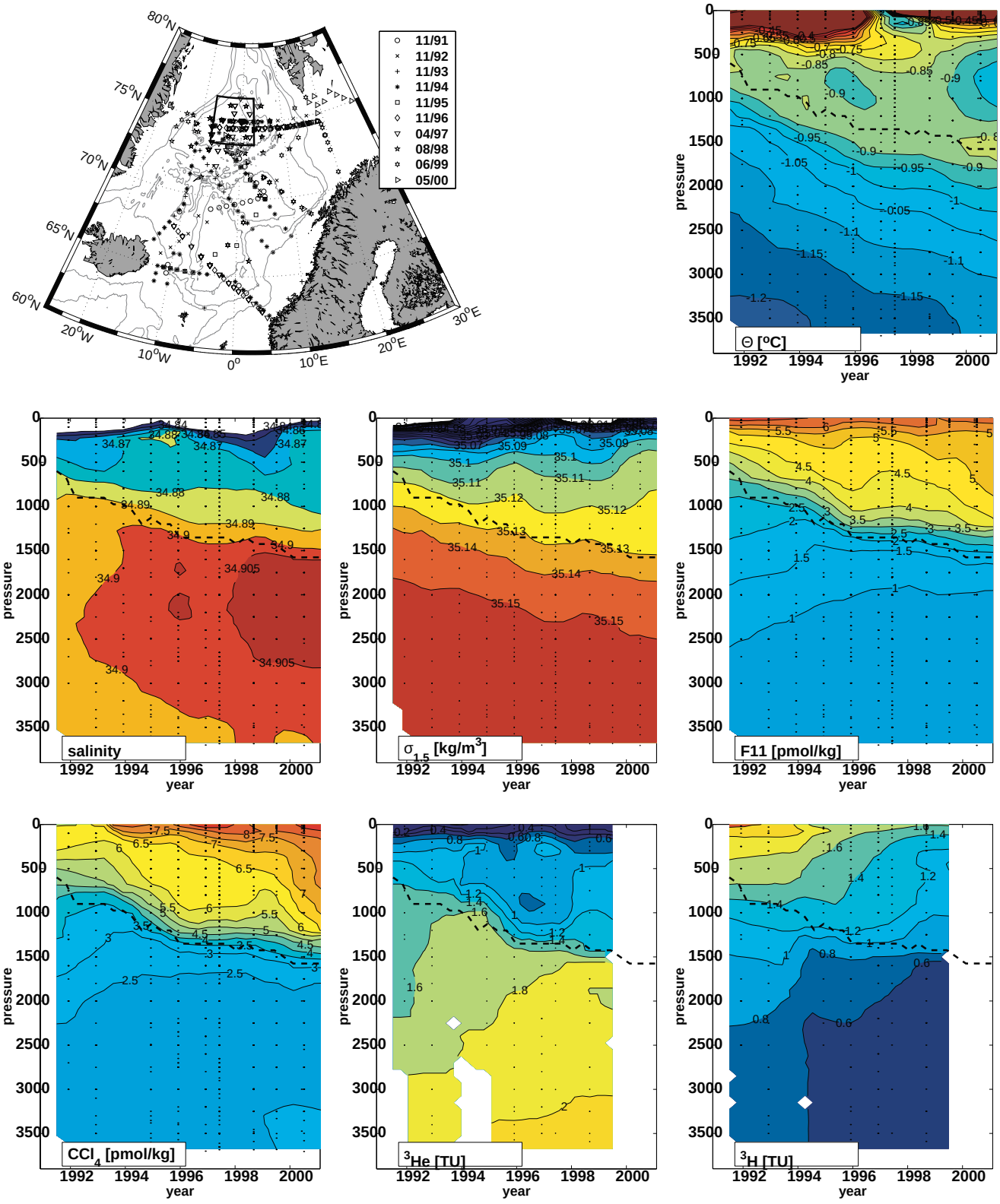

Fig. 1: Station map (upper left) and time series of (from the top right then in sequence to lower right): potential temperature, salinity, density anomaly referenced to 1500 dbar, F11, CCl_4, ^3He and tritium (^3H). A gaussian weighted interpolation scheme of all data between 7°W and 3°E and 73.5°N to 76.5°N (area indicated in map) was applied. The broken line indicates the temporal evolution of the intermediate temperature maximum (Tmax).

From Dickson and Boscolo: The Arctic-Subarctic Ocean Flux Study (ASOF): Rationale, Scope and Methods (page 64)

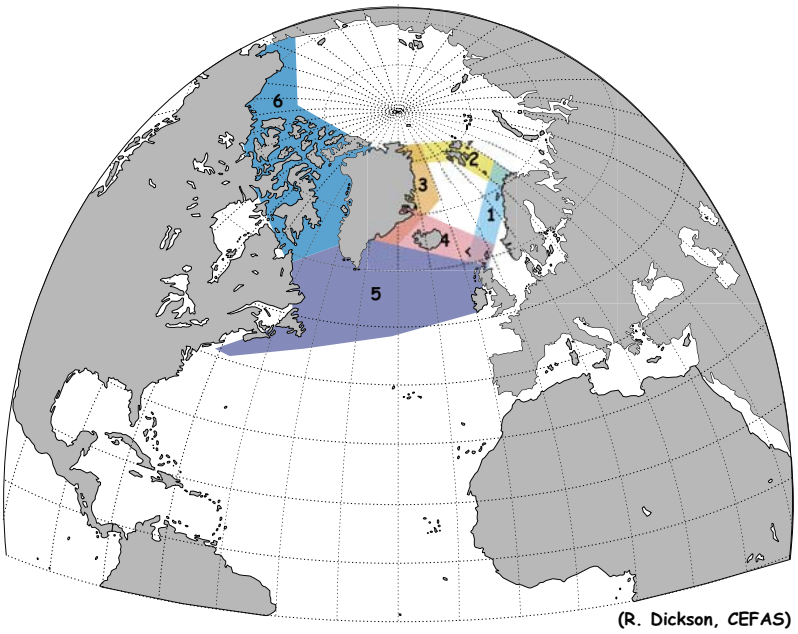

Fig. 1: The ASOF domain. (1) Warm water inflow to Nordic Seas; (2) Exchanges with Arctic Ocean; (3) Ice and fresh water outflow; (4) Greenland-Scotland Ridge exchanges; (5) Overflows and storage basins to Deep Western Boundary Current (DWBC); (6) Canadian Arctic Archipelago (CAA) throughflow.

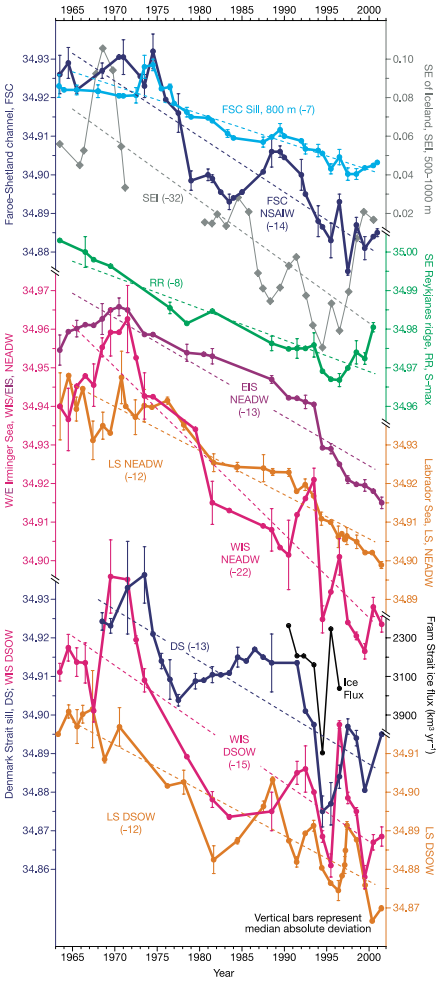

Fig. 2: Evidence that the following change in the upper Nordic Seas, the entire system of overflow and entrainment that ventilates the deep Atlantic has steadily changed in character over the past four decades, resulting in a sustained and widespread freshening of the deep and abyssal ocean (Dickson et al., 2002).

From Gabaldon et al.: Temperature Profiles contained in the CORIOLIS Database during its two first years (2000–2001) (page 68)

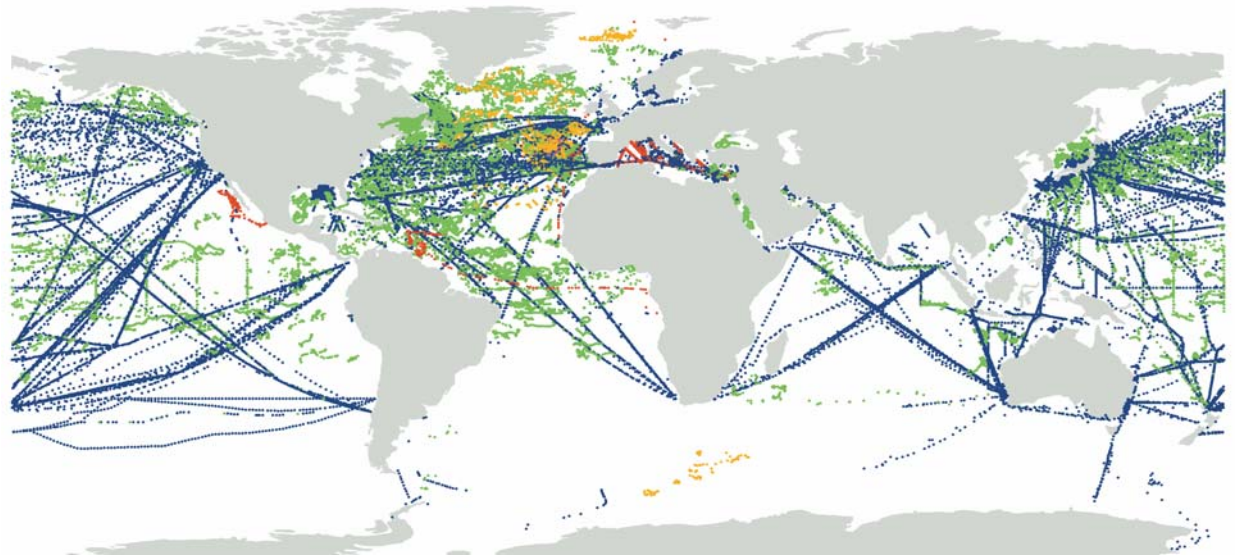

*Fig. 1: Total content of temperature profiles in the CORIOLIS Database on the 26th April, 2002. **TE** (green), **BA** (blue), **XB** (red), **PF** (orange) and **CT** profiles (pink).*

From Gabaldon et al.: Temperature Profiles contained in the CORIOLIS Database during its two first years (2000–2001) (page 68)

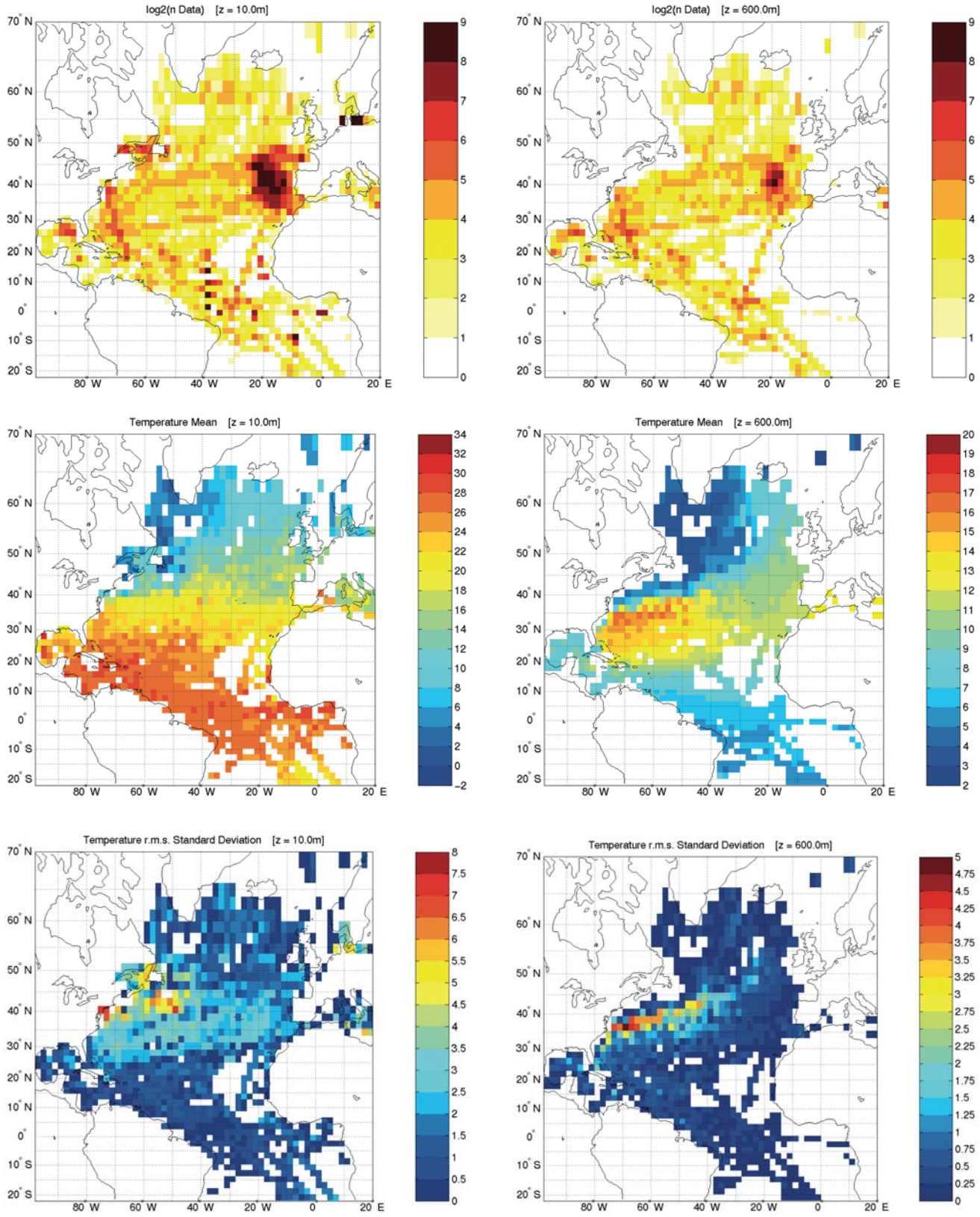

Fig. 5: Number of profiles by depth, mean temperature and standard deviation at 10 (left column) and 600 meters (right column), during the period [January'2000 – December'2001].

continued from page 34

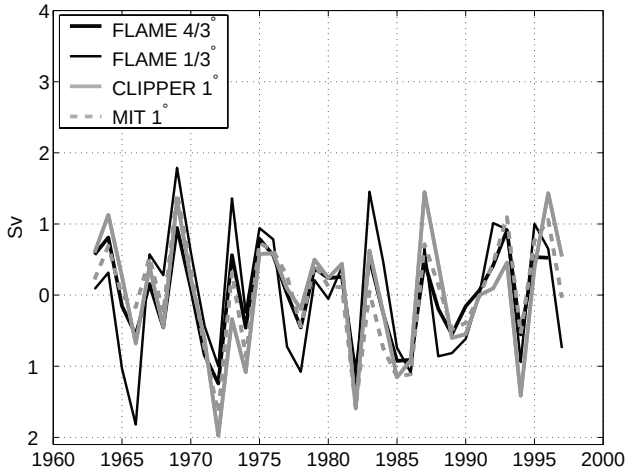

Fig. 1: Anomalies of the MOC transport at 45°N in the Atlantic over the last 40 years (annual means) from model experiments forced with atmospheric fluxes based on NCEP/NCAR reanalysis data (cf. text for details of the model setups).

freshwater flux for the period 1958 - 1997 taken from the NCEP/NCAR reanalysis project. An additional restoring of surface temperature and salinity to climatological values has been used following the formulation of Barnier (1998).

- An isotropic 4/3° MOM simulation from the FLAME hierarchy (Family of Linked Atlantic Model Experiments; see EW01 and http://www.ifm.uni-kiel.de/fb/fb1/tm/research/FLAME/index.html). The model configuration and forcing are similar to the experiments in EW01. This model has been forced with monthly NCEP/NCAR anomalies of wind stress and net heat flux for the period 1958 - 1996 added onto monthly climatological means based on an analysis of the ECMWF model (Barnier et al., 1995), including an SST restoring as mentioned above for the CLIPPER model. The freshwater flux in this model has been calculated by a restoring of the sea surface salinity to Levitus data. A number of sensitivity studies are available for the FLAME model that address the respective roles of interannual variations in wind and thermal forcing (EW01). Eddy induced tracer transport has been parameterized following Gent & McWilliams (1990; hereafter GM90)

- A 50 year forward run of the MIT ocean model (http://mitgcm.org/sealion) carried out in the framework of the ECCO project (http://www.ecco-group.org). This model has a regular 1° grid and has been forced with daily NCEP/NCAR reanalysis fluxes of wind stress, net heat and freshwater for the period 1948 - 2001. Surface temperature and salinity were relaxed additionally towards Reynolds SST and Levitus salinity fields, respectively. The model used a full mixed layer model (KPP; Large et al., 1994) and the GM90 parameterization. In the vertical the model used a lopped-cell formulation (Adcroft et al., 1997) which allows an improved representation of bottom slopes.

In addition we analyse an eddy-permitting FLAME experiment that has been set up and forced as the one described above, but uses an isotropic grid with 1/3° resolution. Although the forcing fields differ in their mean components, their variability is identical in the first two cases.

Results

Our focus here is on interannual changes of the MOC and their physical causes. For that purpose we start with an analysis of the strength of the MOC as a function of time on inter-annual and longer time scales.

Fig. 1 shows time series of the maximum of the annual mean overturning stream function at 45°N from the above mentioned simulations. The mean value and its multi-decadal trend have been eliminated from each time series since they are not of primary interest in this note. The mean overturning values lie in the range between 15.7 and 17.2 Sv. These quantities might be regarded to be model constants, the actual values of which depend critically on grid spacing (horizontally and vertically), choice of mixing parameterizations, mean forcing fields, and other details.

There is a striking similarity in phase and amplitude of the inter-annual fluctuations from all four simulations, regardless of resolution. Since the fluctuating part of the atmospheric forcing is essentially the same in all simulations it seems likely that the oceanic response to these fluctuations is a robust feature which in principle does not depend on model details, but represents a physical phenomenon that should be inferable from models given precise wind fields. Variations of ±1 Sv between successive years seem to be common, but they can reach more than 3 Sv in some years. It is noteworthy that the temporal trends in the three runs vary between enhancements of 1 Sv to 3 Sv over the four decades, with the largest trend being present in the MIT model. One way to interpret this trend is to associate it with density-driven long-term variations. Barotropic and baroclinic changes together thus could lead to decadal changes in the strength of the overturning within ±3-4 Sv (RSS).

To demonstrate similarities in the simulated oceanic response we will compare typical overturning differences between 1993 and 1994 as a function of latitude and depth (Fig. 2). We note that changes in the overturning are basically vertically coherent and are aligned with those in zonal wind stress. The modifications of the overturning circulation are a manifestation of the changes in the Ekman transport due to enhanced or reduced zonal winds in 1994. Between 35°N and 55°N, e.g., the increase in the zonal wind stress causes an enhanced Ekman transport to the south, thereby reducing the meridional transport to the north that forms the upper limb of the over-

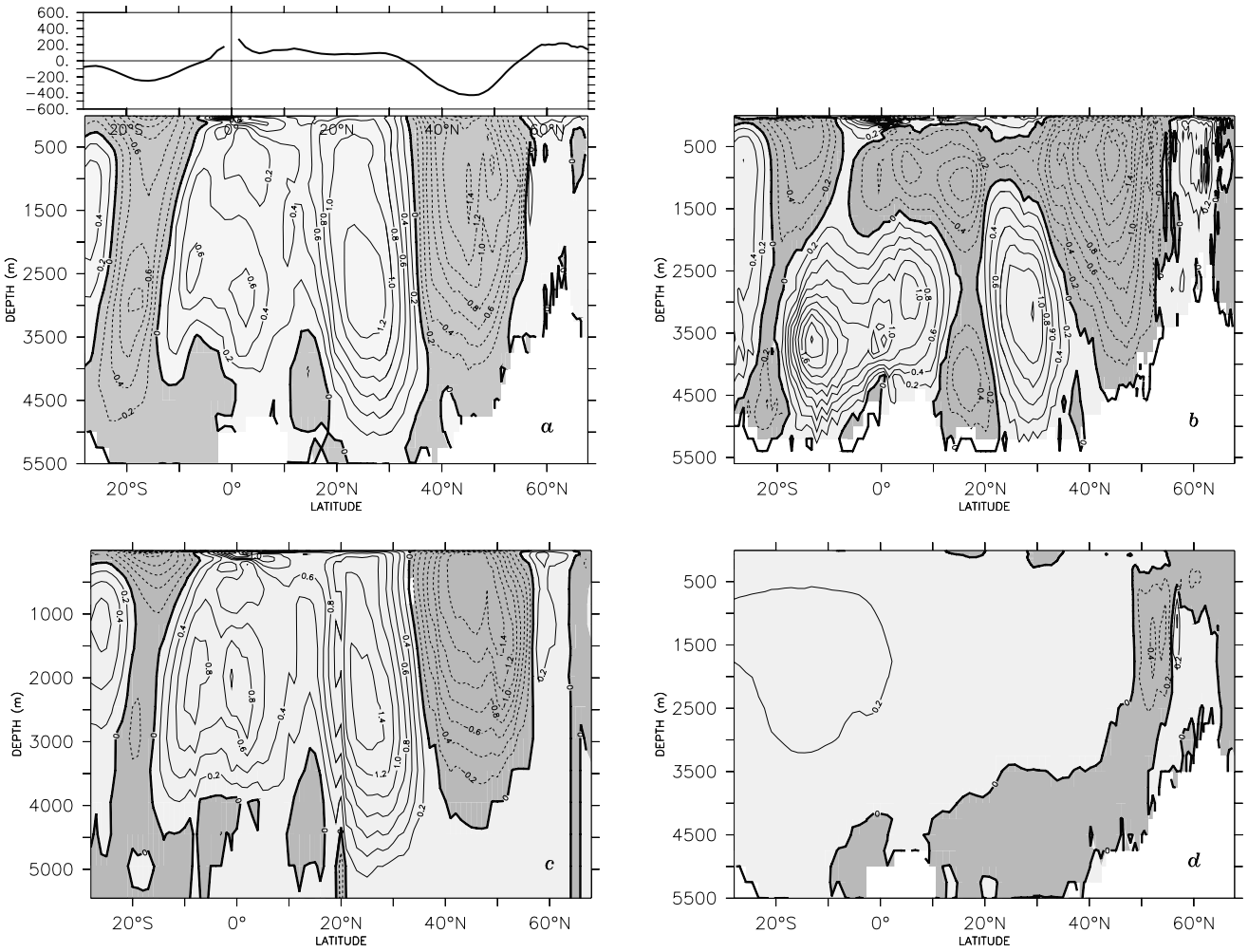

Fig. 2: Differences between the annual mean overturning fields in the Atlantic for 1994 and 1993 from (a) the FLAME 4/3° model, (b) the CLIPPER 1° model, (c) the MIT/ECCO 1° model, and (d) the 4/3° FLAME model with interannual fluctuations only in the buoyancy forcing. The top panel shows the 1994-1993 difference in the zonally averaged zonal wind stress divided by the Coriolis parameter (taken from the FLAME forcing data).

turning cell (Fig. 2a). This behaviour is similar to the one described by Dong and Sutton (2001) who found that the inter-annual variability of the oceanic heat transport is dominated by windstress-driven Ekman fluctuations.

The 1994-1993 difference pattern from the CLIPPER model (Fig. 2b) is similar to the one from FLAME in shape and magnitude, with the exception of the upper 1500m between 10°S and 40°N. This CLIPPER simulation did not include the GM90 parameterization, and comparison with a FLAME sensitivity run without GM90 shows that some of the discrepancies between the difference plots can be explained by this factor (not shown here). The difference pattern from the MIT model (Fig. 2c) is in very close agreement with the FLAME pattern, although the 1994-1993 changes have a slightly higher amplitude in the MIT model. We recall, however, that the forcing of the MIT model contained much higher frequencies, and it needs to be investigated if a rectifying effect on the overturning circulation exists on various time scales.

A summary of the relation between wind stress fluctuations and variations in the overturning is given in Fig. 3 showing the correlation of local changes of the zonal wind stress component with changes in MOC as a function of depth and latitude in the FLAME 4/3° model. Surprising is the significant correlation between both quantities, even at depth in mid-latitudes. Interesting is also the clear deviation from this behaviour near the equator, but especially north of 60°N (GIN Sea). Recent studies show the enhanced impact of bottom topography and the associated bottom torque as well as the reduced direct wind impact in the vorticity balance of the high latitudes (e.g., Hughes and de Cuevas, 2001; Lu and Stammer, 2002).

For completeness it needs to be mentioned that the correlation shown in Fig. 3 is dominated by inter-annual variations. For these frequencies wind is the dominating force leading to predominantly barotropic changes. Baroclinic changes are less pronounced as shown in Fig. 2d. It shows results from a FLAME case study with inter-annual fluctuations only in the buoy-

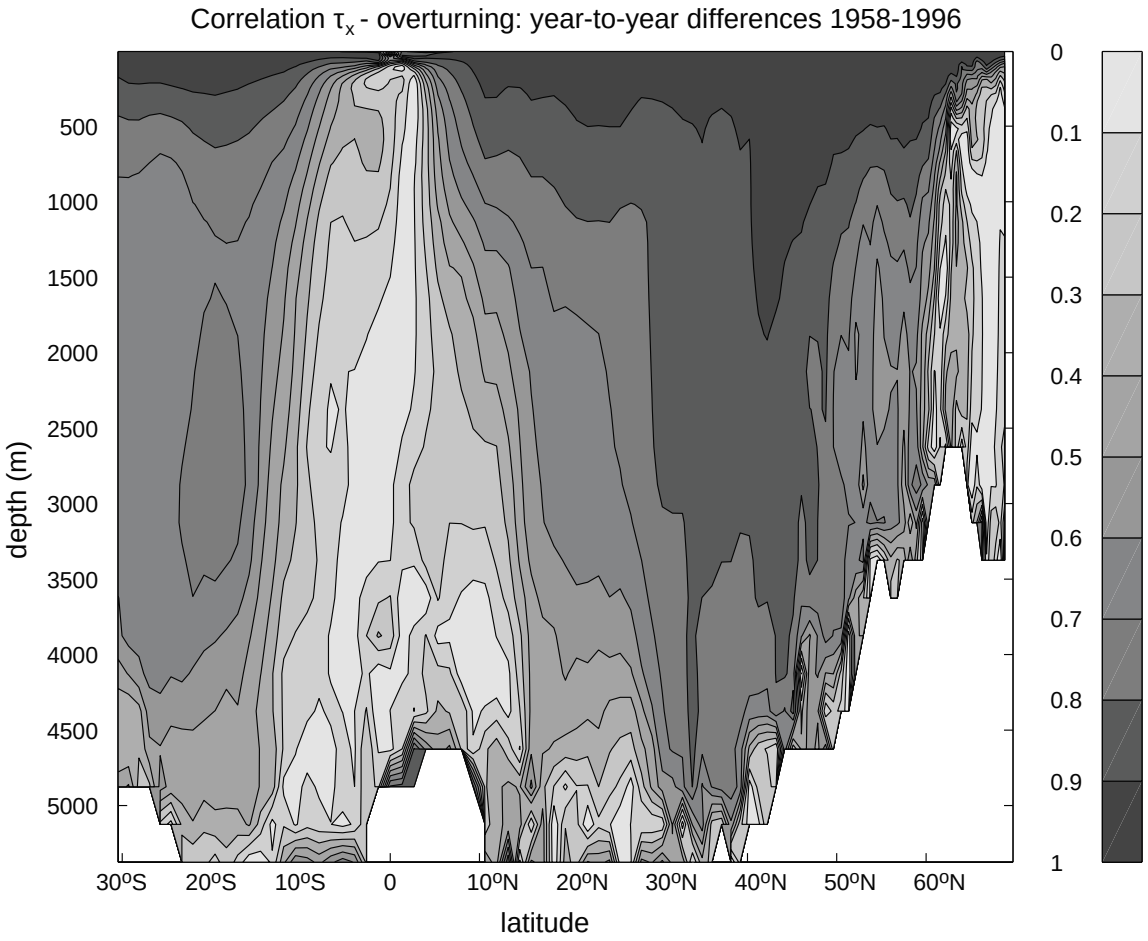

Fig. 3: Correlation of local overturning changes to changes in the zonal wind stress as function of latitude and depth for the FLAME 4/3° model.

ancy forcing. Comparing the 94-93 differences in the MOC strength to the case with both interannually varying buoyancy and wind forcing (Fig. 2a) shows that the wind effect (local or remote) clearly dominates the year-to-year variability.

Perspectives

An important result from our intercomparison effort is the indication that different ocean models (using different numerical methods, e.g. for describing horizontal advection or vertical convection processes, and a variety of parameterizations for subgridscale mixing) that are being forced with similar atmospheric fluxes show strong similarities in their reaction of climatically important features such as the strength of the MOC to inter-annual variations in the wind stress forcing. A closer inspection of the model fields reveals, however, a number of differences between the models due to the different physical parameterizations and the different underlying numerics. Whereas inter-annual overturning fluctuations seem to be entirely due to changes in the zonal wind stress over the North Atlantic, we expect to see a trend towards increased buoyancy driven changes on longer time scales.

Our investigations will have an impact on the design of observing systems for meridional ocean transports of mass and heat. Besides the question which variables need to be measured the model results might also be of help for the spatial arrangement of moorings, e.g., by providing information about whether transport changes are concentrated near the western boundary or not.

References

Adcroft, A.J., C.N. Hill, and J. Marshall, 1997: Representation of topography by shaved cells in a height coordinate ocean model. *Mon. Wea. Rev.*, **125**, 2293-2315.

Barnier, B., 1998: Forcing the ocean. In: *Ocean Modelling and Parameterization*, E. Chassignet and J. Verron (eds.), Kluwer Academic Publishers, 45-80.

Barnier, B., L. Siefridt, and P. Marchesiello, 1995: Thermal forcing for a global ocean circulation model using a three-year climatology of ECMWF analysis. *J. Mar. Sys.*, **6**, 363-380.

Beismann, J.-O., and B. Barnier, 2002: Variability of the thermohaline circulation of the North Atlantic: Sensitivity to overflows of dense water masses. *Ocean Dynamics*, to be submitted.

Curry, R.G., M.S. McCartney, and T.M. Joyce, 1998: Oceanic transport of subpolar climate signals to mid-depth subtropical waters. *Nature*, **391**, 575-577.

Dong, B.W., and R.T. Sutton, 2001: The dominant mechanisms of variability in Atlantic ocean heat transport in a coupled ocean-atmosphere GCM. *Geophys. Res. Lett.*, **28**, 2445-2448.

Eden, C., and J. Willebrand, 2001: Mechanism of interannual to decadal variability of the North Atlantic circulation. *J. Climate*, **14**, 2266-2280.

Gent, P.R., and J.C. McWilliams, 1990: Isopycnal mixing in ocean circulation models. *J. Phys. Oceanogr.*, **20**, 150-155.

Gulev, S.K., B. Barnier, H. Knochel, J.-M. Molines, and M. Cottet, 2002: Water mass transformation in the North Atlantic and its impact on the meridional circulation: insights from an ocean model forced by NCEP/NCAR reanalysis fluxes. *J. Climate*, submitted.

Häkkinen, S., 1999: Variability of the simulated meridional heat transport in the North Atlantic for the period 1951-1993. *J. Geophys. Res.*, **104** (C5), 10991-11007.

Hughes, C.W., and B.A. de Cuevas, 2001: Why western boundary currents in realistic oceans are inviscid: a link between form stress and bottom pressure torques. *J. Phys. Oceanogr.*, **31**, 2871-2885.

Kalnay, E., M. Kanamitsu, R. Kistler, W. Collins, D. Deaven, L. Gandin, M. Iredell, S. Saha, G. White, J. Woollen, Y Zhu, M. Chelliah, W. Ebisuzaki, W. Higgins, J. Janowiak, K.C. Mo, C. Ropelewski, J. Wang, A. Leetma, R. Reynolds, R. Jenne, and D. Joseph, 1996: The NCEP/NCAR 40-Year Reanalysis Project. *Bull. Amer. Meteor. Soc.*, **77**, 437-471.

Kanzow, T., 2000: Integrale Erfassung langperiodischer Transporte: Simulation und Optimierung eines verankerten Systems. Master's thesis, Institut für Meereskunde Kiel, Germany.

Large, W.G., J.C. McWilliams, and S.C. Doney, 1994: Oceanic vertical mixing: A review and a model with a nonlocal boundary layer parameterisation. *Rev. Geophys.*, **32**, 363-403.

Lu, Y., and D. Stammer, 2002: Vorticity balance in a global ocean circulation model. *J. Phys. Oceanogr.*, to be submitted.

Madec, G., P. Delecluse, M. Imbard, and C. Lévy, 1998: OPA8.1 Ocean General Circulation Model reference manual. Notes du Pôle de modélisation 11, Institut Pierre-Simon Laplace, France, 91 pp.

Marotze, J., S.A. Cunningham, and H.L. Bryden, 2002: Monitoring the Atlantic Meridional Overturning Circulation at 26.5°N. Proposal to the NERC Rapid Climate Change Thematic Programme (http://www.nerc.ac.uk/funding/thematics/rcc/).

Marshall, J., A. Adcroft, C. Hill, L. Perelman, and C. Heisey, 1997: A finite-volume, incompressible navier-stokes model for studies of the ocean on parallel computers. *J. Geophys. Res.*, **102** (C3), 5753-5766.

Pacanowski, R., 1995: MOM 2 documentation, user's guide and reference manual. GFDL Tech. Rep. 3, 123 pp.

Tréguier, A.-M., T. Reynaud, T. Pichevin, B. Barnier, J.-M. Molines, A.P. de Miranda, C. Messager, J.-O. Beismann, G. Madec, N. Grima, M. Imbard, C. Le Provost, 1999: The CLIPPER Project: High Resolution Modelling of the Atlantic. *International WOCE Newsletter*, **36**, 3-5, Southampton, UK.

Conference Announcement

OCEANS: Ocean Biogeochemistry and Ecosystems Analysis
Open Science Conference, January 7-10, 2003

This conference is designed to gather community input to develop a new ten-year international research project, OCEANS. The Transition Team developing the OCEANS project outlines below some ideas to seed discussion at the Open Science Conference. The conference will include plenary presentations, discussion sessions and poster presentations.

The primary goal of OCEANS is to understand the sensitivity of the ocean to global change within the context of the broader Earth System, focusing on biogeochemical cycles, marine food webs and their interactions. The overarching questions to seed discussion are:

- How does global change, represented by changes in natural climatic modalities and anthropogenic forcings, impact marine biogeochemical cycles and ecosystem dynamics?
- How do these impacts alter the mechanistic relationship between elemental cycling and ecosystem dynamics?
- What are the feedback mechanisms to the Earth System from these changes?

OCEANS will seek a comprehensive understanding of the impacts of climate and anthropogenic forcings on food-web dynamics (i.e., structure, function, diversity, and stability) and elemental cycling (i.e., geochemical pathways, transfers, and cycling), including the impacts of underlying physical dynamics of the ocean. It will also strive for mechanistic and predictive understanding of how these linked systems respond to global change resulting from natural climate modes (e.g., the El Niño-Southern Oscillation [ENSO] and the North Atlantic Oscillation [NAO]) and anthropogenic perturbations, and then feedback to climate, ocean physics, and marine resources). An integral tool for this research is palaeoceanography, including the reliable calibration of proxies for macro and micro-nutrients, productivity, plankton composition, temperature, and other physical changes.

Some areas of the ocean are likely to be particularly sensitive to gradual long-term changes and will be subject to intensive studies. These "hot spots" often occur in critical domains such as regions of upwelling and deep mixing, continental margins, high-latitude areas, the sediment-water interface, the mesopelagic layer and intermediate waters.

For full programme and registration details, visit www.igbp.kva.se/obe/

Changes of Water Mass Properties observed in the Bermuda Time Series (BATS)

Heidi Leffanue and Matthias Tomczak
School of Chemistry, Physics and Earth Sciences
Flinders University of South Australia
Adelaide, Australia
corresponding e-mail: heidi.leffanue@flinders.edu.au

Introduction

The world's oceans play a major role in climate variability and climate change as the exchange of heat and momentum with the atmosphere results in a closely coupled relationship of global influence. Water masses receive their signatures from atmospheric processes and are therefore good indicators for changes in climatic conditions.

Some of the most important water masses of the global ocean are formed in polar regions during wintertime, when observations of atmospheric conditions and resulting water mass formation are difficult if not impossible. This study explores the possibility of inferring climate-induced changes of water mass properties in polar and subpolar regions from hydrographic observations in the subtropics.

Data from the BATS station in the Sargasso Sea (Bermuda Atlantic Time-series Study, nominal location 31°40'N, 64°10'W) were utilised for the project. This is a high quality time series comprising monthly observations of hydrographic parameters including temperature, salinity, oxygen, nitrate, phosphate and silicate. These parameters are requirements for Optimum Multiparameter (OMP) analysis, an inverse modelling technique which determines the relative contributions of various water masses to a water sample. The most recent development of the method (Karstensen and Tomczak, 1998) accounts for the non-conservative behaviour of oxygen and nutrients by applying Redfield ratios, thereby allowing extended OMP analysis to be applied at basin-wide scales, using water masses which originate in areas remote from the study region.

The study aimed at identifying decadal changes in water mass properties – this is reflected in the time-behaviour of the residuals i.e., periods of "unusual" water mass properties (which do not match the predetermined source water types) will be seen as periods of abnormally large residuals.

Results

The analysis generally produced realistic models of the distribution and contribution of the various water masses present in the Sargasso Sea. Low residuals were obtained for each depth range indicating a good match between source water types and the actual data set. A major outcome was the irregular distribution of Labrador Sea Water (LSW).

Figs. 1a and 1b (page 37) show the contribution of LSW to the make-up of the water at depths between 900m and 2400m. Much vertical structure and temporal variation can be seen, with an apparent absence of LSW in the interval from mid 1995 to early 1998.

This is an unlikely scenario as LSW is the major component of the water column between depths of 900 to 1800m in the western Atlantic Ocean. It is more likely that this is a record of property modifications of LSW and the subsequent time lag between the source region and Bermuda. Such modifications could also explain the large rise in error levels associated with the apparent variations in Labrador Sea Water content (Fig. 2, page 37).

These mass conservation residuals, plotted as a percentage, indicate the quality of the solution. The absolute size of the error is of no significance (the equations for the model matrix are weighted by the user and therefore the residuals can be made as small as desired by increasing the weight for mass conservation); but changes of the residuals in space and time can reveal significant changes or errors in source water types or water mass distribution.

The largest residuals in the 900-1300m depth range appear mainly in time intervals which correspond to an 'absence' of LSW in the water column (compare Fig. 1b), with the remainder of the data displaying near zero mass conservation errors.

Discussion

LSW forms convectively during winter in the central Labrador Sea. This has been shown to be a sporadic process (Talley and McCartney, 1982; Clarke and Gascard, 1983), although the water mass produced generally exhibits consistent properties with LSW classically defined as relatively warm and of low salinity.

Dickson et al. (1996) have suggested that long term changes in convective activity in the North Atlantic are in response to atmospheric forcing, namely the North Atlantic Oscillation (NAO). The NAO is a large scale alternation of the atmospheric masses between the Icelandic low and the Azores high pressure cells. A 'high index' pattern indicates strong mid-latitude westerlies, which blow cold, dry air from Canada across the Labrador basin and are a significant factor in determining the depth of winter convection in the Labrador Sea (Curry and McCartney, 1996).

From records of the ocean weather ship (OWS) Bravo, increased production of deeply convected water has intensified from 1988 (Lazier, 1995). Dickson et al. (1996) found that continued deepening convection eventually reached into the lower layers of the water column,

entraining Iceland Scotland Overflow Water and Denmark Strait Overflow Water. This resulted in a cooler but more saline LSW, from around 1990 to 1995. These findings are of interest, as a colder and saltier LSW corresponds to the initial proposition that classically defined LSW has been modified during the study period. The time lapse between LSW formation and its arrival in the subtropics is the remaining consideration in supporting this proposal.

Early studies estimated a LSW transit time from source to the subtropics of eighteen years (Smethie, 1993; Doney and Jenkins, 1994), but more recent analysis of temperature, salinity and tracer data suggests a time lag of 10 years from the Labrador Sea to the Bahamas (26.5^{0}N) (Molinari et al., 1998). These contrasting results were interpreted by the researchers as possible fluxes in the energy state of the Gulf Stream and its recirculation, with the Deep Western Boundary Current linking more directly with the Labrador Sea when energy levels are relatively low and therefore establishing a shorter route.

Pickart et al. (1996) argue that increased forcing due to the harsh winters of the 1980s and 1990s has led to formation of LSW outside of the Labrador Sea, where it is easily entrained into the Deep Western Boundary Current and carried southward quickly, evading the recirculating gyre of the Labrador Sea. Curry et al. (1998) showed that the correlation between strong subpolar convection and temperature changes near Bermuda was highest at a five to six year time lag, implying that after extreme convection in the Labrador Sea, the subtropical basins receive large volumes of LSW with a cooler temperature signal five to six years later.

To summarise, severe winters brought on by strong NAO events and/or simultaneous NAO/ENSO episodes in the 1980s and 1990s created suitable conditions for very deep convection in the Labrador Sea. Since 1990, prolonged intensification has pushed the convection process into the more saline water masses below, resulting in LSW which is colder and saltier than the classical definition. Assuming a lag time of around 5 to 6 years, this denser LSW may account for the large gap showing in the distribution plots between 1995 and 1998.

Future Directions

OMP analysis has proved to be an effective tool for identifying subpolar climate changes using observations made in the subtropics. Future work will have to concentrate on development of OMP analysis into a nonlinear minimisation scheme that allows simultaneous variation of the water mass contribution and the user-defined source water type matrix. This would allow not only the identification of periods of unusual water mass properties (such as in this case) but also a quantitative determination of the change that occurred. The result could be a time history of source water type properties for several water masses formed in different regions, derived from observations at a single location in the easily accessible subtropics. Work in that direction is proceeding.

References

Clarke, R.A., and J.C. Gascard, 1983: The formation of Labrador Sea Water Part I: large-scale processes. *J. Phys. Oceanogr.*, **13**, 1764-1778.

Curry, R.G., and M.S. McCartney, 1996: Labrador Sea Water Carries Northern Climate Signal South. *Oceanus*, **39**, 2, 24-28.

Curry, R.G., M.S. McCartney, and T.M. Joyce, 1998: Oceanic transport of subpolar climate signals to mid-depth subtropical waters. *Nature*, **391**, 575-577.

Dickson, R.R., J. Lazier, J. Meincke, P. Rhines, and J. Swift, 1996: Long term coordinated changes in convective activity of the North Atlantic. *Progr. Oceanogr.*, **38**, 241-295.

Doney, S.C., and W.J. Jenkins, 1994: Ventilation of the Deep Western Boundary Current and abyssal western North Atlantic: Estimates from tritium and ^{3}He distributions. *J. Phys. Oceanogr.*, **24**, 638-659.

Karstensen, J., and M. Tomczak, 1998: Age determination of mixed water masses with CFC and oxygen data. *J. Geophys. Res.*, **24**, 2777-2780.

Lazier, J.R.N., 1995: The Salinity Decrease in the Labrador Sea over the Past Thirty Years. In: *Natural Climate Variability on Decade-to-Century Time Scales*, Martinson D.G., K. Bryan, M. Ghil, M.M. Hall, T.M. Karl, E.S. Sarachik, S. Sorooshian, and L.D. Talley (eds), National Academy Press, Washington DC, 295-302.

Molinari, R.L., R.A. Fine, W.D. Wilson, R.G. Curry, J. Abell, and M.S. McCartney, 1998: The arrival of recently formed Labrador Sea Water in the Deep Western Boundary Current at 26.5^{o}N. *Geophys. Res. Lett.*, **25**, 2249-2252.

Pickart, R.S., M.A., Spall, and J.R.N. Lazier, 1996: Mid-depth ventilation in the western boundary current system of the sub-polar gyre. *Deep Sea Research*, **44**, 1025-1054.

Smethie, W.M., 1993: Tracing the thermohaline circulation in the western North Atlantic using chlorofluorocarbons. *Progr. Oceanogr.*, **31**, 51-99.

Talley, L.D., and M.S. McCartney, 1982: Distribution and circulation of Labrador Sea Water. *J. Phys. Oceanogr.*, **12**, 1189-1204.

Impact of Individual El Niño Events on the North Atlantic European Region

Pierre-Philippe Mathieu[1], Rowan T. Sutton[1], and Buwen Dong[2]
[1]Department of Meteorology, University of Reading, Reading, UK.
[2]Met Office, Bracknell, UK.
corresponding e-mail: mathieu@met.rdg.ac.uk

1. Introduction

In the special issue of CLIVAR Exchanges on Tropical-Extratropical interactions (No. 23), several papers addressed the important problem of understanding the remote impacts of ENSO. In the North Atlantic / European (NAE) region the impacts of ENSO are generally weaker that those seen in the Pacific / North American (PNA) sector. Nevertheless, significant climate anomalies do occur, and progress in understanding these anomalies is important to ongoing efforts in seasonal prediction.

Most of the past research into the impacts of ENSO on the NAE region has employed composite analyses (e.g. Fraedrich, 1994). The purpose of such an approach is to highlight the common impacts and average out "contaminating" variability. A limitation is that, in reality, every ENSO event is unique and the averaging process obscures the unique aspects. These aspects may include potentially predictable climate anomalies that arise in response to the particular distribution of SST anomalies associated with the individual ENSO event.

The impact of individual ENSO events on the PNA sector has been researched by Hoerling and Kumar (1997). We are investigating the impacts on the NAE region. As an integral part of this work we are examining the respective roles of (a) SST anomalies in the Indian and Pacific Oceans, and (b) SST anomalies in the Atlantic Ocean.

2. Methodology

We conducted two ensemble experiments of 10 integrations with the UK Met Office atmospheric model HadAM3 (Cox et al., 1999). The first experiment, "GLOB", was forced over the 1986-2001 period by the global observed Sea Surface Temperatures (SST) from Reynolds et al. (2002). For the second experiment, "IPAC", the SST is identical to GLOB in the Indian and Pacific basins but differs in the Atlantic basin (between 30°S and 75°N) where climatological SST values are imposed. Our analyses focus on the ensemble means of each experiment. Comparison of GLOB with the model's time mean climatology provides information about the pattern and predictability of the ENSO response, while the IPAC experiment provides insight into the specific contribution of Indian and Pacific SST forcing. The difference between the GLOB and IPAC, referred to as "ATL", provides a measure of the influence of Atlantic SST on the atmosphere.

Our experimental methodology and objectives are similar to the study of Dong et al. (2000) but we extend their study by analysing 6 ENSO events, 3 El Niños and 3 La Niñas. For reasons of space, however, we restrict our attention here to two El Niño events, 1987/88 (EN1) and 1991/92 (EN2), and also focus solely on the model results without discussing the comparison with observations. The reader is referred to Mathieu et al. (2002) for a more comprehensive discussion.

3. Results

Fig. 1 shows results for the two El Niño events. Shown in the figure are the observed SST anomalies (relative to a 1986-2001 climatology) and simulated anomalies in 500hPa geopotential height (GPH) for GLOB, IPAC and ATL. Shading indicates significance at the 95% level. Comparison of the results for GLOB shows that both events were associated with potentially predictable atmospheric signals in the NAE region. Over North America both events feature a dipole pattern of anomalies characteristic of the tail end of the PNA pattern. Further east, however, there are major differences. In EN1 a band of negative anomalies is sandwiched to the north and south and by positive anomalies. This pattern is similar to that identified in past composite studies of the ENSO influence on the NAE region (Fraedrich, 1994). By contrast, the pattern for EN2 is quite different. Positive anomalies are located in the midlatitudes over the North Atlantic and the pattern overall is suggestive of a wave train emanating from the Carribean region. The contrast between EN2 and EN1 illustrates the fact that different El Niño events may give rise to very different climate impacts in the NAE region.

Comparison of the results for IPAC shows that, even when the influence of Atlantic SST anomalies is removed, there is a potentially predictable signal in both cases. Furthermore, the circulation anomalies for the two events differ considerably. These differences stem from the different SST anomalies in the Pacific and Indian Oceans. For example, the weaker SST anomalies in the tropical Pacific during EN1 excite a weaker response in the NAE region than is seen for EN2.

Lastly, the results for ATL show clearly that, for both events, SST anomalies in the Atlantic Ocean had a significant impact on the climate of the NAE region. Moreover, the Atlantic conditions had very different impacts for the two events. In EN1 the pattern of GPH anomalies is similar to that seen in GLOB, with a band of negative anomalies in midlatitudes sandwiched to the

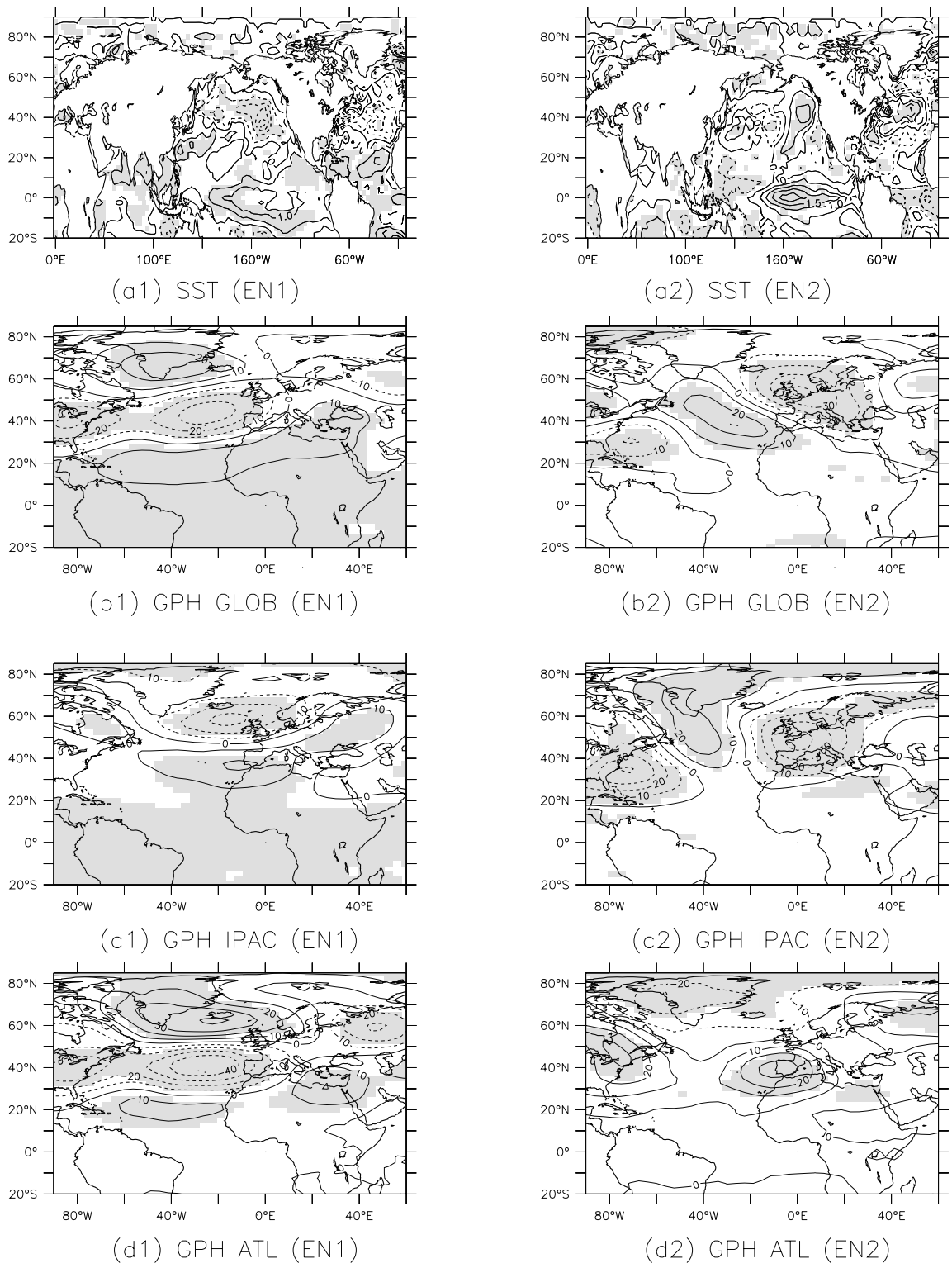

Fig. 1: Oceanic forcing and atmospheric response during the 1987/88 (EN1) and 1991/92 (EN2) El Niño events. Winter (December-January-February) anomalies of observed Sea Surface Temperature (SST) [a] and simulated Geopotential Height at 500mb (GPH) for GLOB [b], IPAC [c] and ATL [d]. In [a-b-c], SST and GPH anomalies are calculated with respect to 1986-2001 climatological period, and the model GPH climatology is derived from the GLOB experiment. In [d], GPH anomalies are calculated as the difference between the ensemble means of the GLOB and IPAC experiments. Shading in the GPH plots indicates 95% significance from a t-test. Shading in the SST plots [a] indicates regions where anomalies exceed one standard deviation of the inter-annual variability.

north and south and by positive anomalies. The pattern for EN2, on the other hand, is almost opposite with positive anomalies in midlatitudes sandwiched by negative anomalies to the north and south. Our research has shown that these different patterns can be understood as responses to the different SST anomalies that were found in the Atlantic Ocean during the two events. In particular, during EN1 positive SST anomalies were located in the tropical Atlantic Ocean. These SST anomalies caused an intensification, and small southward shift, of the ITCZ (not shown). Associated with this shift is an anomalous divergent circulation and Rossby wave source (Sardeshmukh and Hoskins, 1988). Other research that we have conducted (Sutton et al., 2001) suggests that the pattern of extra-tropical anomalies can be understood as, primarily, a remote response to this tropical Rossby wave forcing.

In the case of EN2, negative SST anomalies were located in the tropical Atlantic. These SST anomalies caused a weakening of the ITCZ and therefore, to the extent that the behaviour is linear, a Rossby wave forcing of the opposite sign to EN1. In reality nonlinearities are present but it appears that linear theory provides the first order explanation for the different impacts of Atlantic SST anomalies during EN1 and EN2.

4. Conclusions

The present study refines the traditional composite view of ENSO-NAE teleconnections by shedding light on the way in which the climate impacts can vary between individual El Niño events. Our results support the existence of significant, and hence potentially predictable, El Niño related impacts on the climate of the NAE region, but also demonstrate that these impacts can differ considerably from event to event. The differences originate in part from differences in the SST forcing in the Pacific and Indian oceans. In addition, however, we have shown that SST anomalies in the Atlantic Ocean can also have an important influence, and sometimes dominate the influence from the Pacific. It is interesting, for example, that the GLOB response in EN1 that - as we noted - resembles traditional composite views is in fact forced primarily by conditions in the Atlantic rather than those in the Pacific. This result invites us to revisit the classical focus on Niño3-averaged SST (or similar indices) as the sole important predictor of remote ENSO impacts. In the development of systems for seasonal prediction of NAE climate, attention must not be limited to a narrow focus on the tropical Pacific.

References:

Cox, P.M., R.A. Betts, C.B. Bunton, R.L.H. Essery, P.R. Rowntree, and J. Smith, 1999: The impact of new land surface physics on the GCM simulation of climate and climate sensitivity. *Clim. Dyn.*, **15**, 183-203.

Dong, B.-W., R.T. Sutton, S.P. Jewson, A. O'Neill, and J.M. Slingo, 2000: Predictable winter climate in the North Atlantic sector during the 1997-1999 ENSO cycle, *Geophys. Res. Lett.*, **27**, 985-988.

Fraedrich, K., 1994: An ENSO impact on Europe? A review. *Tellus*, **46A**, 541-552.

Hoerling, M.P., and A. Kumar, 1997: Why do North American climate anomalies differ from one El Niño to another? *Geophys. Res. Lett.*, **24** (9), 1059-1062.

Mathieu, P-P., R.T. Sutton, B.-W. Dong, and M. Collins, 2002: Predictability of winter climate over the North Atlantic European region during ENSO events. *J. Climate*, submitted.

Reynolds, R. W., N. A. Rayner, T. M. Smith, D. C. Stokes, and W. Wang, 2002: An improved in situ and satellite SST analysis. *J. Climate*, in press.

Sardeshmukh, P.D., and B.J. Hoskins, 1988: The generation of global rotational flow by steady idealised tropical divergence. *J. Atmos. Sci.*, **45**, 1228- 1251.

Sutton, R.T., W.A. Norton, and S.P. Jewson, 2001: The North Atlantic Oscillation - What Role for the Ocean?. *Atmospheric Science Letter*, doi:10.1006/asle.2000.0018.

A Change in the Summer Atmospheric Circulation over the North Atlantic

James W. Hurrell[1] and Chris K. Folland[2]
[1]National Center for Atmospheric Research
Boulder, CO, USA
[2]Hadley Centre for Climate Prediction and Research
Met Office, Bracknell, UK
corresponding e-mail: jhurrell@ucar.edu

1. Introduction

The North Atlantic Oscillation (NAO) has been identified as one of the five principal research areas of the DecCen component of CLIVAR. One reason is that the NAO and its time dependence appear central to the current global change debate. A substantial fraction of the warming of the Northern Hemisphere continents over recent decades is linked to the behaviour of the NAO, in particular a change in the boreal winter atmospheric circulation toward enhanced middle latitude westerly flow (the positive NAO index phase). But what about changes in the Atlantic climate during other times of the year?

The hitherto general focus on the variability of the wintertime Atlantic climate is understandable: the winter months are dynamically the most active, so perturbations in the atmosphere can grow to large amplitudes. However, "climate noise" associated with weather variations is also larger during winter. Because strong climate anomalies can be detected during other times of the year and the noise of natural variability is less, useful insights into the mechanisms responsible for those signals can be obtained. This is especially true of summer, when variability is particularly important from the perspective of droughts and heat waves.

We are examining the annual cycle of climate and climate change over the Atlantic and investigating the mechanisms responsible for the variability through analyses of both observed and climate model data. Coherent fluctuations of surface pressure, temperature and precipitation occur throughout the year, and decadal and longer-term variability is not confined to winter. In the following, we briefly describe one of our more interesting results. A more complete description, including numerical experiments to elucidate physical mechanisms, will be described elsewhere.

2. Results

The spatial pattern of the leading eigenvector of Northern Hemisphere sea level pressure (SLP) during high summer (July-August) is a dipole with a southern center of action extending over the northeast Atlantic across western Europe into Scandinavia and a northern center over the Arctic. This may be viewed as the "summer NAO" (e.g., Hurrell and van Loon, 1997), although the amplitudes of the SLP anomalies are substantially weaker and further north and east relative to winter. A time series of July-August SLP area-averaged over the southern center reveals strong variations on interannual to multi-decadal time scales (Fig. 1). Most striking, perhaps, is the transition from an extended period of below-average SLP to positive SLP anomalies since about 1967 (see also Rodwell and Folland, 2002). The spatial pattern of this change (not shown) reveals locally statistically significant increases in SLP greater than 2 hPa over much of northern Europe during 1967-2001 relative to 1921-1966. This change toward persistent anticyclonic flow during high summer in recent decades is reflected in other variables as well, which increases our confidence that the signal is real. For instance, mean central England surface air temperature (CET) has increased ~0.35°C decade^{-1} since 1965 during both July and August (more than the mean rate of warming in winter), with the warming concentrated in maximum temperature (Sexton et al., 2002). Over the longer period 1900-1998 high summer CET shows more (significant) warming (0.09°C decade^{-1}) than does the annual mean (0.06°C decade^{-1}).

The changes in the mean circulation during high summer have been accompanied by a pronounced shift in the storm tracks and associated synoptic eddy activity. We have examined transient eddy statistics from more than 50 years of NCEP/NCAR reanalyzed atmospheric data, band-passed filtered to retain fluctuations on time scales of 2-8 days. The distribution of 300 hPa height variance for July-August reveals a climatological variance maximum near 55°N to the south of Greenland and Iceland (Fig. 2). The change in recent decades has been a northward shift and eastward extension of storm activity, with the largest reduction in variance near 50°N over

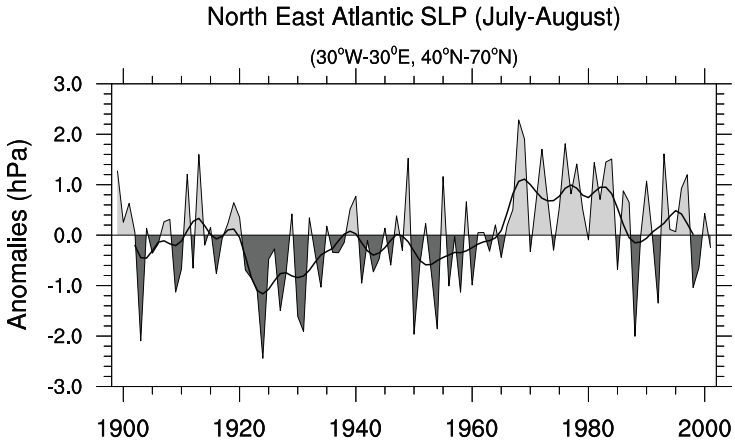

Fig. 1: Anomalies of July-August sea level pressure (SLP) area-averaged over the domain 30°W-30°E, 40°N-70°N from 1899-2001. The heavy solid line represents the SLP variations smoothed with a low-pass filter that eliminates fluctuations with periods less than about 4 years.

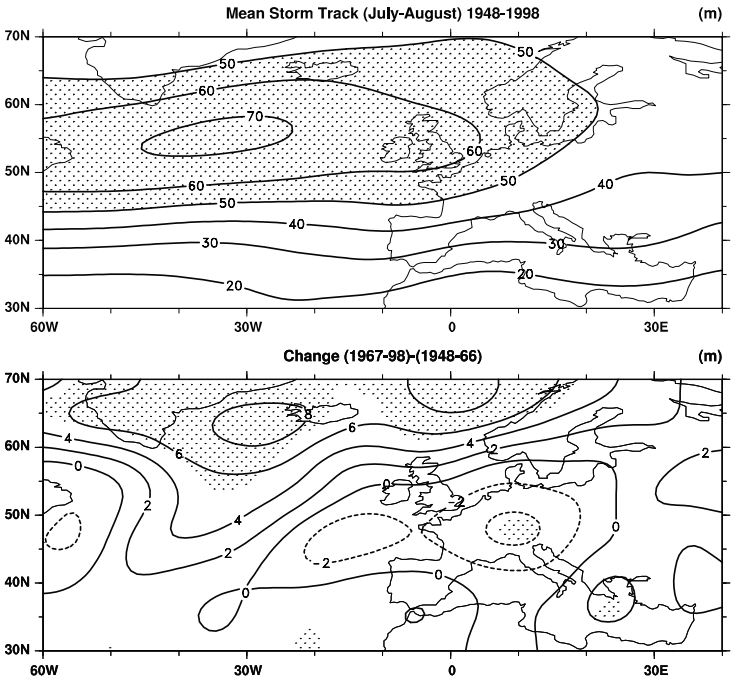

Fig. 2: Mean storm track for 1948-1998 high summers (July-August), and the change after 1966, as revealed by the 300 hPa root mean square transient geopotential height (m) band-pass filtered to include 2-8 day period fluctuations. Differences significantly different from zero at the 5% level using a t-test are stippled on the lower panel.

Europe. These changes in the mean and eddy components of the flow affect the transport and convergence of moisture and, therefore, can be directly related to changes in regional precipitation. Indeed, summer precipitation over much of northern Europe has been about 15% lower compared to earlier decades (e.g., Fig. 3, page 38). An analysis of more than 200 years of data from stations throughout England and Wales reveals a significant drying trend since the 1950's with several of the driest high summers on record occurring since 1970 (not shown).

A regression of July-August streamfunction anomalies throughout the troposphere onto the SLP time series of Fig. 1 reveals a strong equivalent barotropic component to the circulation anomalies over the northeast Atlantic and Europe (not shown). At lower latitudes, when SLP is anomalously high over the North Atlantic, the dominant global feature is a lower tropospheric anticyclonic couplet that straddles the equator over the tropical Atlantic and tropical North Africa with a more extensive cyclonic couplet in the upper troposphere. This structure suggests a relationship between changes in tropical Atlantic diabatic heating, including rainfall variations over the Sahel, and extra-tropical Atlantic circulation anomalies during high summer. Indeed, Fig. 3 shows the pronounced drying in recent decades across tropical North Africa that is well documented in the literature, and suggests a possible extension of the drying across the tropical North Atlantic.

The long record of precipitation over the Sahel is well known as one of the clearest examples of a regional, interdecadal climate signal. This region receives most (80-90%) of its annual mean rainfall (100-500 mm) during July to September. The linear correlation between annual Sahel rainfall and the SLP time series of Fig. 1 is -0.53 over 1901-1998. A plot of the squared coherence between the two time series reveals that variations on interdecadal time scales (periods greater than 20 years) contribute the most to the observed correlation, as the squared coherency is greater than 0.7 at these lower frequencies (not shown; see also Ward, 1998). The lower correlations on sub-decadal time scales are to be expected, given the internal variability of the extra-tropical atmosphere.

3. Discussion

The causes of observed seasonal rainfall variations over tropical North Africa, and the Sahel region in particular, have been of interest for a long time, and a large body of literature exists on the topic. Of particular interest on decadal time scales has been the association between Sahel rainfall and a leading mode of global, seasonal sea surface temperature (SST) variability that describes a tendency for out-of-phase variations between Northern Hemisphere and Southern Hemisphere SST anomalies (e.g., Folland et al., 1986; Palmer, 1986; Ward, 1998). The correspondence between the record of Sahel rainfall and a time series of the interhemispheric SST mode is quite strong (r~0.6 over 1901-1998), especially on interdecadal time scales (not shown). But are such SST variations fundamental to the observed link between Sahel rainfall and high summer circulation anomalies over the extra-tropical North Atlantic?

We are addressing this question in part through analysis of several different atmospheric general circulation model (AGCM) ensembles, where the AGCMs were forced with the time history of observed SSTs. Most of the models are able to reproduce the observed Sahel-extra-tropical North Atlantic relationship, whereby a summer season of higher-than-average surface pressure over northern Europe is accompanied by reduced rainfall over the tropical North Atlantic and North Africa. Initial results, based on analysis of variance techniques that separate climate variability into forced (i.e., due to SST variations) and unforced (i.e., due to internal atmospheric dynamics) components, suggest the link occurs primarily through mechanisms internal to the atmosphere (D.P. Rowell, personal comm.), whereby variations in the tropical Atlantic and Sahel rainfall force changes in high summer North Atlantic climate through an atmospheric bridge mechanism similar to that over the Pacific sector during ENSO. The observed low frequency changes in summer climate over Europe, then, may arise indirectly from processes that affect tropical Atlantic precipitation on long time scales, such as the inter-hemispheric gradient in tropical Atlantic SST. The results also suggest, however, a weaker direct atmospheric circula-

tion response to SST forcing. This would be consistent with Rodwell and Folland (2002), who argue that the high summer anticyclonic trend over northern Europe is, at least partly, an ocean-forced signal.

References

Folland, C.K., T.N. Palmer, and D.E. Parker, 1986: Sahel rainfall and worldwide sea temperature 1901-1985. *Nature*, **320**, 602-607.

Hurrell, J.W., and H. van Loon, 1997: Decadal variations in climate associated with the North Atlantic Oscillation. *Clim. Change,* **36**, 301-326.

Palmer, T.N., 1986: The influence of the Atlantic, Pacific and Indian Oceans on Sahel rainfall. *Nature*, **322**, 251-253.

Rodwell, M.J., and C.K. Folland, 2002: Atlantic air-sea interaction and model validation. *Annali di Geofisica,* in press.

Sexton, D.M.H., Parker D.E., and C.K. Folland, 2002: Natural and human influences on Central England temperature. *J. Climate*, submitted.

Ward, M.N., 1998: Diagnosis and short-lead time prediction of summer rainfall in tropical North Africa at interannual and multidecadal timescales. *J. Climate*, **11**, 3167-3191.

The winter North Atlantic Oscillation: Roles of Internal Variability and Greenhouse Gas Forcing

Timothy J. Osborn
Climatic Research Unit, School of Environmental Sciences, University of East Anglia, Norwich, UK
corresponding e-mail: t.osborn@uea.ac.uk

1. Introduction

The North Atlantic Oscillation (NAO) has been an important driver of circum-Atlantic climate variability during the extended boreal winter, especially over recent decades (Hurrell, 1995; Wanner et al., 2001). The NAO is relevant, therefore, to seasonal predictability during the wintertime in these regions (e.g., Rodwell et al., 1999). The fact that it has also exhibited (Fig. 1) strong multi-decadal variations since the mid-twentieth century means that the NAO has also become relevant to climate change issues (e.g., Hurrell, 1996; Osborn et al., 1999; Gillett et al., 2000). Fig. 1a shows the winter NAO index time series of Jones et al. (1997), updated through winter 2001/2 (data courtesy of Phil Jones). The multi-decadal variations that have been strong since 1900 are clear, together with the strong trend from the low-index 1960s to the high-index early 1990s. Recent winters have an average NAO index that is only slightly above the 1961-1990 mean, and the trend from the 1960s to the early 1990s has not continued. Nevertheless, it is important to understand the causes of the multi-decadal variations, particularly whether they are related to anthropogenic forcing of climate or are an expression of natural climate variability.

Results from an analysis of forced and unforced coupled climate model simulations are reported here, focusing on the two issues of (i) whether the internally-generated variability exhibited by the climate models is sufficiently strong to be a possible explanation of recent NAO changes; and (ii) whether these climate models' responses to increased greenhouse gas concentrations includes a change in the NAO index that might have contributed to recent changes and that might continue into the future. Analyses along these lines have been undertaken before (e.g., Osborn et al., 1999; Ulbrich and Christoph, 1999; Fyfe et al., 1999; among others), but the advance made here is that seven different climate models (Table 1) have been utilised, with very similar experiments being available from each, and all models are analysed using exactly the same methods. This enables a multi-model comparison that is quantitative rather than just qualitative in nature. Results from the average of the seven model analyses will be published in Gillett et al. (2002), while full results (including an analysis of changes in the characteristics of inter-annual NAO variability under enhanced greenhouse forcing) will be presented elsewhere (Osborn, manuscript in preparation, available from the author).

2. Data and methods

2.1 Observed data

Monthly-mean sea level pressure (SLP) from 1873 to 1997 on a 5° latitude by 10° longitude grid covering much of the northern hemisphere were used. This data set is derived from the Met Office analyses (Jones, 1987; also see Basnett and Parker, 1997, for further discussion, though note that their GMSLP2 data set was not used here). A December to March (DJFM) average is formed from the monthly data to provide the mean winter SLP used here [Osborn et al. (1999) gave reasons for the use of this four month seasonal mean].

2.2 Simulated data

Monthly sea level pressure fields, averaged across the December to March season, were taken from the seven different coupled ocean-atmosphere climate models listed (with acronyms and references) in Table 1. Data from five of these models were obtained from the Intergovernmental Panel on Climate Change (IPCC) Data Distribution Centre (http://ipcc-ddc.cru.uea.ac.uk/), while data from the HadCM2 and HadCM3 simulations were obtained from the Climate Impacts LINK Project (http://www.cru.uea.ac.uk/link/); all the modelling centres are gratefully acknowledged for allowing their data to be distributed for research and impacts use.

For each model, data were taken from control integrations with unchanging external forcing, varying in length from 200 to 1400 years. Winter SLP was also taken

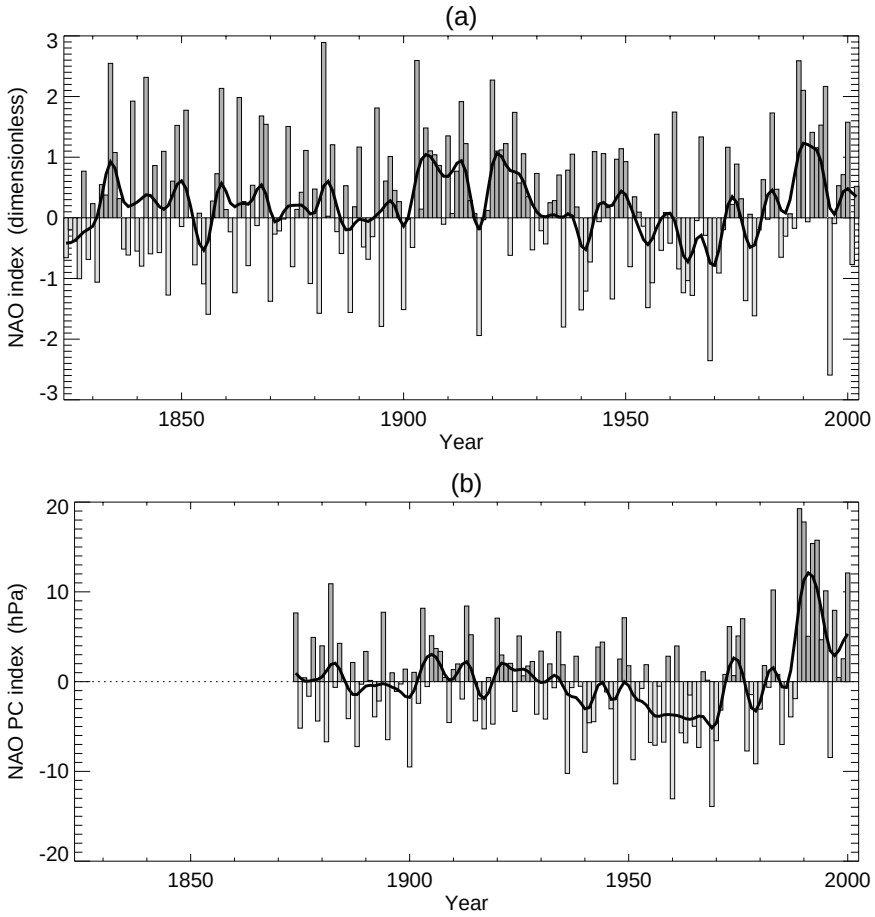

Fig. 1: Observed winter NAO indices: (a) based on the difference in normalised SLP between Gibraltar and Iceland (dimensionless), updated to the most recent winter; and (b) based on the leading principal component of the Atlantic-sector SLP field (hPa).

from integrations with increasing greenhouse gas concentrations, forced with historic levels prior to 1990 and thereafter by a compounded 1% per year increase in effective carbon dioxide. Not all models (notably HadCM2 and HadCM3) conserve mass perfectly and this can manifest itself as a trend in global-mean SLP (see Fig. A1 of Osborn et al., 1999). In all simulations used here, any such artificial variations in globally-averaged sea level pressure are removed by making a geographically-uniform adjustment to the pressure at each grid box.

2.3 Measuring the North Atlantic Oscillation

Osborn et al. (1999) discuss and illustrate (see their Fig. 2) a range of indices of the observed NAO, and find that they are all quite highly correlated (in the range 0.83 to 0.98). Two distinct approaches are to use (i) pressure differences between station pairs; or (ii) a pattern-based measure of the NAO. The station-based approach (Fig. 1a) has the advantage of producing a longer observed record; but a disadvantage is that circulation variability that is unrelated to the NAO (i.e., with a different spatial structure) can have an influence on either or both stations used. Because of this disadvantage with the station-based index, a pattern-based approach is mainly used here, identifying the pattern with principal component analysis (PCA) and then projecting time series of SLP anomaly fields on to this pattern (i.e., computing the vector dot product between field and pattern) to obtain an index time series (Fig. 1b). PCA (using the covariance matrix and with no rotation) is always performed on the Atlantic half (110°W to 70°E) of the northern hemisphere SLP field and the leading empirical orthogonal function (EOF) is retained as the NAO pattern [if SLP from the entire hemisphere had been used, then the resulting pattern might resemble the Arctic Oscillation (Thompson and Wallace, 1998) rather than the NAO].

The EOF from each model simulation is used to define the NAO index for that simulation (Fig. 2). This makes allowance for small variations in the EOF patterns between simulations, though the comparison would lose its validity if the pattern differences were large. Care has to be taken with the scaling of the EOF patterns and their associated time series, especially when using different patterns and from different model grids, to ensure that the magnitudes of the associated principal component time series can be compared on a like-with-like basis. Osborn (manuscript in preparation) gives full details of the scaling used.

2.4 Estimating the range of internal variability

The focus here is on 30-year trends in the NAO index, since Osborn et al. (1999) and others have already suggested that 30-year trends beginning between 1960 and 1967 are unusually strong. From each model control integration, the distribution of 30-year trends is obtained by computing all overlapping trends during the run. From each of these distributions, the 2.5 and 97.5 percentiles are estimated, to obtain a range encompassing 95% of the internally-generated NAO trends.

3. Internally-generated variability of the North Atlantic Oscillation

Fig. 3 shows the 30-year trends computed in a sliding window applied to the observed NAO index shown in Fig. 1b. The horizontal lines mark the 2.5 and 97.5 percentiles estimated from the seven model control runs. Most observed trends fall within these estimates of the range of natural internally-generated NAO variability,

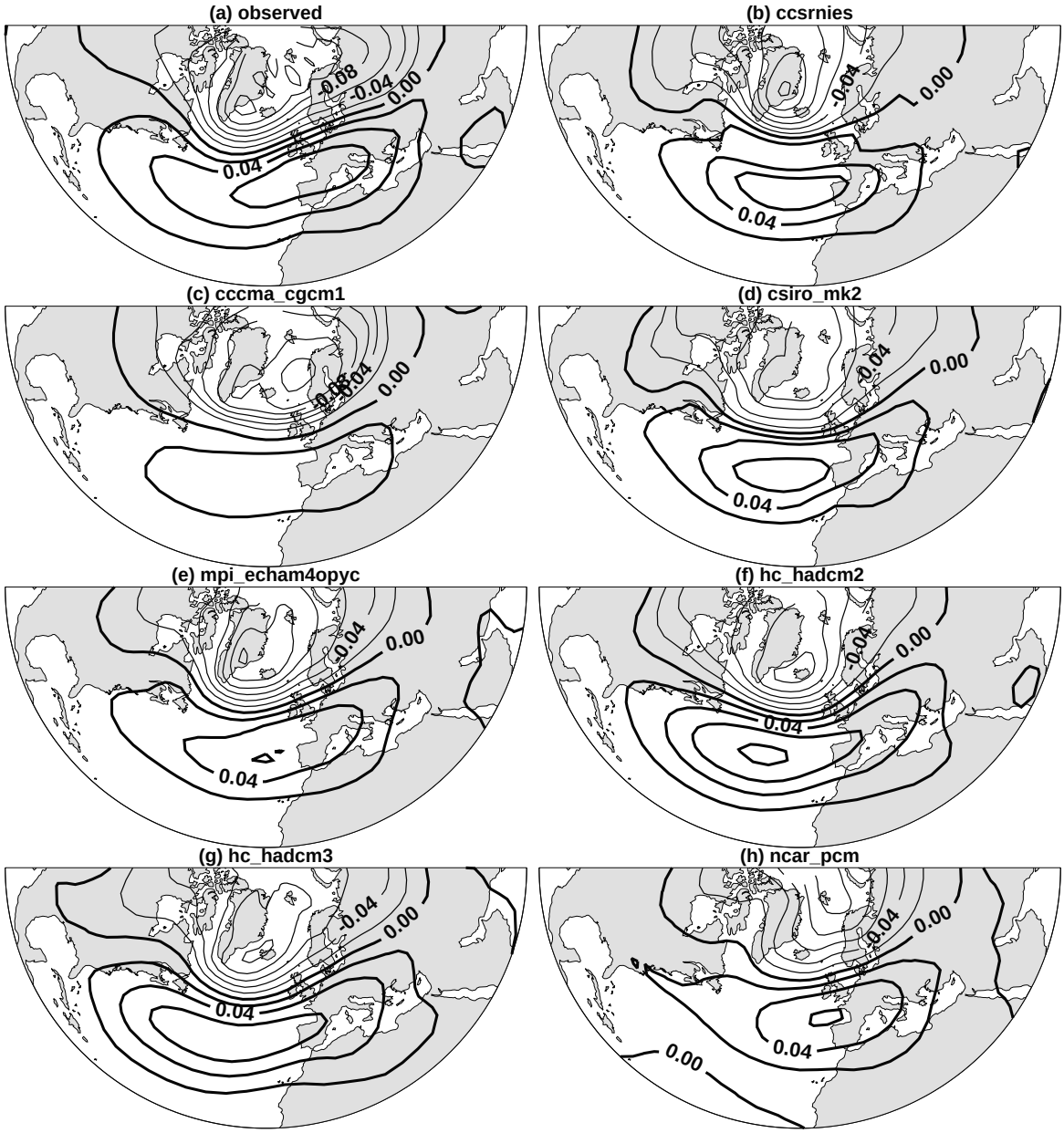

Fig. 2: Leading EOF patterns of Atlantic-sector SLP from (a) observations; and control simulations of models (b) CCSR/NIES; (c) CGCM1; (d) CSIRO Mk2; (e) ECHAM4/OPYC; (f) HadCM2; (g) HadCM3; and (h) NCAR PCM.

Table 1: Climate model acronyms, references and simulation lengths (years).

Acronym	Modelling centre and reference	Reference	Control length	Climate change run
CCSR/NIES	CCSR and NIES, Japan	Emori et al. (1999)	210	1890-2099
CGCM1	CCCMA, Canada	Flato et al. (2000)	200	1900-2099
CSIRO Mk2	CSIRO, Australia	Gordon & O'Farrell (1997)	210	1890-2099
ECHAM4	DKRZ, Germany	Bacher et al. (1998)	240	1870-2099
HadCM2	Hadley Centre, Met Office, UK	Johns et al. (1997)	1400	1870-2099 (4 runs)
HadCM3	Hadley Centre, Met Office, UK	Gordon et al. (2000)	240	1860-2099
NCAR PCM	NCAR, USA	Washington et al. (2000)	300	1960-2099

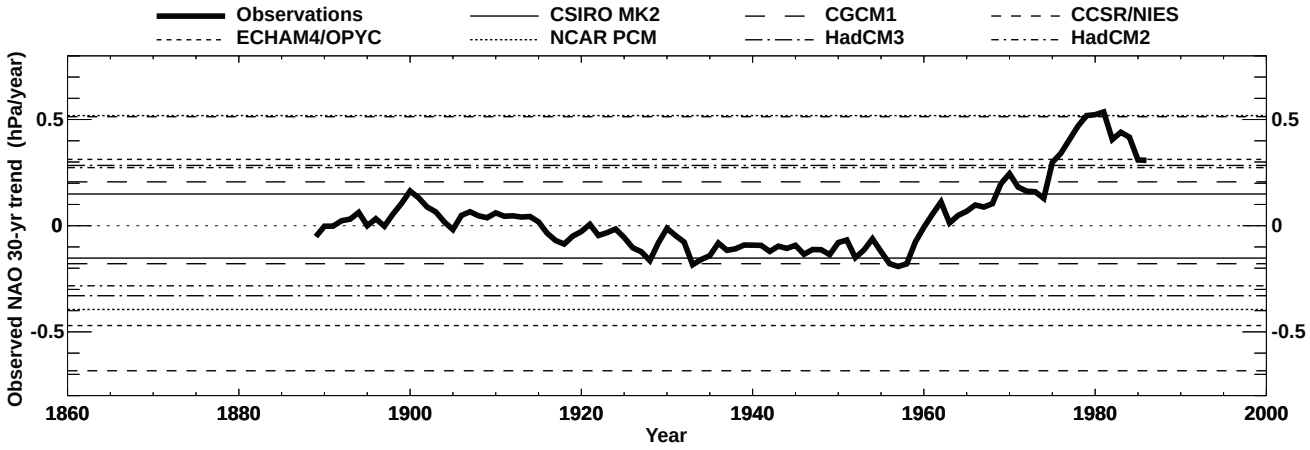

Fig. 3: Thick black line shows the 30-year trends (hPa/yr) in the observed NAO index (shown in Figure 1b) computed in a 30-year sliding window and plotted against the central year of the window. Horizontal lines indicate the 2.5 and 97.5 percentiles of the control simulation distributions of 30-year trends, with models indicated according to the key.

with the main exception being those trends in 30-year windows centred near 1980 (i.e., 1965-1994). A number of these trends exceed the 97.5 percentile of five models, while only 3 trends exceed the 97.5 percentile of all the models, including CCSR/NIES and NCAR PCM. It should be noted, however, that these latter two models have an inter-annual NAO variance that is significantly greater than that observed; if the time series from these two models are scaled so that their high-frequency (intra-decadal) variance matches that observed, then the 97.5 percentiles are reduced and a sequence of twelve 30-year trends (starting from years between 1960 and 1971) exceed all the model 97.5 percentiles. These results strongly support one of two conclusions: either these seven models all underestimate the level of internally-generated multi-decadal variability of the winter NAO, or that some natural or anthropogenic forcing (or combination of forcings) is contributing to the change in wintertime circulation.

4. Simulated response of the North Atlantic Oscillation to greenhouse gas forcing

When measured using a pattern-based index, all seven models produce a gradual shift towards a stronger NAO index when greenhouse gas forcing is increased (Fig. 4, page 38), though the magnitude of this change varies from small, non-significant changes (e.g., CSIRO Mk2, CGCM1) to changes that, by the later decades of this century, reach values similar to those observed during the early 1990s. The sign of this response to greenhouse gases is more consistent than when a station-based index is used (e.g., Osborn et al., 1999, found a *decreased* HadCM2 NAO index using this type of index).

5. Conclusions

There is some confidence, based on the similarity between model simulations, that the response to enhanced greenhouse forcing is a strengthening of the westerly circulation during the Northern Hemisphere winter. The regional details (not shown) are not consistent between models, but a large-scale consistent feature is a strengthening of the pressure gradient between the Mediterranean Sea and the Arctic Ocean, manifested as an increase in the NAO index. According to current model simulations, neither internally-generated variability nor greenhouse gas forcing are sufficient alone to explain the recent observed NAO index changes. The two together, possibly in concert with additional external forcings (see Gillett et al., 2002, for further discussion), might be sufficient to explain the observations, or perhaps a systematic deficiency in the models is to blame, such as insufficient stratospheric resolution (Shindell et al., 1999).

Acknowledgements

This study was funded by the UK Natural Environment Research Council (GR3/12107), with additional support from the Tyndall Centre for Climate Change Research (IT1.15).

References

Bacher, A., J.M. Oberhuber, and E. Roeckner, 1998: ENSO dynamics and seasonal cycle in the tropical Pacific as simulated by the ECHAM4/OPYC3 coupled general circulation model. *Clim. Dyn.,* **14**, 1659-1672.

Basnett, T.A., and D.E. Parker, 1997: Development of the Global Mean Sea Level Pressure Data Set GMSLP2. *Hadley Centre Climate Research Technical Note,* **79**, Met Office, Bracknell, UK.

Emori, S., T. Nozawa, A. Abe-Ouchi, A. Numaguti, M. Kimoto, and T. Nakajima, 1999: Coupled ocean-atmosphere model experiments of future climate change with an explicit representation of sulfate aerosol scattering. *J. Meteorol. Soc. Japan,* **77**, 1299-1307.

Flato, G.M., G.J. Boer, W.G. Lee, N.A. McFarlane, D. Ramsden, M.C. Reader, and A.J. Weaver, 2000: The Canadian Centre for Climate Modelling and Analysis global coupled model and its climate. *Clim. Dyn.,* **16**, 451-467.

Fyfe, J.C., G.J. Boer, and G.M. Flato, 1999: The Arctic and Antarctic Oscillations and their projected changes under global warming. *Geophys. Res. Lett.,* **26**, 1601-1604.

Gillett, N.P., G.C. Hegerl, M.R. Allen, and P.A. Stott, 2000: Implications of changes in the Northern Hemisphere circulation for the detection of anthropogenic climate change. *Geophys. Res. Lett.*, **27**, 993-996.

Gillett, N., H.F. Graf, and T. Osborn, 2002: Climate change and the NAO. In: *North Atlantic Oscillation,* Hurrell J.W., Y. Kushnir, M. Visbeck, and G. Ottersen (eds.), American Geophyscial Union, Washington, in press.

Gordon, H.B., and S.P. O'Farrell, 1997: Transient climate change in the CSIRO coupled model with dynamic sea ice. *Mon. Wea. Rev.,* **125**, 875-907.

Gordon, C. , C. Cooper, C.A. Senior, H. Banks, J.M. Gregory, T.C. Johns, J.F.B. Mitchell, and R.A. Wood, 2000: The simulation of SST, sea ice extents and ocean heat transports in a version of the Hadley Centre coupled model without flux adjusments. *Clim. Dyn.,* **16**, 147-168.

Hurrell, J.W., 1995: Decadal trends in the North Atlantic Oscillation: regional temperatures and precipitation. *Science,* **269**, 676-679.

Hurrell, J.W., 1996: Influence of variations in extratropical wintertime teleconnections on Northern Hemisphere temperature. *Geophys. Res. Lett.*, **23**, 655-668.

Johns, T.C., R.E. Carnell, J.F. Crossley, J.M.Gregory, J.F.B. Mitchell, C.A.Senior, S.F.B. Tett, and R.A. Wood, 1997: The second Hadley Centre coupled ocean-atmosphere GCM: model description, spinup and validation. *Clim. Dyn.*, **13**, 103-134.

Jones, P.D., 1987: The early twentieth century Arctic High – fact or fiction? *Clim. Dyn.,* **1**, 63-75.

Jones, P.D., T. Jonsson, and D. Wheeler, 1997: Extension to the North Atlantic Oscillation using early instrumental pressure observations from Gibraltar and South-West Iceland. *Int. J. Climatol.,* **17**, 1433-1450.

Osborn, T.J., K.R. Briffa, S.F.B Tett, P.D. Jones, and R.M.Trigo, 1999: Evaluation of the North Atlantic Oscillation as simulated by a coupled climate model. *Clim. Dyn.,* **15**, 685-702.

Rodwell, M.J., D.P. Rowell, and C.K. Folland, 1999: Oceanic forcing of the wintertime North Atlantic Oscillation and European climate. *Nature,* **398**, 320-323.

Shindell, D.T., R.L. Miller, G.A. Schmidt, and L. Pandolfo, 1999: Simulation of recent northern winter climate trends by greenhouse-gas forcing. *Nature,* **399**, 452-455.

Thompson, D.W.J., and J.M. Wallace, 1998: The Arctic Oscillation signature in the wintertime geopotential height and temperature fields. *Geophys. Res. Lett.,* **25**, 1297-1300.

Ulbrich, U., and M. Christoph, 1999: A shift of the NAO and increasing storm track activity over Europe due to anthropogenic greenhouse gas forcing. *Clim. Dyn.,* **15**, 551-559.

Wanner, H., S. Bronnimann, C. Casty, D. Gyalistras, J. Luterbacher, C. Schmutz, D.B. Stephenson, and E. Xoplaki, 2001: North Atlantic Oscillation – concepts and studies. *Surveys in Geophysics,* **22**, 321-382.

Washington, W.M., J.W. Weatherly, G.A. Meehl, A.J. Semtner, Jr., T.W. Bettge, A.P. Craig, W.G. Strand, Jr., J.M. Arblaster, V.B. Wayland, R. James, and Y. Zhang, 2000: Parallel climate model (PCM) control and transient simulations. *Clim. Dyn.,* **16**, 755-774.

Conference Announcement:
2nd Euroconference "Achieving Climate Predictability Using Paleoclimate Data"
Barcelona (Spain), October 11-16, 2003

The second Euroconference "Achieving Climate Predictability Using Paleoclimate Data", will be held near Barcelona (Spain) from October 11 to 16, 2003.

The goal of this conference is to continue to build a platform for scientific exchange between two climate research communites who are working on similar topics but come from different angles. Climate variability and predictability is an important theme in both CLIVAR and PAGES, which are the two leading international research initiatives under the umbrellas of WCRP and IGBP, respectively.

Martin Visbeck (Lamont-Doherty, Palisades) and Thomas Stocker (University of Bern) are co-chairing the organising committee of this meeting. The draft programme that is currently under development will cover observational and modelling aspects of climate predictability and will attempt to integrate knowledge on past variability into the framework of what we know from present-day observations. Preliminary titles of the main sessions are:

- Session 1: Paleoclimate variability of the North Atlantic and beyond – data and models;
- Session 2: Modern circulation in the North Atlantic - data and models;
- Session 3: The North Atlantic Oscillation, past, present and future;
- Session 4: Potential future North Atlantic circulation changes and climate predictability.

Invited speakers are currently contacted and a more detailed programme will become available by end of the year through the PAGES and CLIVAR Project Officces and the European Science Foundation.

The European Science Foundation, through the EURESCO programme, is handling the administrative and organisational aspects of this conference.

Preliminary contact:

Keith Alverson, PAGES Project Office, Bern Switzerland
keith.alverson@pages.unibe.ch

Modelling the Late Maunder Minimum with a 3-dimensional Ocean-Atmosphere GCM

Irene Fischer-Bruns[1], Ulrich Cubasch[1], Hans von Storch[2], Eduardo Zorita[2], J. Fidel Gonzáles-Rouco[3] and Jürg Luterbacher[4]

[1] **Modelle und Daten, Max-Planck-Institut für Meteorologie, Hamburg, Germany**
[2] **GKSS, Institut für Küstenforschung Geesthacht, Germany**
[3] **Depto. de Astrofísica y Ciencias de la Atmósfera Universidad Complutense de Madrid, Spain**
[4] **Nationaler Forschungsschwerpunkt Klima, Universität Bern, Switzerland**
corresponding e-mail: fischer-bruns@dkrz.de

Abstract

A fully coupled Ocean - Atmosphere GCM (OAGCM) has been forced with the solar variability, the volcanism and the greenhouse gas concentrations for the last 450 years. The simulation shows almost global cooling during the Late Maunder Minimum (LMM, 1675-1715) with the lowest values in the North Atlantic. This is consistent with the available historic reconstructions. The rate of cooling at the onset of the LMM and the rate of warming at the end of the LMM are in the same range or even larger than what has been experienced since the industrialization. During the first half of the LMM the NAO has a negative phase allowing cold Siberian air to penetrate deeply into Europe. During the second half, the NAO shifts into a positive phase, thus contributing to the warming, which eventually marked the end of the LMM. The North Atlantic experiences a "Great Salinity Anomaly", which leads to an increased ice-coverage in the Denmark Strait.

1. Introduction

So far, fully coupled 3-dimensional OAGCM's have successfully simulated the present day climate, the climate since the beginning of the industrialization, and have been used to calculate future climates (IPCC, 2001). In the study presented here, such a model is used to simulate the climate since 1550. These simulations are performed in response to the discussion about the attribution of the recently observed climate change to anthropogenic factors. In this context it is debated whether the climate change experienced since the beginning of industrialization is unique in its rate and magnitude, and how this change compares to the climate change during the Little Ice Age (LIA). It is also an interesting test for the models, where we can gain more confidence in their ability to simulate a future climate, if we can calculate realistically historic climate events. Furthermore such a simulation can be used to validate historic climate reconstructions, for example from tree rings.

Cubasch et al. (1997) and Cubasch and Voss (2000) performed the first numerical experiments of this kind. They forced an earlier version of the model, which has been used to run climate change simulations with the solar variability since the 17th century. They found a significant response to long periodic large amplitude variations of the solar radiation. These data were further analysed by Hegerl et al. (1997). They could distinguish between a natural forcing signal and a greenhouse gas signal and could prove that during the recent decades the anthropogenic signal was significantly larger than the natural forcing signal. Tett et al. (1999, 2000) extended this approach running multiple experiments and the inclusion of volcanic forcing. They confirmed the results of Hegerl et al. (1997) and Cubasch et al. (1997) that the natural forced variability is smaller than the anthropogenically forced climate change and does not explain the temperature increase recently observed. Both sets of experiments did, however, not go far back enough in time to be able to simulate the LIA.

Crowley (2000) performed a simulation starting at the year 1000, but using only a 1-dimensional energy balance model. Shindell et al. (2001) performed an equilibrium study with an atmosphere model coupled to a mixed layer ocean for the LMM.

In the present study the natural and anthropogenic forcing described by Crowley (2000) has been used to drive a fully coupled 3-dimensional ocean atmosphere in a transient mode, i.e. the time evolution of the climate before, during and after the LMM is calculated.

The experimental set up and the model used are described in section 2, the results are discussed in section 3. Besides an analysis of the temperature evolution, particular emphasis has been placed on the investigation of the role of the NAO during this time. This is followed by a general discussion in section 4.

2. The model and the experimental set up

The T30 version of the ECHAM4 atmosphere model (Roeckner et al., 1992) coupled to the HOPE ocean model (Wolff et al., 1997; Legutke and Maier-Reimer, 1999; Legutke and Voss, 1999) is used for the simulation. The ocean model has a resolution of 2.8° which increases to 0.5° near the equator in order to be able to simulate ENSO events. Two simulations have been performed: a 1000 year long control simulation, in which the solar and greenhouse gas forcing have been held fixed to present day conditions, and a historic climate change simulation with time dependent forcing. For the latter experiment, the solar forcing (reconstructed from ^{10}Be data), the volcanic forcing and the greenhouse gas forcing have been prescribed using the same data, which Crowley (2000) applied in his experiments. The albedo effect of the volcanoes is implemented as a reduction of the solar forc-

ing. Fig. 1 (page 39) shows the different forcings prescribed during the forced simulation. The simulation starts from present-day forcing conditions. These are slowly changed in 35 model years to the estimated values for year 1500 AD. This time period is not sufficient to obtain a deep ocean circulation at equilibrium with the forcing, but it is long enough to obtain a realistic response in the top layers of the ocean and in the atmosphere. The model achieves a stable state around year 1550 AD.

3. Results

Temperature Evolution

The mean temperature evolution can be found in Fig. 2, page 39. In order to make it comparable to the observational data by Mann et al. (1998), for the years prior to 1860 only the Northern Hemisphere (NH) has been displayed. The temperature has two distinct minima, one during the LMM, and one during the Dalton Minimum (circa 1780-1829). These minima have a larger amplitude than in the reconstruction by Mann et al. (1998). Their amplitude is more comparable to the recent reconstructions by Esper (2002). It is interesting to note that the warming (cooling) rates are in the same range or even larger than what has been observed during the 20th century.

The global mean temperature change for the LMM period shows a cooling over the whole globe with the lowest temperatures in the NH, and particularly in the North Atlantic region (Fig. 3, page 39). This is in contrast to the findings by Shindell et al. (2001) and Cubasch et al. (1997), which more or less obtain the global warming pattern with an inverse sign once the solar input is reduced. This shows the importance of the volcanic forcing, which had been neglected in these two studies, as Shindell (pers. com.) has been able to show.

The largest cooling can be found in the western North Atlantic, where south of Greenland and close to Iceland a large ice covered area emerges. This ice cover diminishes the heat flow of the ocean into the atmosphere. It bears the signature of a "Great Salinity Anomaly" (GSA) as described by Dickson et al. (1988) and Mysak et al. (1990). Such an anomaly has been found in simulations by Hall and Stouffer (2001), where it has been generated by non-linear dynamics without additional forcing. In the case presented here it is caused by increased precipitation in the years before the LMM. The LMM simulation by Shindell et al. (2001) cannot simulate a GSA since it is a transient feature and demands a fully interactive ocean, because it needs the dynamical interplay of atmosphere, ocean and sea-ice.

North Atlantic Oscillation

The North Atlantic Oscillation (NAO) characterizes atmospheric variability at monthly to decadal time scales. Since the interdecadal variability appears to be most evident during the winter season, an EOF analysis of the mean sea level pressure anomalies for the North Atlantic region based on winter data (DJF) has been performed. The model produces a realistic representation of the winter NAO pattern (Fig. 4, page 39) in the historic climate change simulation (1550-1990).

The NAO index is defined as the difference between the area averaged and normalized mean sea-level pressure anomalies representing the teleconnectivity centres located northwest of Portugal and over Iceland (Ulbrich and Christoph, 1999, Portis et al., 2001). The principal component time series corresponding to the leading EOF is highly correlated (r=0.92) with the NAO index in the simulation. The simulated NAO index has also been compared with the reconstructed NAO index by Luterbacher et al. (1999, 2002), who used long-term instrumental time series and high-resolution documentary proxy data for his reconstruction. Both time series show considerable variability and differences in phase. They never enter a quasi-permanent low index phase during the LMM associated with weaker mean westerlies over the North Atlantic as suggested by Shindell et al. (2001).

Furthermore, an analysis of the modelled annual global mean temperature in relation to the modelled NAO index for the time period 1550-1800 reveals that during approximately the first half of the LMM (LMM1, 1671-1684) the NAO index is negative, together with a sharp drop in temperature in Europe, while it turns positive approximately during in the second half of the LMM (LMM2, 1685-1708) with an increase in temperature (Fig. 5, page 39). During the first phase of the LMM the advection of continental cold air dominates in central Europe, while in the second phase the NAO contributes with an enhanced advection of warmer Atlantic air masses to the decay of the LMM. This cooling-warming transition can be verified with the temperature reconstruction of van den Dool et al. (1978).

The NAO index calculated here is positively correlated with the North Atlantic storm track (defined as the 2.5 to 6 day band pass filtered variance of the 500 hPa geopotential height) with a maximum correlation of 0.6 in the central North Atlantic (cf. Osborn et al., 1999). During the first half of the LMM a significant decrease of storm track activity in the North Atlantic and West European region is found, while for the second half of the LMM an significant increase of storm track activity over the European continent is simulated.

4. Discussion

The model simulation presented here agrees with the equilibrium mixed layer model simulation of Shindell et al. (2001) by simulating a distinct Maunder Minimum with a global drop of temperature and a particularly large drop of temperature over Europe. Contrary to the simulation by Shindell et al. (2001), it shows a large cooling connected to a GSA in Denmark Strait. Also, its NAO is variable, which agrees well with the observational re-

constructions. The more stable NAO in Shindell et al.'s calculation might be caused by their experimental design, but might also be caused by their more elaborate representation of the stratosphere.

It has to be stressed that our result is just one realization. Multiple experiments have to be run to enhance the significance of the findings. The excessive amount of computing resources was so far prohibitive.

Acknowledgement

The model simulations have been performed by GKSS at the DKRZ computing center. Irene Fischer-Bruns has been supported by the SFB 512 sponsored by the DFG. The experiments have been part of the KIHZ-project of the Helmholtz-Society. The authors also wish to express thank to D. Shindell for the useful discussion during the AGU Spring Meeting in Washington (2002), and to T. Crowley for making the data available.

References

Albritton, D.L., T. Barker, I.A. Bashmakov, O. Canziani, R. Christ, U. Cubasch, O. Davidson, H. Gitay, D. Griggs, J. Houghton, J. House, Z. Kundzewicz, M. Lal, N. Leary, C. Magadza, J.J. Mccarthy, J.F.B. Mitchell, J.R. Moreira, M. Munasinghe, I. Noble, R. Pachuri, B. Pittock, M. Prather, R.G. Richels, R.B. Robinson, J. Sathaye, S. Schneider, R. Scholes, T. Stocker, N. Sundararaman, R. Swart, T. Taniguchi, and D. Zhou, 2001: Climate Change 2001: Synthesis Report. R.T. Watson ed., Cambridge University Press, 200pp.

Crowley, T.J., 2000: Causes of climate change over the past 1000 years. *Science*, **289**, 270-277

Cubasch, U., G.C. Hegerl, R. Voss, J. Waszkewitz, and T.C. Crowley, 1997: Simulation with an O-AGCM of the influence of variations of the solar constant on the global climate. *Climate Dynamics*, **13**, 757-767

Cubasch, U., and R. Voss, 2000: The influence of total solar irradiance on climate. *Space Science Reviews*, **94**, 185-198.

Dickson, R.R., J. Meincke, S.-A. Malmberg, and A.J. Lee, 1988: The „Great Salinity Anomaly" in the Northern North Atlantic 1968-1982. *Prog. Oceanog.*, **20**, 103-151.

Esper, J., E.R. Cook, and F.H. Schweingruber, 2002: Low-frequency signals in long tree-ring chronologies for reconstructing past temperature variability. *Science*, **295**, 2250-2254.

Hall, A., and R.J. Stouffer, 2001: An abrupt climate event in a coupled ocean-atmosphere simulation without external forcing. *Nature*, **409**, 171-174.

Hegerl, G.C., K. Hasselmann, U. Cubasch, J.F.B. Mitchell, E. Roeckner, R. Voss, and J. Waszkewitz, 1997: Multi-fingerprint detection and attribution analysis, of greenhouse gas, greenhouse gas-plus-aerosol and solar forced climate change. *Climate Dynamics*, **13**, 613-634.

IPCC, 2001: Projections of future climate change. In: Climate Change 2001: The Scientific Basis. Contribution of Working Group I to the Third Assessment Report of the Intergovernmental Panel on Climate Change [Houghton, J.T., Y. Ding, D.J. Griggs, M. Noguer, P. van der Linden, X. Dai, K. Maskell, and C.I. Johnson (eds.)]. Cambridge University Press, ISBN 0521 01495 6.

Legutke, S., and R. Voss, 1999: The Hamburg Atmosphere-Ocean Coupled Circulation Model ECHO-G. Technical Report No. 18, DKRZ, Hamburg.

Legutke, S., and E. Maier-Raimer, 1999: Climatology of the HOPE-G Global Ocean - Sea Ice General Circulation Model. Technical Report No. 21, DKRZ, Hamburg.

Luterbacher, J., C. Schmutz, D. Gyalistras, E. Xoplaki, and H. Wanner, 1999: Reconstruction of monthly NAO and EU indices back to AD 1675. *Geophys. Res. Lett.*, **26**, 2745-2748.

Luterbacher, J., E. Xoplaki, D. Dietrich, P.D. Jones, T.D. Davies, D. Portis, J.F. Gonzalez-Rouco, H. von Storch, D. Gyalistras, C. Casty, and H. Wanner, 2002: Extending North Atlantic Oscillation Reconstructions Back to 1500. *Atmos. Sci. Lett.*, **2**, 114-124.

Mann, M.E., R.S. Bradley, and M.K. Hughes, 1998: Global scale temperature patterns and climate forcing over the past six centuries. *Nature*, **392**, 779 – 787.

Mysak, L.A., D.K. Manak, and R.F. Marsden, 1990: Sea-ice anomalies observed in the Greenland and Labrador Seas during 1901-1984 and their relation to an interdecadal Arctic climate cycle. *Climate Dynamics*, **5**, 111-133.

Osborn T.J., K.R. Briffa, S.F.B. Tett, P.D. Jones, and R.M. Trigo, 1999: Evaluation of the North Atlantic Oscillation as simulated by a coupled climate model. *Climate Dynamics*, **15**, 685-702.

Portis, D.H., J.E. Walsh, M. El Hamly, and P.J. Lamb, 2001. Seasonality of the North Atlantic Oscillation. *J. Climate*, **14**, 2069-2078.

Roeckner, E., K. Arpe, L. Bengtsson, S. Brinkop, L. Dümenil, M. Esch, E. Kirk, F. Lunkeit, M. Ponater, B. Rockel, R. Sausen, U. Schlese, S. Schubert, and M. Windelband, 1992: Simulation of the present-day climate with the ECHAM model: Impact of model physics and resolution. Report No. 93, Max-Planck-Institut für Meteorologie, Bundesstr 55, Hamburg.

Shindell, D.T., G-A. Schmidt, M.E. Mann, D. Rind and A. Waple, 2001: Solar forcing of regional climate change during the Maunder minimum. *Science*, 294, 2149-2154.

Tett, S.F.B., P.A. Stott, M.R. Allen, W.J. Ingram und J.F.B. Mitchell, 1999: Causes of twentieth-century temperature change near the Earth's surface. *Nature*, **399**, 569 - 572.

Tett, S. F.B., G.S. Jones, P.A. Stott, D.C. Hill, J.F.B. Mitchell, M.R. Allen, W.J. Ingram, T.C. Johns, C.E. Johnson, A. Jones, D. L. Roberts, D.M.H. Sexton, and M.J. Woodage, 2000: Estimation of natural and anthropogenic contributions to 20th century. Hadley Centre Tech Note 19, Hadley Centre for Climate Prediction and Response, Meteorological Office, RG12 2SY, UK pp52.

Ulbrich, U., and M. Christoph, 1999: A shift of the NAO and increasing storm track activity over Europe due to anthropogenic greenhouse gas forcing. *Climate Dynamics*, **15**, 551-559.

van den Dool, H.M., H.J. Krijnen, and C.J.E. Schuurmans, 1978: Average winter temperatures at De Bilt (The Netherlands): years 1634-1977. *Climatic Change*, **1**, 319-330.

Wolff, J.-O., E. Maier-Raimer, and S. Legutke, 1997: The Hamburg Ocean Primitive Equation Model HOPE, Technical Report No. 13, DKRZ, Hamburg.

Hydrographic and Transient Tracer Response to Atmospheric Changes over the Nordic Seas

Johannes Karstensen[1], Peter Schlosser[2], John Bullister[3] and Douglas Wallace[4]
[1] Programa Regional de Oceanografia Fysika y Clima Universidad de Concepcion, Chile
[2] Lamont-Doherty Earth Observatory of Columbia University, Palisades, NY, USA
[3] NOAA PMEL, Seattle, WA, USA
[4] Institut für Meereskunde, Universität Kiel, Kiel, Germany
corresponding e-mail: karstens@profc.udec.cl

Introduction

Knowledge of the timing and intensity of convection in the Nordic Seas is important for our understanding of the global thermohaline circulation because it generates waters that flow over the sills between Greenland and Scotland and contribute to the ventilation of the lower branch of the North Atlantic Deep Water. At present most of the overflowing waters are generated by rather shallow convection in the Norwegian and Iceland seas (Hansen and Osterhus, 2000). However, deep water ventilation in the region is also important as it maintains the interior overturning of the Nordic Seas/Arctic Ocean system. A key region for direct deep water ventilation is the central Greenland Sea. It is the region with the lowest stratification and the densest outcrop in winter and, although never directly observed, it is hypothesized that ventilation of the deep waters down to the bottom occurs in the center of the gyre. Water mass formation and hence ventilation rely on the forcing at the air/sea interface. Model studies have shown that in the Nordic Seas changes in the freshwater flux (including sea ice) may inhibit convection and in turn have major impact on the patterns and strength of the thermohaline circulation (e.g. Broecker et al., 1990; Marotzke and Willebrand, 1991).

As part of repeat hydrographic cruises by the Institute of Marine Research in Bergen, transient tracer measurements have been carried out in the Nordic Seas between 1991 and 2000 on an annual basis. Although the station spacing did not follow an exact pattern (Fig. 1, page 40), the cruises followed quasi-standard lines. One of those lines, at about 75°N, crossed the central Greenland Sea each year and, in conjunction with data from earlier cruises, provides one of the longest time series of transient tracer measurements (see Bönisch et al., 1997 for the earlier data). Karstensen et al., (2002) documented the temporal changes of hydrographic properties and transient tracers during the last decade in the Nordic seas. They derived formation rates of water in the Greenland Sea and mapped the spreading of these waters. In this note we report on possible forcing mechanisms that are responsible for the properties observed in the hydrographic and transient tracer time series, as well as their variability.

Greenland Sea gyre time series 1991 to 2000

Time series for temperature, salinity, chlorofluorocarbons (CFC11, CFC12, CFC113, Carbontetrachloride (CCl_4)), tritium and helium isotopes were constructed for the central Greenland Sea gyre. This was done by applying a Gaussian weighted interpolation considering a region of 5° by 2.5° from the gyre center (2°W/75°N) which was identified through the low stability of the water column. Stations with very deep mixed layers or chimney-type structures were excluded from the time series because they reflect small scale features rather than representing the large scale temporal evolution of the gyre (Send and Marshall, 1995).

The time series show pronounced changes over the last decade for all tracers. The data show that the trends of quasi-linear increases in temperature and salinity of the deep water (about 0.01 Ky^{-1} and 0.001 psu y^{-1}, respectively; e.g., Bönisch et al., 1997) continued through the end of the 1990's. The tracer inventories (not shown here) indicate strongest ventilation between 1994/95 and 1999/2000. If we assume that a 500 m deep mixed layer is responsible for the observed tracer inventory increases, we obtain a ten year average water mass formation rate of roughly 0.2 Sv, equivalent to about 1 Sv during the individual events. In contrast, using only temperature and salinity, Budeus et al. (1998) concluded that no intensive convection took place in the three years following 1993. This observation emphasizes the usefulness of transient tracers in detecting and quantifying deep convection.

At intermediate depth (above 2000 m) the apparent propagation of a relative temperature maximum (Tmax) into deeper layers can be seen. This feature developed during the end 1980's/early 1990's (Budeus et al., 1998) and is reflected in all tracer data sets as it aligns with a strong vertical gradient. The gradient separates the waters that are exposed to direct (air/sea) ventilation from those influenced by mainly by lateral mixing from the rim. The deepening of Tmax slowed down in the second half of the last decade and at present the Tmax layer is located at about 1800 m (D. Quadfasel, pers. communication). Budeus et al. (1998) used a linear extrapolation of the deepening of Tmax between 1993 and 1996 (order 150 m y^{-1}) to estimate the period of time required for ventilation of the deep waters to be about 20 to 30 years. In view of the slowing down of the deepening of the Tmax waters, this time seems to be too short. The slow-down may be related to the fact that Tmax enters a depth range which is dominated by lateral exchange of the gyre with water of Arctic Ocean origin, entering via Fram Strait. The core of this water is marked by the salinity maximum at about 2000 m and for convectively renewed water it needs to be more salty to penetrate this layer. The deepening of the Tmax layer could

be triggered by a number of factors and is discussed below.

For the deep water ventilation different theories exist based on double diffusion (e.g., Clarke et al., 1990), 'dome collapse' (e.g. Meincke et al., 1997), or vertical mixing (e.g., Visbeck and Rhein, 2000). At present lateral/diffusive renewal plays a dominate role in deep water transformation and is mainly fed by warmer and more salty water of Arctic Ocean origin. If sustained over a long period of time such mixing reduces the strength of the overturning circulation in the Nordic Seas as it lowers the potential energy of the system.

Forcing at the air/sea interface and the deepening of Tmax

To explore if and how the ventilation (hence the deepening of Tmax) is related to local forcing at the air/sea interface, time series of heat flux and wind stress curl based on NCEP/NCAR reanalysis data were constructed. Monthly mean NCEP/NCAR data were used to address the 'memory' of the gyre on long term forcing factors rather than considering short fluctuations which we expect to be of important in triggering rather small scale individual convective events. Annual mean anomalies of heat flux and wind stress are calculated by subtracting the average seasonal cycle (Fig. 2).

Annual mean heat loss averaged over the period 1981 to 2001 where about 10 Wm^{-2} and a positive wind stress curl of about 2.3 10^{-7} Nm^{-3} was calculated. Of particular interest in interpreting the deepening of Tmax is the forcing during 1993 and 1995, i.e., the years that exhibit the strongest deepening. From Fig. 2 it is evident that during these periods the annual mean heat loss was twice as large as the average and the wind stress curl was three times larger.

From the changes in temperature (Fig. 1, page 40) the changes in heat content of the gyre can be calculated. For convenience a heat flux was deduced for a scenario that would bring the system back to its 1991 state assuming uniform exchange over the area of the gyre. For the deep water (2000 to 3700m) a heat gain of about 25 Wm^{-2} was found between 1991 and 2000. As the deep water warming appears to be rather linear, at least since the mid 1970's (Bönisch et al., 1997), an annual mean heat loss of about 60 Wm^{-2} is needed to bring the deep layer back to its high energy state of the 1970's. These are large numbers considering the present isolation of the deep waters from surface fluxes. For the intermediate waters (500 to 2000m) variable fluxes of heat loss and gain were found while in 2000 an overall heat gain of 15 Wm^{-2} relative to 1991 was found. The heat content related to the latter heat flux appears to be sufficiently small to be removed during a single intensified convection event. However, centered at 1700m depth, the Tmax layer carries a heat content that is equivalent to a sustained heat flux of about 10 Wm^{-2} between 1991 and 2000. For the upper layer with its seasonal warming and freshening cycle we can not estimate the heat balance due to lack of adequate data.

In conclusion, the gyre interior experienced a heat gain while the average surface heat flux is negative (-10 W m^{-2}). We interpret this apparent curiosity as a result of the physics of convection, specifically, an eddy-induced circulation (Send and Marshall, 1995; Kathiwala and Visbeck, 2000). The winter surface heat/buoyancy loss generates eddies which in turn drive a meridional overturning of the water column. This circulation incorporates water from the periphery. The mixing of water from the periphery with waters from the mixed layer and the 'old gyre water' determines the observed heat content.

Eddy activity is related to baroclinicity and hence to the slope of and spacing between isopycnals (Visbeck et al., 1997). Each year in summer heat gain and freshwater fluxes establish a stratified mixed layer over the central Greenland Sea while in winter buoyancy flux destroys it, mainly through eddy processes. We do not know the seasonal upper water stratification of the gyre over the years but some hypotheses can be derived: During the summers of 1993 and 1994 the freshwater

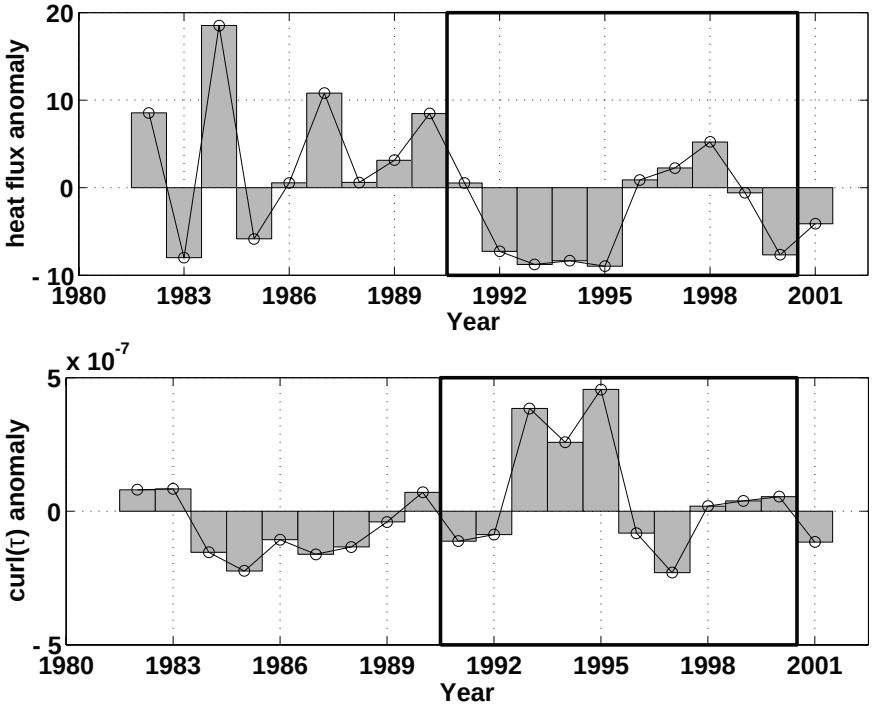

Fig. 2: NCEP/NCAR reanalysis (upper panel) annal heat flux anomaly and (lower panel) wind stress curl anomaly.

export through Fram Strait was two to three times larger than the average between 1990 and 1996 (Vinje et al. 1998). Assuming that sea-ice transport is the main freshwater source of the gyre it should have established a very light surface layer, which, in combination with the subsurface penetration of Atlantic Water towards the gyre center, produces strong baroclinicity. In turn the gyre was 'preconditioned' to support a vigorous eddy field established through the intense heat losses (Fig. 2) during the winters of 1993, 1994 and 1995. The so eddy-driven meridional overturning generated by these processes should have been very intense and incorporated more (upper) water from the periphery which would explain the increase in tracer concentrations. In addition, the intensified overturning would explain the deepening of the layer characterized by Tmax. With increasing wind stress curl over successive years we expect an increased deepening of the doming allowing the water of the intermediate layers to participate in the secondary circulation. In contrast, between 1996 and 1999 the forcing was closer to average conditions (Fig. 2) and even if convective cells have been generated in winter it is not expected that an intensive deep-reaching secondary circulation had been established and Tmax did not deepen further. In winter 1999/2000 intensive heat loss again drove a secondary circulation which increased the transient tracer inventories but did not reach deep enough to deepen the Tmax layer.

The interplay between local vertical (convection) and advective components contributing to the water mass formation and transformation in the Greenland Sea suggests that the region may have an 'intrinsic' time scale governed by the interaction of local forcing and advection to generate deep convection. Hence, modelling and predicting the thermohaline circulation in the Arctic Mediterranean and the resulting contribution of waters to the overflows is a challenging task for ocean modelers.

Acknowledgment

The NCEP/NCAR reanalysis data and reconstructed Reynolds SST data is available from the NOAA-CIRES Climate Diagnostics Centre, Boulder, Colorado, USA, from their Web site http://www.cdc.noaa.gov/. Financial support from NOAA through grant NA86GP0375 is acknowledged.

References

Bönisch, G., J. Blindheim, J.L. Bullister, P. Schlosser, and D.W.R. Wallace, 1997: Long term trends of temperature, salinity, density and transient tracers in the Greenland Sea. *J. Geophys. Res.,* **102**, 18553-18571.

Broecker, W., T.-H. Peng, J. Jouzel, and G. Russel, 1990: The magnitude of the global fresh-water transports of importence to ocean circulation. *Climate Dyn.*, **4**, 73-79.

Budeus, G., W. Schneider, and G. Krause, 1998: Winter convective events and bottom water warming in the Greenland Sea. *J. Geophys. Res.,* **103**, 18513-18527.

Clarke, R., J. Swift, J. Reid, and K.P. Koltermann, 1990: The formation of Greenlandic Sea Deep Water: Double diffusion or deep convection? *Deep-Sea Res.*, **37**, 1385-1424.

Hansen, B., and S. Osterhus, 2000: North Atlantic - Nordic Seas exchange. *Prog. Oceanogr.*, **45**, 109-208

Karstensen, J., and P. Schlosser, D. Wallace, J. Bullister and J. Blindheim, 2002: Variability of water mass formation in the Greenland Sea during the 1990's. *J. Geophys. Res.*, in preparation.

Khatiwala, S., and M. Visbeck, 2000: An estimate of the eddy-induced circulation in the Labrador Sea. *Geophys. Res. Letts.*, **27**, 2277-2280.

Marotzke, J., and J. Willebrand, 1991: Multiple equilibria of the global thermohaline circulation. *J. Phys. Oceanogr.,* **21**, 1372- 1385.

Meincke, J., B. Rudels, and H.J. Friedrich, 1997: The Arctic Ocean-Nordic seas thermohaline system. *ICES J. Mar. Science*, **54**, 283-299.

Rudels, B., 1990: Haline convection in the Greenland Sea. *Deep-Sea Res.*, **37**(9), 1491-1511.

Send, U., and J. Marshall, 1995: Integral effects of deep convection *J. Phys. Oceanogr,* **25**, 855-872.

Vinje, T., N. Nordlund, and Å. Kvambekk, 1998: Monitoring ice thickness in Fram Strait. *J. Geophys. Res.*, **103** (C5), 10437-10449.

Visbeck, M., and M. Rhein, 2000: Is bottom boundary layer mixing slowly ventilating Greenland Sea deep water? *J. Phys. Oceanogr.,* **30**, 215-224.

Visbeck, M., J. Marshall, T. Haine, and M. Spall, 1997: Specification of eddy transfer coefficients in coarse resolution ocean circulation models. *J. Phys. Oceanogr.,* **27**, 381-402.

The Arctic-Subarctic Ocean Flux Study (ASOF): Rationale, Scope and Methods

Robert Dickson[1] and Roberta Boscolo[2]
[1]CEFAS, Lowestoft, UK.
[2]CSIC-Instituto de Investigaciones Mariñas, Vigo, Spain
corresponding e-mail: rbos@iim.csic.es

According to the last IPCC projections (2001), the ocean – and in particular the Atlantic – response to an increase of greenhouse gases would result in a slowdown of the Meridional Overturning Circulation (MOC) in the North Atlantic.

Regional models have highlighted specific "vulnerabilities" of the MOC to changes in the Arctic heat and freshwater budget (Wadley and Bigg, 2002). Nevertheless questions remain as to whether they yet deal adequately with the complexities of the ocean's thermohaline circulation and its many sources of variability. These controls on the MOC are believed to include: the poleward flux of warm and salty Atlantic surface water; the freshwater and ice flux out of the Arctic; the speed and density of the deep overflows crossing the Greenland-Scotland ridge; open-ocean convection; mixing near the ocean margins, including the sea surface; ice-ocean and atmosphere-ocean interactions; freshwater input from the atmosphere and rivers.

These processes and transports are poorly observed and understood. We have no systematic measurements of the freshwater flux between the Arctic Ocean and the Atlantic by either of its two main pathways; we have new measurements of the heat and salt flux to the Arctic Ocean but not yet of its variability on any scale; we have a growing knowledge of the long-term variability of the hydrography of the dense water overflows which "drive" the MOC but embryonic ideas as to their causes, etc…; and our present observations of the MOC (in the North Atlantic or anywhere else) are insufficient to detect whether it is changing. Understandably then, we would take the view that these key mechanisms and processes are too crudely represented in the present generation of the global climate models.

It is the aim of ASOF to supply these missing observations. More specifically: to measure and model the variability of the fluxes between the Arctic Ocean and the Atlantic Ocean with a view to implementing a long-term system of critical measurements needed to understand the high latitude ocean's steering role in decadal climate variability.

The ASOF domain is illustrated in Fig. 1 (page 41) in terms of the 6 main tasks around which this programme is structured. ASOF does not intend to cover the whole or even a large part of the thermohaline circulation of the North Atlantic. Instead, the focus is on understanding the broad range of upstream influences that may impose changes on the Deep Western Boundary Current (DWBC). Since we cannot yet identify which may be the dominant upstream influences on the DWBC, the ASOF observing programme proposes simultaneous rather than sequential observations for a period long enough to identify the slow shifts of global change. The various ocean measurements techniques that very recently have made considerable advances in the field will allow all the observations needed for ASOF to be made with some degree of confidence.

There are several other reasons for implementing ASOF in addition to those mentioned before: (a) the modelling and paleo-evidence that anthropogenic effects on the stability of the thermohaline circulation may be rapid in their onset (Stocker and Schmittner, 1997); (b) the fact that we are beginning to know what the "fingerprint" of the anthropogenic climate change should look like in the ocean (Banks and Wood, 2002); (c) the recent observational evidence that large scale decadal changes are already passing through the Atlantic thermohaline system (Dickson et al., 2002; Fig. 2, page 41). As such an extended and extensive effort would be beyond the resources of any single institute or nation, ASOF implementation will benefit from the several agencies from different countries that are currently contributing to the study of the ocean's role in rapid climate change (the UK RAPID thematic programme, the Norwegian NOClim project, aspects of EC Framework 5 and programme solicitations of the NSF Office of Polar Programmes and the interagency SEARCH programme).

The ASOF International Scientific Steering Group will meet for the second time during October 18-19, 2002 in Hamburg. The agenda of the meeting includes discussion and eventual approval of the ASOF structure (proposed to be divided into 6 regional tasks) with the selection of Chairmen and Teams for each component. The ISSG will also discuss the ASOF data policy which will conform with the data management model for CLIVAR in order to ensure (a) that ASOF can access the multidisciplinary data sets that will be generated by CLIVAR and that (b) the datasets generated by the individual regional tasks of ASOF will be directed into CLIVAR data stream and available to the wider community.

More information on ASOF can be found at:
http://asof.npolar.no/

References

Banks, H., and R. Wood, 2002: Where to look for Anthropogenic Change in the Ocean. *J. Climate*, **15**, 879-891.

Dickson, R. R., I. Yashayaev, J. Meinke, W. Turrell, S. Dye, and J. Holford, 2002: Rapid Freshening of the Deep North Atlantic Ocean over the past four decades. *Nature*, **416**, 832-837.

IPCC, 2001: Climate Change 2001: The Scientific Basis. J.T. Houghton, Y. Ding, D.J. Griggs, M. Noguer, P.J. van der Linden, and D. Xiaosu (Eds.), Contribution of Working Group I to the Third Assessment Report of the Intergovernmental Panel on Climate Change, Cambridge University Press.

Stocker, T.F., and A. Schmittner, 1997: Influence of CO_2 emission rates on the stability of the thermohaline circulation. *Nature*, **388**, 862-865.

Wadley M.R., and G.R. Bigg, 2002: Impact of flow through the Canadian Archipelago and Bering Strait on the North Atlantic and Arctic Circulation. *Q. J. Roy. Met. Soc.*, submitted.

Rapid Climate Change (RAPID) – a new UK Natural Environment Research Council (NERC) programme

Meric A. Srokosz, RAPID Science Coordinator
Southampton Oceanography Centre, Southampton, UK
corresponding e-mail: M.Srokosz@soc.soton.ac.uk

Background

A wide range of model studies show that the presence of the oceanic thermohaline circulation (THC) and its associated heat transport produces a substantially warmer climate in western Europe than would otherwise be the case (see, for example, Manabe and Stouffer, 1988; Schiller et al. 1997; Vellinga and Wood, 2002). The THC consists of deep convection induced by surface cooling at high latitudes, sinking to depth, and upwelling of deep waters at lower latitudes, with horizontal shallow and deep currents feeding these vertical flows. The deep convection and sinking in the North Atlantic (in the Labrador and Greenland Seas) have no counterpart in the North Pacific Ocean, where northward heat transport is consequently much weaker. However, the Atlantic THC has not always been like today's. Palaeo climate records indicate that abrupt climate change has occurred in the Northern Hemisphere, especially during and just after the last cold stage (see, for example, Broecker and Denton, 1989; Dansgaard et al., 1993; Broecker, 2000), with THC change as the most plausible mechanism. Similar change might occur in the future. Model results suggest that the human-induced increase in the atmospheric concentration of CO_2 and other greenhouse gases will lead to a significant reduction in strength of the Atlantic THC (for example, Manabe and Stouffer, 1993; Wood et al., 1999). This in turn will modify substantially the projected rate of climate change over western Europe. Furthermore, it is possible that changes could occur rapidly, perhaps over as short a period as10-20 years. Such rapid climate change would make adaptation to, and mitigation of, the impacts exceedingly difficult for the affected countries. Therefore, it would be useful to estimate the probability of such changes. However, while most climate models indicate that there will be THC weakening, there is considerable spread between their projections (Cubasch et al., 2001), and at least two models show no change at all (Latif et al., 2000, Gent, 2001).

Thus, while there is a possibility that the North Atlantic THC will undergo changes that will result in substantial and rapid climate change for western Europe and Scandinavia, the probability of this occurring cannot be reliably quantified. In order to assess the probability of a future rapid climate change, it is also necessary to understand other potential drivers of rapid change and the intrinsic variability of the climate system. Over recent years, progress has been made in acquiring high quality palaeo observations of past rapid climate change (see, for example, Dansgaard et al., 1989; Alley et al., 1993; Koç Karpuz and Jansen, 1992) and Holocene climate variability (see, for example, Mann et al., 1998; 1999, Briffa et al., 2001). The challenge is to bring together the palaeo data and the climate models, in order to validate the models and develop estimates of uncertainty. This would improve understanding of rapid climate change and of the intrinsic variability of the system, and test the models' abilities across a range of time scales that exceeds the period of instrumental records. (McAvaney et al., 2001 summarise the current state of climate models and the uses of palaeo data that have been made so far for model testing).

Finally, it is important to note that present-day observations of the Atlantic THC (or of the meridional overturning circulation - MOC - of which the THC is the dominant component) are insufficient to detect whether it is changing. Recent observations are suggestive of significant changes occurring in the North Atlantic. These include changes in the characteristics of the cold deep overflows (Hansen et al., 2001) and a freshening of the deep waters (Dickson et al., 2002). Thus a weakening of the MOC may already be in progress, unnoticed.

The RAPID programme

In view of the above, NERC has funded the RAPID programme to investigate and understand the causes of rapid climate change, with a main (but not exclusive) focus on the role of the Atlantic Ocean's THC. Using a combination of present day observations, palaeo data and a hierarchy of models (from local process models to global general circulation models) the programme intends to improve understanding of the roles of the THC and other processes in rapid climate change, and of the global and regional impacts of such change. As a result, the ability to monitor and predict future rapid climate change, particularly in the North Atlantic region, will be enhanced. Specific objectives are:

1) To establish a pre-operational prototype system to continuously observe the strength and structure of the Atlantic meridional overturning circulation (MOC).

2) To support long-term direct observations of water, heat, salt, and ice transports at critical locations in the northern North Atlantic, to quantify the atmospheric and other (e.g. river run-off, ice sheet discharge) forcing of these transports, and to perform process studies of ocean mixing at northern high latitudes.

3) To construct well-calibrated and time-resolved palaeo data records of past climate change, including error estimates, with a particular emphasis on the quantification of the timing and magnitude of rapid change at annual to centennial time-scales.

4) To develop and use high-resolution physical models to synthesise observational data.

5) To apply a hierarchy of modelling approaches to understand the processes that connect changes in ocean convection and its atmospheric forcing to the large-scale transports relevant to the modulation of climate.

6) To understand, using model experimentation and data (palaeo and present day), the atmosphere's response to large changes in Atlantic northward heat transport, in particular changes in storm tracks, storm frequency, storm strengths, and energy and moisture transports.

7) To use both instrumental and palaeo data (see 1-3) for the quantitative testing of models' abilities to reproduce climate variability and rapid changes on annual to centennial time-scales. To explore the extent to which these data can provide direct information about the THC and other possible rapid changes in the climate system and their impact.

8) To quantify the probability and magnitude of potential future rapid climate change, and the uncertainties in these estimates.

These objectives are clearly inter-linked. Thus the ability to predict future climate change (8), rapid or otherwise, is predicated on understanding the current state of the climate (particularly a key component like the THC; 1-2) and past changes in climate (3), on developing models necessary to investigate the THC and climate (4), on using the models to investigate how the climate system works (5-6) and to test the response of the whole system (7).

RAPID has been funded by NERC at a level of £20M (~$30M) over a period of 6 years. The deadline for full proposals in response to the first Announcements of Opportunity (AOs) was July 2002. One of the AOs was specifically focussed on the design and implementation of a prototype Atlantic MOC monitoring system, which is considered a key component of the RAPID programme. Funding decisions will be made in November 2002, with studies beginning early in 2003. Given the scale of the problem, RAPID is actively developing international collaborations that will complement and enhance the work carried out in the UK. As a result of this, an Expression of Interest for a European Union Framework 6 Programme Integrated Project (called WATCHER = Will the Atlantic Thermohaline Circulation Halt; is Europe at Risk?) was submitted to the EU in June 2002. A key collaboration, arising from discussions between the Prime Ministers of the UK and Norway, is with the Norwegian Ocean Climate project (NOClim; http://www.noclim.org). The RAPID programme will contribute to CLIVAR (in the areas of GOALS, DecCen, ACC) and to IGBP PAGES. More details of the programme, including the science and implementation plans and proposed project titles, can be found on the RAPID web page http://rapid.nerc.ac.uk/. For further information about RAPID (or WATCHER) contact the RAPID Science Coordinator (see contact details above).

References

Alley, R.B., D.A. Meese, C.A. Shuman, A.J. Gow, K.C. Taylor, P.M. Grootes, J.W.C. White, M. Ram, E.D. Waddington, P.A. Mayewski, and G.A. Zielinski, 1993: Abrupt increase in Greenland snow accumulation at the end of the Younger Dryas event. *Nature*, **362**, 527-529.

Briffa, K.R., T.J. Osborn, F.H. Schweingruber, I.C. Harris, P.D. Jones, S.G. Shiyatov, and E.A. Vaganov, 2001: Low-frequency temperature variations from a northern tree ring density network. *J. Geophys. Res.*, **106**, 2929-2941.

Broecker, W.S., 2000: Abrupt climate change: causal constraints provided by the paleoclimate record, *Earth-Science Reviews*, 51, 137-154.

Broecker W.S., and G.H. Denton, 1989: The role of ocean-atmosphere reorganisations in glacial cycles. *Geochim. Cosmochim. Acta*, **53**, 2465-2501.

Cubasch, U., G.A. Meehl, G.J. Boer. R.J. Stouffer, M. Dix, A. Noda, C.A. Senior, S. Raper, and K.S. Yap, 2001: Projections of future climate change. In: *Climate Change 2001: the scientific basis. Contribution of Working Group 1 to the Third Assessment Report of the Intergovernmental Panel on Climate* (J.T. Houghton et al., editors), Cambridge University Press, 881pp.

Dansgaard, W., J.W.C. White, and S.J. Johnsen, 1989: The abrupt termination of the Younger Dryas climate event. *Nature*, **339**, 532-4.

Dansgaard, W., S.J. Johnsen, H.B. Clausen, D. Dahl-Jensen, N.S. Gundestrup, C.U. Hammer, C.S. Hvidberg, J.P. Steffensen, A.E. Sveinbjornsdottir, J. Jouzel, and G. Bond, 1993: Evidence for general instability of past climate from a 250-kyr ice-core record. *Nature*, **364**, 218-220.

Dickson, R.R., I., Yashayaev, J. Meincke, B. Turrell, S. Dye, and J. Holfort, 2002: Rapid freshening of the deep North Atlantic Ocean over the past four decades. *Nature*, **416**, 832-837.

Gent, P.R., 2001: Will the North Atlantic Ocean thermohaline circulation weaken during the 21st century? *Geophys. Res. Lett*., **28**, 1023-1026.

Hansen, B., W.R.Turrell, and S. Østerhus, 2001: Decreasing overflow from the Nordic seas into the Atlantic Ocean through the Faroe Bank Channel since 1950. *Nature*, **411**, 927-930.

Koç Karpuz, N., and E. Jansen, 1992: A high resolution diatom record of the last deglaciation from the S.E. Norwegian Sea: documentation of rapid climatic changes. *Paleoceanography*, **7**, 499-520.

Latif, M., E. Roeckner, U. Mikolajewicz, and R. Voss, 2000: Tropical stabilisation of the thermohaline circulation in a greenhouse warming simulation *J. Climate,* **13**, 1809-1813.

Manabe, S., and R.J. Stouffer, 1988: Two stable equilibria of a coupled ocean-atmosphere model. *J. Climate*, **1**, 841-866.

Manabe, S., and R.J. Stouffer, 1993: Century scale effects of increased atmospheric CO_2 on the ocean-atmosphere system. *Nature*, **364**, 215-218.

Mann, M.E., R.S. Bradley, and M.K. Hughes, 1998: Global-Scale Temperature Patterns and Climate Forcing Over the Past Six Centuries. *Nature*, **392**, 779-787.

McAvaney, B.J., C. Covey, S. Joussaume, V. Kattsov, A. Kitoh, W. Ogana, A.J. Pitman, A.J. Weaver, R.A. Wood, and Z.-C. Zhao, 2001: Model Evaluation. In: *Climate Change 2001: the scientific basis. Contribution of Working Group 1 to the Third Assessment Report of the Intergovernmental Panel on Climate* (J.T. Houghton et al., editors), Cambridge University Press, 881pp.

Schiller, A., U. Mikolajewicz, and R. Voss, 1997: The stability of the thermohaline circulation in a coupled ocean-atmosphere general circulation model. *Climate Dyn.*, **13**, 325-347.

Vellinga, M., and R.A. Wood, 2002: Global climate impacts of a collapse of the Atlantic thermohaline circulation. *Climatic Change*, in press.

Wood, R.A., A.B. Keen, J.F.B. Mitchell, and J.M. Gregory, 1999: Changing spatial structure of the thermohaline circulation in response to atmospheric CO_2 forcing in a climate model. *Nature*, **399**, 572-575.

New: The CLIVAR Data Section

Temperature Profiles contained in the CORIOLIS Database during its two first Years (2000–2001)

Jesús E. Gabaldón[1,2], Fabienne Gaillard[2] and Thierry Carval[1]
IFREMER - Centre de Brest
[1]Ingeniérie des Systèmes Informatiques
[2]Laboratoire de Physique des Océans
Plouzané, France
corresponding e-mail: Jesus.Gabaldon@ifremer.fr

Abstract

*This article represents a first evaluation of the CORIOLIS Database, a fundamental resource of the French ARGO Data Centre. The database has global coverage containing, at the end of July 2002, 296,935 quality-proof profiles, representing respectively 8,137,242 and 1,229,894 independent temperature and salinity measurements worldwide. The database is continuously loaded in real-time after a quality check-up procedure. Here we shall only describe the content in the North Atlantic Ocean (included in the so-called "**CLIPPER - MNATL**" area), which accounts approximately for the 45% of the total content of the database. We report its content after the two first years (2000–2001), describing the countings by depth, type of profile and spatial distribution. The full data set can be downloaded from http://www.coriolis.eu.org.*

1. Introduction

The Coriolis data centre was initiated in 1999 as a contribution to operational oceanography in the context of the *Global Ocean Data Assimilation Experiment* (GODAE) (http://www.bom.gov.au/bmrc/ocean/GODAE) and *Array for Real-time Geostrophic Oceanography* (ARGO) (http://www.argo.ucsd.edu, http://argo.jcommops.org) programmes, aimed at building up a global ocean observing system. The set up period has given place to a more stable regime, and the data centre is now collecting and daily distributing a database representative of its future activity. The CORIOLIS Project is an operational effort to deliver data and synthetic products (like objectively analysed temperature and salinity fields) at both real-time and delayed modes. The data represent a fundamental resource, e.g., for a real-time prediction system of the North Atlantic Ocean (MERCATOR, (http://www.Mercator.com.fr/en/)). One of the main difficulties for developing an ocean prediction system compared with global weather prediction is that the horizontal scales of the most relevant ocean processes are quite small (down to the order of a few tens of kilometres), and so the information and computational requirements for global systems are consequently huge. On the other hand, due to the many data sources, types of sensors and distribution means, gathering together all data in a proper manner for rapid availability and distribution was a challenging task that required a big organisational and management effort. In a European context the Coriolis Project is leading the move in oceanography towards the field of operations in the domain of *in situ* data. It has established a daily data delivery procedure of quality-proof temperature and salinity profiles at a global scale and, in a weekly rate, it delivers also synthetic products like objectively analysed 4D fields. As it will be shown in this report, only two years after the creation of the database the spatial density of data which is now available from the CORIOLIS data centre represents already a valuable information set suitable for real-time and delayed ocean analysis. The whole data set will become valuable for climate researchers also. It already represents a useful information resource for those charged with ocean management and protection, among other potential users.

The work presented here is meant to prepare further analysis of the temperature field, for which it is necessary to define what time and space resolution can be achieved and which smoothing (or correlation) will have to be applied. To be consistent with the development of the MERCATOR Project, the analysis is performed over the North-Atlantic area of their prototype based on the **CLIPPER - MNATL**". The CLIPPER - MNATL area is defined over the ocean area within 98° W to 20° E, and from 20° S to 70° N. Anticipating that the data coverage would be rather non-uniform and in order to take into account the variation of scales with latitude, the CLIPPER - MNATL area has been divided into twelve subareas (named, *Elementary Areas*) of 30 degrees square.

Resolutions and correlation scales that vary from one to the other can then be defined for each.

The most recent count of the CORIOLIS Database (July 31st, 2002) yields 296,935 profiles. In terms of independent measurements,this represents 8,137,242 and 1,229,894 temperature and salinity values respectively (see Fig. 1, page 41). The database contain mostly temperature profiles during the years 2000 and 2001, however since mid 2001 it is progressively enriched from salinitymeasurements. The CORIOLIS Project, specifically its database, benefits from the projects POMME (French), GYROSCOPE and MFSPP (European) and ARGO (international). The data set can be downloaded from http://www.coriolis.eu.org.

2. Data Types

Data-types are general families of profiles. There are 6 data-types for vertical profiles. Data-types are defined by the GTSPP programme.

XB: An **XB** profile is performed by an XBT probe. It allows a full resolution profile. The reference parameter is depth.

CT: A **CT** profile is performed by a CTD equipment. The vertical resolution of the profile is usually decimated to 10 dbar. It is therefore a high resolution profile, but not a full resolution profile (a full resolution profile has a vertical resolution of less than 1 dbar). The reference parameter is pressure.

PF: A **PF** profile is performed by a drifting profiler. It is a full resolution profile. The reference parameter is pressure.

TR: A **TR** profile is performed by a thermistor chain from drifting buoys or moorings. It is a full resolution profile. The reference parameter is depth.

BA: A **BA** (BATHY) profile is a low resolution profile received from the GTS network. It is a real-time profile. The measurements are performed by XBT, CTD, profilers, buoys or moorings. A **BA** profile contains only temperature measurements with a resolution of 1/10 of Celsius degrees. The reference parameter is depth.
When a profile with full resolution is available, the corresponding BA low resolution profile is removed from the database.

TE: A **TE** (TESAC) profile is a low resolution profile received from the GTS network. It is a real-time profile. The measurements are performed by XBT, CTD, profiler, buoys or moorings. A **TE** profile contains temperature measurements with a resolution of 1/100 of °C. A **TE** message may also contain salinity measurements with a resolution of 1/100 p.s.u. The reference parameter is depth.
When a profile with full resolution is available, the corresponding TE low resolution profile is removed from the database.

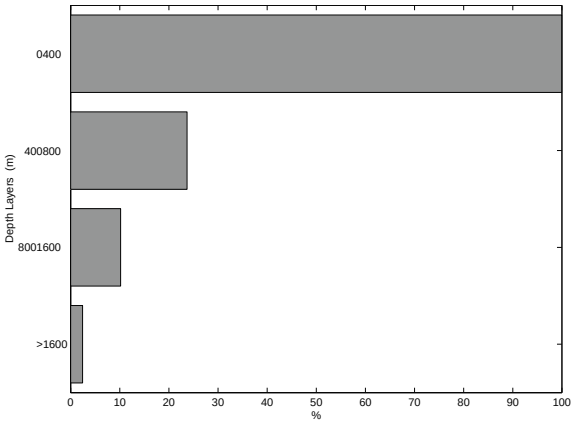

*Fig. 2: Percentual coverage of the depth layers, in the **CLIPPER - MNATL** area during the period [January'2000 – December'2001].*

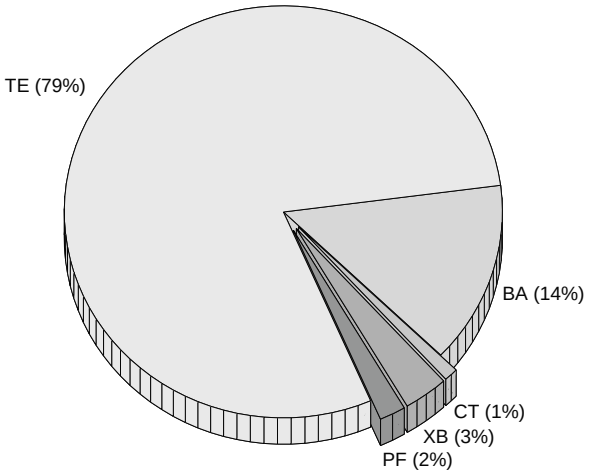

Fig. 3: Percentual type composition of the profiles, in the CLIPPER - MNATL area during the same period.

Probe Codes: Probe codes are defined by the World Meteorological Agency (WMO). These codes describe accurately XBT versions. But, the description of CTD, buoys or moorings is very general.

3. Content of the Database in the CLIPPER - MNATL Area

The evaluation of the database presented here refers to the temperature profiles collected over the **CLIPPER - MNATL** area during its first two years (2000–2001). The content of the Coriolis data centre is, however, not horizontally and vertically homogeneous due to the intrinsic differences between the origin of the data, source of distribution and type of sensor. We have classified the depth of the profiles into four levels: [0–400], [400–800], [800–1600] and [>1600]. Indeed, this classification tries to group the profiles according to the maximum depth that each type of sensor may attain[1].

[1]*This classification will change in spring 2002, when the Coriolis version 2 will be operative. The second version will considerably reduce some possible ambiguities between type of sensor and means of distribution of the profiles.*

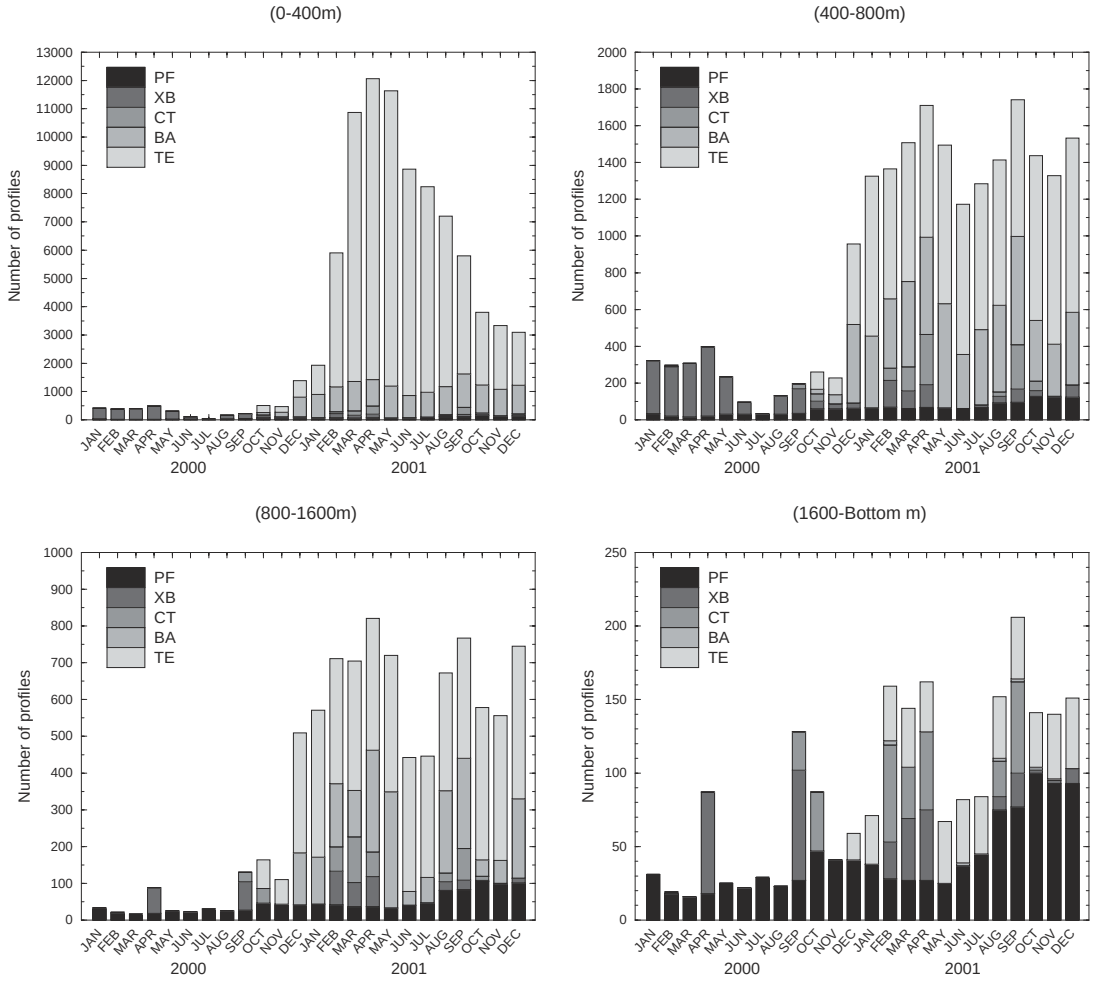

Fig. 4: Number of profiles at the different Elementary Areas by depth layers and type of sensor [January'2000 – December'2001].

Table 1: Loading rates during 2001 in the **CLIPPER - MNATL** area (profiles/month), and proportions for each depth layer

	0–400 m	400–800 m	800–1600 m	>1600 m
$\bar{x} \pm s.d.$	6894.3 ± 3493.4	1442.8 ± 167.2	644.5 ± 123.9	129.9 ± 43.5
%	100	20.9	9.3	1.9

The uppermost level in the **CLIPPER - MNATL** area is almost totally covered by the database (99.96%). XBT and mooring profiles both represent a high proportion of the total input of the database, and these cover only the upper few hundred meters of the water column. The next layer [400–800] is still fairly covered but nonetheless represents approximately only 24% of the total profiles. Half of this is represented by the [800-1600] layer. Finally, the deepest layer is covered by the 2% of the profiles (Fig. 2).

During the period 2000–2001 79% of the profiles loaded into the database came through the GTS-TESAC change to"(**TE**) network, 14% through the GTS-**BA** network and 6% through the three remaining types (**XB**, **PF** and **CT**) (Fig. 3). The three remaining types (**XB**, **PF** and **CT**) represent by the moment approximately the 6%. However, one must stress that the percentage values represented by the last three types are, in fact, misrepresented in the present report. This is because both **TE** and **BA** types contain profiles type **XB**, **PF** and **CT**, as well as other types of profiles from moorings, drifting buoys, ships of opportunity or research vessels, etc.

During the first months of 2000 the number of profiles grew at nearly a constant rate of 400 profiles a month (Figure 4). In terms of loading the Coriolis Data centre took off actually in February 2001, though at the end of year 2000 the rate was about 1330 profiles / month (December), raising up to 1697 in January 2001, and 5724 in February. The high loading rate registered during the period February-September 2001, with a maximum loading rate of nearly 12000 profiles / month in April, was due to the loading of delayed mode data. Finally, in December 2001 the database was holding a total number of **99762** profiles, in the **CLIPPER - MNATL** area. The mean

loading rates for 2001 are presented in Table 1. During the last months (October-Decembre 2001) the database was enriched by 9440 profiles. This means an average input rate of approximatively 3146 profiles / month. This rate is approximatively of the same order than the values registered during the first months of 2002 (not shown).

Fig. 5, (page 42) shows the profile distribution at 2x2 degrees for two different depths. Overall, the POMME area[2] shows the highest profile density from the surface down to 2000 meters. This makes it the best represented area in the CORIOLIS Database at all depths, accounting for about 45% of the profiles in the **CLIPPER - MNATL** area. At such spatial resolution the North Atlantic Ocean appears nearly covered down to almost 800 meters, except of some areas of the northern seas (the Baffin Bay, the Icelandic Plateau and the Norwegian Basin), the Cape Verde Plateau and Monaco Basin (in front of the Mauritanian and Senegal coasts), and the Brazilian and Angola basins. At 1000 meters and deeper the central Atlantic appears uncovered, and between 1200 and 1600 meters only the eastern North American and north Brazilian coasts are scarcely covered by the CORIOLIS Database.

[2]The POMME area, defined between 33–45° N and 8.5–25°W, was intensively studied during 2000–2001 by the French project of the same name.

Workshop on Advances in the Use of Historical Marine Climate Data

Henry Diaz[1], Chris Folland[2], Teruko Manabe[3], David Parker[2], Richard Reynolds[4], and Scott Woodruff[1]
[1]NOAA/CDC, Boulder, CO, USA
[2]Met Office, Bracknell, UK
[3]WMO/ , Geneva, Switzerland
[4]NOAA/NCDC, Asheville, NC, USA
corresponding e-mail: sdw@cdc.noaa.gov

A Workshop on Advances in the Use of Historical Marine Climate Data was held at the NOAA Climate Diagnostics Center, Boulder, Colorado, USA on 29th January - 1st February 2002. It was organized by NOAA, the Met Office, and Japan Meteorological Agency, and was sponsored by the Global Climate Observing System (GCOS) and the World Meteorological Organization (WMO). A full report will appear in WMO Bulletin later this year.

Scope

The overall scope of the workshop was to build on the recent blend of the US Comprehensive Ocean-Atmosphere Data Set (COADS) with the Met Office Marine Data Bank and several million newly digitized data. This blend provides the climate research community with an unprecedented assembly of *in situ* marine data. The new observational archive has been named the International Comprehensive Ocean-Atmosphere Data Set (I-COADS).

Proceedings

The Workshop began with over 2 days' presentations to plenary sessions on historical marine data sets, sea surface temperature (SST) and sea ice, marine air temperature, mean sea level pressure (MSLP) and wind, and recommendations from the second CLIVAR Climate of the Twentieth Century (C20C) workshop (see below). The Workshop then split into three breakout groups covering 1) SST, air temperature and sea-ice; 2) MSLP and wind; and 3) technical requirements. These groups made recommendations, summarised below. General background to the recommendations includes the need to reduce the remaining biases in the data; to increase, where possible, coverage and temporal resolution; to specify uncertainty in analyses; to clearly distinguish versions of datasets; and to promote easy access to all data. The Workshop agreed on a staged timetable for implementation. Firstly, a 2-year period would lead to the third C20C Workshop around April 2004; and secondly, a period of about 5 years will lead to the Fourth Assessment Report of the Intergovernmental Panel on Climate Change (IPCC).

Recommendations

1. SST, air temperature and sea-ice

Within 2 years:

1.1. Re-examine the historic bias corrections to SST, especially for the late 1930s through the end of the 1940s.

1.2. All the metadata in the issues of WMO Publication No. 47 (International List of Selected, Supplementary and Auxiliary Ships) should be digitized, biases in recent night marine air temperature (NMAT) data should be evaluated, and NMAT interpolation techniques should be re-assessed.

1.3. Use geostationary satellite and moored buoy data to analyse the diurnal cycle of SST, particularly in the tropical west Pacific warm pool. It is recommended that the Voluntary Observing Ship Climate (VOSClim) Project be extended, or a parallel project be initiated, to include buoys.

1.4. Commence regular comparisons of the quality control (QC) procedures for SST. For these, common *in situ* input data should be used.

1.5. Collate NOAA Pathfinder satellite SSTs for inland seas and large lakes.

1.6 Develop sub-monthly analyses of SST since 1950.

1.7 The Joint Technical Commission for Oceanography and Marine Meteorology (JCOMM) Expert Team on Sea Ice (ETSI) should provide recommendations on the blending of sea-ice data and on the interpretation of microwave observations of sea-ice. This will provide much-needed information on variations in sea ice thickness.

1.8. It is desirable that the ETSI should provide an inventory of historical sea ice data for the Southern Ocean.

1.9. The use of satellite SSTs in relationships between SST and sea ice concentration should be re-assessed owing to possible contamination of these SSTs by the sea-ice. Improved sea-ice data and relationships should be incorporated into SST analyses.

Within 5 years:

1.10. Cloud-clearing techniques for satellite-based infrared SSTs should be compared.

1.11. Regular comparisons of SST analyses should commence.

1.12. All SST analyses need to include gridded fields of analysis error including bias correction error. Error covariances are also needed.

1.13. Create monthly and sub-monthly blended SST/sea-ice products. Estimates of errors, and indications of sources of data, should be included in the product.

2. Mean sea level pressure and wind

Well within the 2-year timeframe, and ideally by early 2003:

2.1. The Hadley Centre global monthly MSLP data set HadSLP should be updated.

2.2. The Terms of Reference of the GCOS MSLP Working Group should be expanded to include surface winds.

2.3. A catalogue of available wind and pressure products should be developed.

Within 2 years:

2.4. Florida State University will have a non-global (Pacific & Indian Oceans) data set of surface wind and MSLP, fluxes, and related variables from 1950 onwards.

2.5. Appropriate techniques for the adjustment of both estimated and measured wind speed observations should be investigated and applied.

2.6. Monthly wind statistics for 1854 to date should be computed using the adjusted estimated and measured winds.

2.7. The Meteorological Service of Canada has created a high-resolution analysis of winds over the North Atlantic for 1958-1997. The use of historical daily MSLP fields to backdate this analysis should be investigated.

2.8. Biases from the US Maury Collection pressure data set should be investigated.

2.9. More observations on pressure are needed to improve historical MSLP analyses.

2.10. The new JCOMM buoy metadata base should be populated with current and historical data. Merged COADS and WMO Publication No. 47 data 1980-97 should be made available.

In the 5-year timeframe:

2.11. Improved monthly (and daily if possible) surface pressure for land stations should be made available for blended land-marine analysis.

2.12. Improved Reanalysis techniques, currently being developed, should be used to produce a combined daily MSLP and surface wind product for as much of the world as possible back to the late 19th Century.

2.13. For all gridded data sets, error estimates of wind and pressures should include grid box uncertainties and error covariance structures.

3. Technical Requirements

For continual action, without a specific timeframe:

3.1. Data that add the most information to the existing database should be given priority for digitisation.

3.2. The research community should have access to preliminary data. Identification and documentation should clearly distinguish final from interim products, and advise users of potential duplication and lack of QC in the interim products.

3.3. Use a new, fully documented format for interim and newly-digitised data.

3.4. Continue development and application of new QC techniques and utilization of metadata.

3.5. Continue wide distribution of all data in appropriate formats, and share software to access and analyse the data. Data should be available freely, e.g. over the Internet, or at a minimum cost for media.

Within 2 years:

3.6. The real-time data collection centres should keep original copies of the GTS data stream. A comparison of GTS receipts at these collection centers should be made.

3.7. Modern high quality data, at a higher observational frequency than standard synoptic periods, should be incorporated in I-COADS.

3.8. There should be a mirror data site for the new I-COADS database.

Conclusion

The Workshop achieved its goals by:

- Creating a timetable for further enhancement of *in situ* marine datasets.
- Developing a strategy for creating and comparing alternative SST, sea-ice concentration and marine air

temperature analyses, to provide estimates of uncertainty in analyses and key diagnostics of climate variability and change, and to allow assessment of the effects on Atmospheric General Circulation Models (AGCMs) of legitimate uncertainties in the analyses.

- Taking account of recommendations made by the second Workshop of the CLIVAR C20C Project. These included acquiring current and historical SST data for inland seas; archiving quality-controlled SSTs and their uncertainties for assimilation into coupled GCMs; assembly of tropical skin SSTs to test model sensitivity to their use and to the diurnal cycle; provision of analyses with estimates of error associated with each grid-box; testing the sensitivity to use of alternative SSTs; creation of sub-monthly historical SST analyses from 1950; acquisition of sea-ice thickness information to improve heat fluxes; incorporation of historical Russian sea-ice data.
- Proposing the further development of analyses of marine surface pressure and winds, with support from the new GCOS MSLP Working Group.

In its final plenary session the Workshop voted in support of the name **International Comprehensive Ocean-Atmosphere Data Set (I-COADS)** for the new blended observational database. This name recognises the multinational input to the database while maintaining continuity of identity with COADS, which has been widely used and referenced. Finally, the Workshop thanked Dr. Joseph O. Fletcher, who inspired the original COADS project in the 1980s, but who was unable to attend on this occasion. Several speakers acknowledged his major contributions, and participants signed a certificate in his honour.

The North Atlantic Oscillation: A Forthcoming American Geophysical Union Monograph

James W. Hurrell[1], Yochanan Kushnir[2], Martin Visbeck[2], and Geir Ottersen[3]
[1]National Center for Atmospheric Research Boulder, CO, USA
[2]Lamont-Doherty Earth Observatory, Palisades, NY, USA
[3]Institute of Marine Research, Bergen, Norway
corresponding e-mail: jhurrell@ucar.edu

Over the middle and high latitudes of the Northern Hemisphere (NH), especially during the cold season months (November-April), the most prominent and recurrent pattern of atmospheric variability is the North Atlantic Oscillation (NAO). The NAO refers to a redistribution of atmospheric mass between the Arctic and the subtropical Atlantic, and swings from one phase to another to produce large changes in the mean wind speed and direction over the Atlantic, the heat and moisture transport between the Atlantic and the neighboring continents, and the intensity and number of storms, their paths, and their associated weather. Agricultural harvests, water management, energy supply and demand, and fisheries yields, among many other things, are directly affected by the NAO. Yet, despite this pronounced influence, many open issues remain about which climate processes govern NAO variability, how the phenomenon has varied in the past or will vary in the future, and whether it is at all predictable. These issues are why the NAO emerges as one of the five principal research areas identified for the DecCen component of CLIVAR, and they were also the fundamental motivation behind a well-attended American Geophysical Union (AGU) Chapman Conference held in Ourense, Spain in late 2000 (Hurrell et al. 2001; Visbeck et al. 2001).

A principal outcome of the Chapman Conference is a new AGU Monograph *The North Atlantic Oscillation.* It is anticipated that the Monograph will be available by the 2002 Fall AGU Meeting (6-10 December, San Francisco, CA, USA). Like the Chapman Conference itself, the Monograph brings together atmospheric scientists, oceanographers, paleoclimatologists and biologists to focus exclusively on the NAO and present a state-of-the-art assessment of current understanding of this important climate phenomenon. Indeed, the outstanding feature of the Monograph is its multidisciplinary content.

The Monograph is thematically organized and provides a comprehensive (multidisciplinary) overview of material (theory, observations and models) related to the NAO. There are 12 chapters, each presenting a thorough overview of a topic, and most contain new research as well. Each chapter was subjected to critical peer review and was revised accordingly. A total of 36 expert referees made substantial contributions to the overall quality and content of the Monograph.

The NAO is one of the oldest known world weather patterns, as some of the earliest descriptions of it were from seafaring Scandinavians several centuries ago. Indeed, the history of scientific research on the NAO is rich, and Stephenson et al. (2002) present a stimulating account of the major scientific landmarks of NAO research through time. They also note that, today, there is considerable renewed interest in the phenomenon, and it is this renewed interest that is the focal point for much of the Monograph. The NAO and its time dependence, for instance, appear central to the current global change debate. Surface temperatures over the NH are likely to be warmer now than at any other time over the past

millennium, and a substantial fraction of this most recent warming is linked to the behavior of the NAO, in particular a trend in its winter index from large amplitude anomalies of one phase in the 1960s to large amplitude anomalies of the opposite phase since the early 1980s. Gillett et al. (2002) assess whether this change in the atmospheric circulation of the North Atlantic is beyond natural variability, and they synthesize a diverse body of literature dealing with how the NAO might change in response to increasing concentrations of greenhouse gases. The relationship between the NAO and anthropogenic climate change has also made it critical to better understand how the NAO and its influence on surface climate have varied naturally in the past. Jones et al. (2002) assess this issue using long, mostly European instrumental records, and they conclude by demonstrating the potential of a new instrumental index dating back to the late 17th century. The need for longer NAO records has also led to the development of numerous extensions from paleoclimate proxies, and Cook (2002) critically reviews these attempts. He also presents a new winter NAO index reconstruction back to AD 1400.

Another reason for invigorated interest in the NAO is that the richly complex and differential responses of the surface-, intermediate- and deep-layers of the ocean to NAO-induced forcing are becoming better documented and understood. The intensity of wintertime convective renewal of intermediate and deep waters in the Labrador Sea and the Greenland-Iceland-Norwegian Seas, for instance, is not only characterized by large interannual variability, but also by interdecadal variations that appear to be synchronized with fluctuations in the NAO. These changes in turn affect the strength and character of the Atlantic thermohaline circulation and the horizontal flow of the upper ocean, thereby altering the oceanic poleward heat transport and the distribution of sea surface temperature (SST). Visbeck et al. (2002) review what is known about the oceanic response to changes in NAO forcing from theoretical, numerical experimentation and observational perspectives. They note that the ocean can respond to NAO-induced forcing with marked persistence or even oscillatory behavior. The extent to which the influence of such oceanic behavior affects the evolution and dynamical properties of the atmospheric flow is probably small, but that it is perhaps significant has stimulated much interest and ongoing work. Czaja et al. (2002) assess the relevance of ocean-atmosphere coupling in determining the overall variability of the NAO.

That the ocean may play an active role in determining the evolution of the NAO is also one pathway by which some limited predictability might exist. New statistical analyses have revealed patterns in North Atlantic SSTs that precede specific phases of the NAO by 6-9 months, a link that likely involves the remarkable tendency of the extratropical ocean to preserve its thermal state throughout the year. On longer time scales, recent modeling evidence suggests that the NAO responds to slow changes in global ocean temperatures, with changes in the equatorial regions perhaps playing a central role. Rodwell (2002) reviews and investigates the predictive role of the ocean circulation using observational, atmospheric and coupled model data, and makes the point that even a limited amount of NAO predictability could be useful.

A second pathway that offers hope for improved predictability of the NAO involves links through which changes in stratospheric wind patterns might exert some downward control on surface climate. A statistical connection between the month-to-month variability of the NH stratospheric polar vortex and the tropospheric NAO was established several years ago, and more recently it has been documented that large amplitude anomalies in the wintertime stratospheric winds precede anomalous behavior of the NAO by 1-2 weeks, perhaps providing some useful extended-range predictability. Thompson et al. (2002) discuss the mechanisms by which the stratosphere might drive NAO-like variability, and they also examine the more dominant tropospheric processes that account for most of the variance of the NAO. Of relevance for the latter is the recasting of the NAO as a regional expression of an annular, hemispheric mode of variability, known as the Northern Annular Mode.

Renewed interest in the NAO has also come from the biological community. Variations in climate have a profound influence on a variety of ecological processes and, consequently, patterns of species abundance and dynamics. Fluctuations in temperature and salinity, vertical mixing, circulation patterns and ice formation of the North Atlantic Ocean induced by variations in the NAO have a demonstrated influence on marine biology and fish stocks through both direct and indirect pathways. The response of marine ecosystems to climate variability associated with the NAO is thoroughly reviewed by Drinkwater et al. (2002). Responses of terrestrial ecosystems to NAO fluctuations have also been documented. In parts of Europe, for example, many plant species have been blooming earlier and longer because of increasingly warm and wet winters, and variations in the NAO are also significantly correlated with the growth, development, fertility and demographic trends of many land animals. Mysterud et al. (2002) review the known effects of the NAO on processes and patterns of terrestrial ecosystems. The NAO has a demonstrated influence on the physics, hydrology, chemistry and biology of freshwater ecosystems as well. Straile et al. (2002) show that the physical impacts of the NAO include effects on lake temperature profiles, lake ice phenology, river runoff and lake water levels. These physical and hydrological responses influence the chemistry and biology of lakes across the NH, so ultimately the population dynamics of freshwater organisms on several trophic levels are affected by climate variability associated with the NAO.

Finally, Hurrell et al. (2002) present an overview and general discussion of the NAO aimed specifically for the non-specialist. In this introductory chapter, they describe the spatial structure of climate and climate vari-

ability, and how the NAO relates to other, prominent patterns of atmospheric circulation variability. They also describe the impact of the NAO on surface temperature, precipitation, and storms, as well as highlight the ocean and ecosystem responses, and the mechanisms that govern NAO variability. They conclude with some thoughts on outstanding issues and future research challenges.

We, the editors, are confident that the Monograph represents a current and an authoritative survey of the ever-growing body of literature on the NAO. It is unique: no other such volume on the NAO exists. As such, we hope it is a valuable resource for students and researchers alike.

Book Reference and Chapters

The North Atlantic Oscillation, **J.W. Hurrell, Y. Kushnir, G. Ottersen, M. Visbeck, (Eds.), AGU, in press.**

Cook, E.R., 2002: Multi-proxy reconstructions of the North Atlantic Oscillation (NAO) index: A critical review and a new well-verified winter index reconstruction back to AD 1400.

Czaja, A., A.W. Robertson, and T. Huck, 2002: The role of Atlantic ocean-atmosphere coupling in affecting North Atlantic Oscillation variability.

Drinkwater, K.F., and co-authors, 2002: The response of marine ecosystems to climate variability associated with the North Atlantic Oscillation.

Gillett, N.P., H.F. Graf, and T.J. Osborn, 2002: Climate change and the North Atlantic Oscillation.

Hurrell, J.W., Y. Kushnir, G. Ottersen, and M. Visbeck, 2002: An overview of the North Atlantic Oscillation.

Jones, P.D., T.J. Osborn, and K.R. Briffa, 2002: Pressure-based measures of the North Atlantic Oscillation (NAO): A comparison and an assessment of changes in the strength of the NAO and in its influence on surface climate parameters.

Mysterud, A., N.C. Stenseth, N.G. Yoccoz, G. Ottersen, and R. Langvatn, 2002: The response of terrestrial ecosystems to climate variability associated with the North Atlantic Oscillation.

Rodwell, M.J., 2002: On the predictability of North Atlantic climate.

Stephenson, D.B., H. Wanner, S. Brönnimann, and J. Luterbacher, 2002: The history of scientific research on the North Atlantic Oscillation.

Straile, D., D.M. Livingstone, G.A. Weyhenmeyer, and D.G. George, 2002: The response of feshwater ecosystems to climate variability associated with the North Atlantic Oscillation.

Thompson, D.W.J., S. Lee, and M.P. Baldwin, 2002: Atmospheric processes governing the Northern Hemisphere Annular Mode/North Atlantic Oscillation.

Visbeck, M., E. P. Chassignet, R. Curry, T. Delworth, B. Dickson, and G. Krahmann, 2002: The ocean's response to North Atlantic Oscillation variability.

Other References

Hurrell, J.W., Y. Kushnir, and M. Visbeck, 2001: The North Atlantic Oscillation. *Science*, **291**, 603-605.

Visbeck, M., J.W. Hurrell, and Y. Kushnir, 2001: First international conference on the North Atlantic Oscillation (NAO): Lessons and challenges for CLIVAR. *CLIVAR Exchanges*, **19**, 24-25.

CLIVAR Calendar

2002	Meeting	Location	Attendance
Oct. 7-9	Working Group on Coupled Modelling, 6th Session	Victoria, Canada	Invitation
Oct. 15-18	NASA-CCR-CRCES Workshop on Decadal Climate Variability	Madison, USA	Open
Nov. 1-9	Indian Ocean GOOS Conference on Observing, Modeling, Data, Management and Capacity Building	Reduit, Mauritius	Open
Nov. 11-15	International AMIP Workshop	Toulouse, France	Limited
Nov. 19-22	Working Group on Seasonal to Interannual Prediction 7th Session	Cape Town, South Africa	Invitation
Nov. 18-22	Final WOCE Conference	San Antonio, USA	Open
Dec. 6-10	AGU Fall Meeting	San Francisco, USA	Open
2003	**Meeting**	**Location**	**Attendance**
Jan. 15-17	CLIVAR Variability of the African Climate System (VACS) Panel - 7th Session	Cape Town, South Africa	Invitation
March 24-28	7th International Conference on Southern Hemisphere Meteorology and Oceanography	Wellington, New Zealand	Open
Oct. 11-16	2nd Euroconference "Achieving Climate Predictability using Paleoclimate Data"	Barcelona, Spain	Open
2004	**Meeting**	**Location**	**Attendance**
June 21-25	First CLIVAR Open Science Conference	Baltimore, USA	Open

Check out our Calendar under: ***http://www.clivar.org/calendar/index.htm*** *for additional information*

Contents

The CLIVAR Newsletter Exchanges is published by the International CLIVAR Project Office.

ISSN No.: 1026 - 0471

Editors: Andreas Villwock and Howard Cattle

Layout: Andreas Villwock

Printed by: Technart Ltd., Southern Road, Southampton SO15 1HG, UK.

CLIVAR Exchanges is distributed free-of-charge upon request (icpo@soc.soton.ac.uk).

If undelivered please return to:

International CLIVAR Project Office
Southampton Oceanography Centre, Empress Dock, Southampton, SO14 3ZH, United Kingdom